This is to certify that the

thesis entitled

Carbon Dioxide Extraction of Aqueous Benzaldehyde Solutions

presented by

Neil Douglas Barnes

has been accepted towards fulfillment of the requirements for

M.S. degree in Chemical Engineering

Major professor

Date November 4, 1994

CARBON DIOXIDE EXTRACTION OF AQUEOUS BENZALDEHYDE SOLUTIONS

By

Neil Douglas Barnes

A THESIS

Submitted to

Michigan State University

in partial fulfillment of the requirements

for the degree of

MASTER OF SCIENCE

Department of Chemical Engineering

1994

ABSTRACT

CARBON DIOXIDE EXTRACTION OF AQUEOUS BENZALDEHYDE SOLUTIONS

By

Neil Douglas Barnes

An apparatus was designed and constructed to measure the phase equilibria of the benzaldehyde-water-carbon dioxide ternary system. Values for the benzaldehyde distribution coefficient determined using this apparatus at a pressure of 1,500 psig and at temperatures of 20 °C and 35 °C were 69 and 52 (mole units) respectively.

A pilot-scale, liquid-liquid extraction column 5 feet high x 1 inch I.D. capable of operating at pressures up to 2,000 psig was designed and constructed. This apparatus was used to extract benzaldehyde from a dilute aqueous solution. Inlet and outlet stream benzaldehyde concentrations were measured using ultraviolet spectroscopy and gas phase chromatography. The measured values were used to perform a benzaldehyde balance for each experimental run of the column. Benzaldehyde recoveries ranged from 81.4% to 105.6%.

The measured inlet and outlet stream benzaldehyde concentrations were used to calculate scale-up parameters for the column. The number of equilibrium stages in the 5 foot tall column was calculated as about 1.0, the number of transfer units by film-transfer theory as 2.5, and the number of stages by the Kremser method as 1.0. The height equivalent to a theoretical stage was determined to be 5 feet and the height of a transfer unit was calculated to be about 2 feet.

To my parents for giving me every opportunity to make something of myself

and

to my sons, Matthew and Justin, who fill me with pride every time I see them.

ACKNOWLEDGEMENTS

The author wishes to express his appreciation to the following people for their contributions and support:

Bharath Rangarajan and Ramkumar Subramanian, Graduate Students, Chemical Engineering, for their assistance, counsel, and perspective;

Carol Barnes for her patience and support;

Julie Caywood, Faith Peterson, and the rest of the Office Staff in the Department of Chemical Engineering for their help with administrative details which was not taken for granted;

and last, but most importantly, to Susan Jones for her help with a long list of things that helped me see this project through to completion.

TABLE OF CONTENTS

LIST OF TABLES

LIST OF FIGURES

CHAPTER 1

INTRODUCTION

The state of Michigan is one of the largest cherry growing states in the United States. Each year, millions of pounds of cherries are processed to separate the fruit from the pits. While the fruit is sold commercially, the cherry pits currently have no commercial value and, in fact, are a liability since there is a cost associated with their disposal.

The Cherry Marketing Institute has undertaken to finance research to find profitable uses for the cherry pits. Research at Michigan State University has shown that benzaldehyde, the chemical commonly referred to as cherry flavoring, is recoverable from the cherry kernel via hydrolysis (Grethlein et al, 1990) and mechanical crushing which produces an oil containing benzaldehyde. The quantities recovered from these two methods are 0.25-0.4 percent of the kernel weight as benzaldehyde for the hydrolysis method (Gribb and Lira, 1992) and 32-36 percent of the kernel weight as an oil containing predominately triglyceride with some benzaldehyde for mechanical crushing (Briggs, 1991). It has also been shown that not only is free benzaldehyde present in the kernel but that two other chemicals, mandelonitrile and amygdalin, are also present. Both mandelonitrile and amygdalin will react during hydrolysis to form benzaldehyde and by-products. The chemical structures of benzaldehyde, mandelonitrile, and amygdalin are shown in Figure 1-1. Although Grethlein's study of cherry pit hydrolysis shows that benzaldehyde is present in significant quantity, methods to recover the benzaldehyde from the dilute hydrolysis broth were not considered.

Since benzaldehyde can be synthesized at a relatively low cost, further investigation of the hydrolysis method is justified only if an economical method of recovery from the dilute hydrolysis broth can be developed. It was thought at the

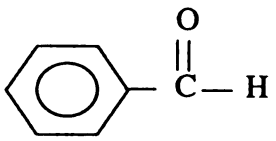

Benzaldehyde

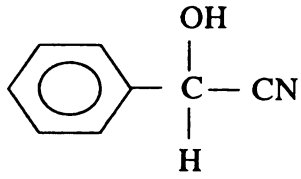

Mandelonitrile

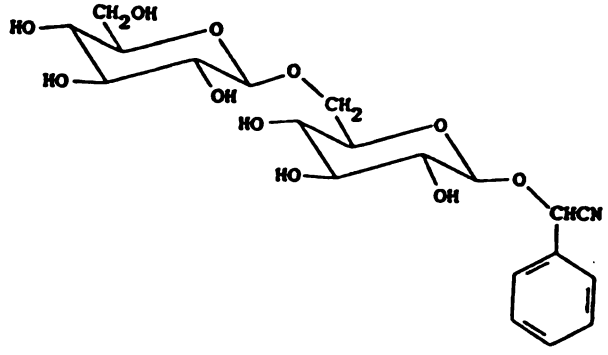

Amygdalin

Figure 1-1. Chemical Structures for Benzaldehyde, Mandelonitrile, and Amygdalin.

beginning of this project that if any processing techniques used to recover the benzaldehyde employed only naturally occurring materials, such as those typically used in food processing, the value of this "natural" benzaldehyde would be sufficient to justify the development of the required recovery process. In fact, the value of "natural" benzaldehyde is close to $100 per pound or approximately one hundred times the value of the synthesized material. This large increase in value could justify processing methods not normally considered because of their high cost.

The low solubility of benzaldehyde in water and inhibition of the hydrolysis by benzaldehyde concentrations greater than 40 parts per million (Grethlein et al, 1990) mean that recovery from a dilute solution must be performed if the hydrolysis method is to be developed to a commercial scale. Three methods that can be considered for recovery of benzaldehyde from a dilute solution are steam distillation, adsorption, and

liquid-liquid extraction.

Steam distillation involves passing steam through the benzaldehyde/water broth and volatilizing the benzaldehyde preferentially to the water. Steam can be added until the benzaldehyde is concentrated into the overhead stream to its solubility limit and then the overhead product can be collected as two phases (Cruess, 1958). This is an inefficient technique because of the large amount of water which must be heated for the recovery of a small amount of product. Also, it is possible that benzaldehyde will react with oxygen present during the distillation to form benzoic acid resulting in an appreciable yield loss.

An alternative to steam distillation is adsorption. In this process, the hydrolysis broth is passed through an adsorbent bed where the benzaldehyde is retained and the water passes through. The benzaldehyde is recovered by passing a new solvent with a high affinity for benzaldehyde through the bed and desorbing the benzaldehyde from the solid. Finally, the benzaldehyde must be recovered from the solvent. It is this final step that generally determines the economic feasibility of the adsorption method since the method usually used for separating the recovery solvent and the desired product is distillation. Distillation has a relatively high capital cost compared to most unit operations because it is energy intensive.

Recovery of the benzaldehyde from the dilute hydrolysis broth is also possible using liquid-liquid extraction with either an organic solvent or liquefied gas as the extraction solvent. Liquid-liquid extraction involves the contacting of a solution with an immiscible solvent in which one or more of the original solution components is soluble. Two liquid phases are formed after the original solution is contacted with the new solvent. These two immiscible phases separate because of a difference in densities. If the desired component of the original solution is more soluble in the new solvent than in the initial solvent, the desired component will be extracted from the original solvent. If organic solvents which are liquids at room temperature are used as

extraction solvents, distillation is usually required to separate the extraction solvent and the solute (desired product). Again, distillation has a relatively high capital cost compared to most unit operations because it is energy intensive.

The use of carbon dioxide as the extraction solvent for benzaldehyde is of interest for four reasons: 1) benzaldehyde is completely soluble in liquid carbon dioxide (Francis, 1954), 2) Related experiments indicate that the distribution coefficient is on the order of 800-1000 which means that efficient extraction of the benzaldehyde is possible in a small column, 3) carbon dioxide will not extract enzymes necessary for hydrolysis which may allow recycle of the spent hydrolysis broth, and 4) carbon dioxide extraction is currently used in food and flavor processing commercially because it meets the strict requirements for extremely low (essentially nondetectable) residual solvent concentrations and because it fulfills the all "natural" requirement for increased product value.

In order to use carbon dioxide as a solvent in an extraction process it must be compressed to a high enough pressure to liquefy it at the chosen operating temperature. For economic reasons, as well as practical ones, this temperature is usually around room temperature. As a general rule, the cost of liquefying carbon dioxide is high and therefore its use as an extraction solvent is limited to high value added products such as "natural" benzaldehyde. It is interesting to note that the critical temperature of carbon dioxide is only slightly above room temperature at 31 degrees Celsius. Therefore, at a temperature only a small amount higher than room temperature and at similar pressures as those used for liquefying carbon dioxide, it becomes a supercritical fluid. This is of particular interest when considering carbon dioxide for liquid-liquid extraction because the diffusivity, viscosity and density are significantly different in the supercritical fluid state than in the normal liquid state. It is possible that if the processing conditions can be carefully controlled so that the carbon dioxide is kept near its critical point, a significant increase in the solubility of benzaldehyde might occur

being greater than the solubility in liquid carbon dioxide. This increase in solubility would reduce the cost of carbon dioxide extraction by decreasing the amount of carbon dioxide used to perform the extraction and, therefore, would reduce the size of the extraction column required for the desired recovery.

Because of the advantages of using liquid-liquid extraction with carbon dioxide as the extraction solvent either in its liquid or supercritical-fluid state versus steam distillation or adsorption, a pilot scale extraction apparatus was built to investigate the recovery of benzaldehyde from a dilute hydrolysis broth. Successful operation of this column could then be used to predict the feasibility of building a commercial-scale column to recover benzaldehyde from hydrolysis broth that would come from processing the fifteen million pounds of cherry pits that are currently disposed of every season in Michigan. Prior to building the extraction apparatus, it was necessary to develop the analytical techniques required to determine the amount of each component in the streams entering and exiting the extraction column in order to determine its performance. It was also necessary to measure the distribution coefficient of benzaldehyde for carbon dioxide and water experimentally since this value could not be found in the literature nor could sufficient data on activity coefficients or solubility be found that could be used to predict the distribution coefficient with any reliability. The theory underlying the principles of liquid-liquid extraction, an explanation of the design of the equipment used in this project, a description of the analytical methods used, and the results of the experiments performed are presented in this report.

CHAPTER 2

BACKGROUND

Many industrially important solutions of liquids form constant boiling mixtures (azeotropes) or have components with such close boiling points that separations of these liquids by ordinary distillation is not practical. Many other compounds, particularly in the foods and flavorings industry, are heat sensitive or are not volatile (e.g. penicillin) and can not be purified by distillation. Various other methods of separation have been applied to such systems including liquid-liquid extraction. Compared to distillation as a means of separation, liquid-liquid extraction is a more recent operation. It has reached industrial significance only since 1930 (Orberg and Jones, 1963). Some examples of liquid-liquid extractions of commercial significance are given in Table 2-1.

Table 2-1. Typical Liquid-Liquid Extractions

Original Solvent	Solute	New Solvent
Water	Acetic Acid	Ethyl Acetate
Water	Adipic Acid	Diethyl Ether
Reformate	Aromatics	Diethylene Glycol
Water	Benzoic Acid	Carbon Tetrachloride
Water	Diethylamine	Toluene
LPG	H_2S	MEA
Naphtha	Mercaptans	NaOH Solution
Water	MEK	Toluene
Lubricating Oil	Naphthenes	Furfural
Water	Phenol	Chlorobenzene

Liquid-Liquid Extraction

Liquid-liquid extraction involves the contacting of a solution with an immiscible solvent in which one or more of the original solution components is soluble. Two liquid phases are formed after the addition of the new solvent. If the new solvent has a different density than the original solvent, the two phases will separate with the less dense phase rising to the top. If the desired component of the original solution is more soluble in the new solvent, this component will be extracted from the original solution through contact with the new solvent.

Extraction may be carried out as a continuous or a batch process. Economics generally favor continuous contacting because of high throughput capacities, ease of handling the feed and shorter down times. There are several types of contactors which may be used for continuous extraction: spray columns, packed columns, sieve tray columns, and mechanically agitated columns of which the two most common are the Scheibel column (Scheibel, 1948) and the Karr column. The spray, packed, and sieve tray columns have the advantage of not using any internal moving parts and have a low capital cost relative to the mechanically agitated type. However, mechanical agitation can provide more surface area for mass transfer between the two phases resulting in a more efficient extraction. A schematic diagram of a liquid-liquid extraction apparatus is shown in Figure 2-1. This particular apparatus was used in pilot scale tests by Schultz and Randall (1974) for the extraction of essences from liquids such as apple, orange and pear juices in pilot scale tests. An interesting feature of this extraction system design is the modifications that allow the use of liquid carbon dioxide as the extraction solvent.

Literature Review

Solvent properties of liquid carbon dioxide were described by Gore (1861) who published information on the solubility of naphthalene, iodine, and similar compounds.

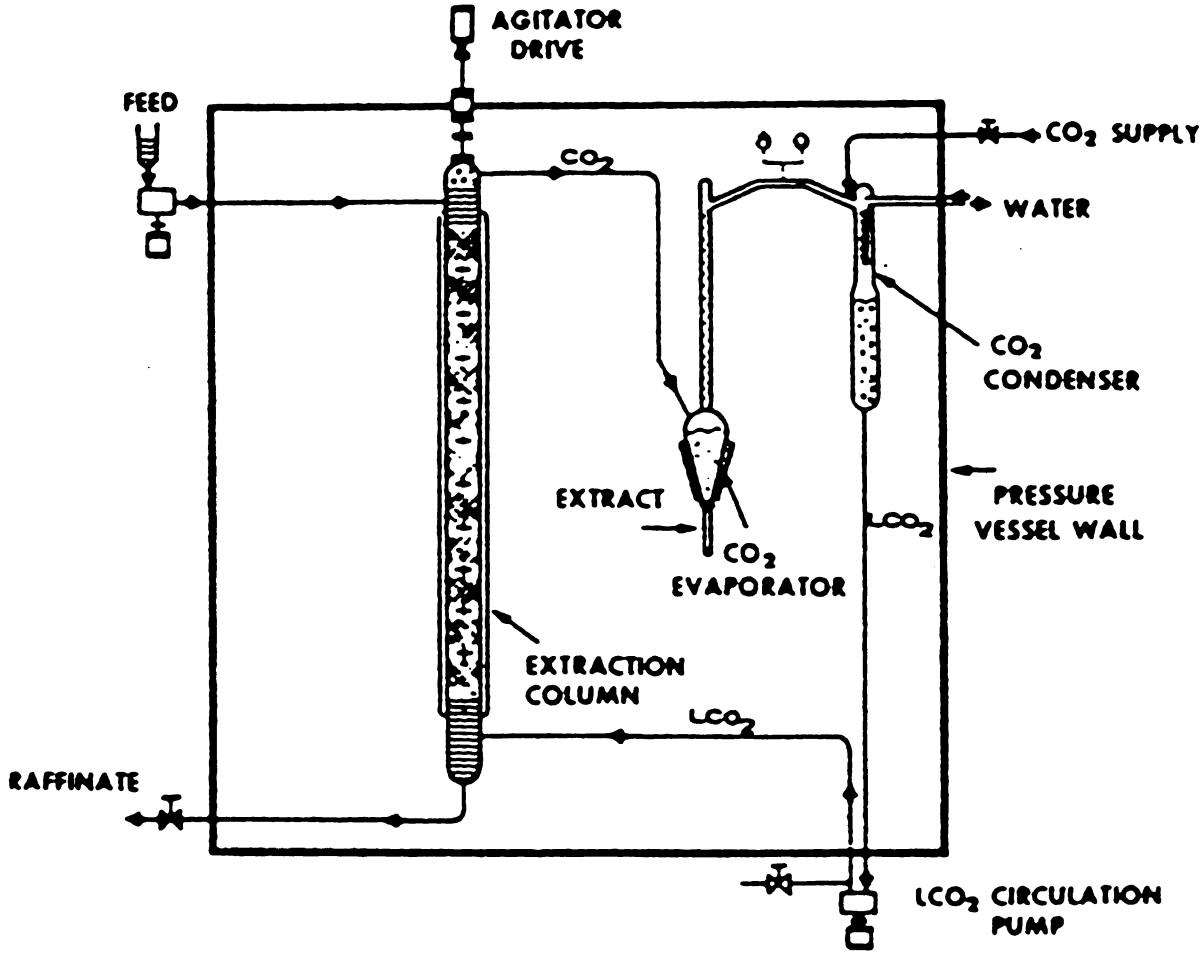

Figure 2-1. Liquid-Liquid Extraction Schematic Diagram.

Low
pate
esse
on t
the
yiel
as a
cor
fru
al.

Di

cit
or
of
be
ho
sc
st
R
h
w

de
di
th

Lowry et al. (1927) measured the solubility of water in liquid carbon dioxide. Early patents that specifically mention carbon dioxide as an extraction solvent for food essences were obtained by Horvath (1939) and Brandt (1942). Francis (1954) worked on the separation of dicyclic hydrocarbons from aliphatics and monocyclics and listed the solubilities of 261 compounds in liquid carbon dioxide. The late 1960's and 1970's yielded a plethora of patents and publications describing uses of liquid carbon dioxide as a solvent; Sivetz (1963) cites usages of liquefied gases for extracting coffee aroma constituents, Schultz (1966) reported on the use of liquid carbon dioxide for extracting fruit aroma constituents, and spice extracts and equipment are described by Pekhov et al. (1969) and others.

Distribution Coefficient

The liquid carbon dioxide extraction of a juice or aqueous essence such as those cited above will follow general extraction principles. The maximum amount of an organic solute that theoretically can be extracted by liquid carbon dioxide in one stage of mixing and settling is determined by the distribution (partition) of the solute between the liquid carbon dioxide and the water. For oxygenated species in a homologous series, as the molecular weight of the solute increases a greater part of the solute will concentrate in the liquid carbon dioxide phase. Thus, fewer extraction stages are needed to extract heavier compounds from an aqueous solution (Schultz and Randall, 1974). It may be expected by inference that this phenomenon occurs in other homologous series of compounds because of the increasing percentage of the structure which is aliphatic.

The ability of liquid carbon dioxide to extract a solute from aqueous solution is determined by the equilibrium distribution of the solute between the liquid carbon dioxide and the water. For extremely dilute solutions Henry's Law is applicable and the distribution coefficient, m, of any compound, i, between the extract phase (solvent

or liquid carbon dioxide phase) and the raffinate phase (aqueous) phase can be expressed as:

$$m_i = \frac{y_i}{x_i} \qquad 2\text{-}1$$

where y_i mole fraction of component i in the extract phase

x_i mole fraction of component i in the raffinate phase

The general significance of the distribution coefficient is that values greater than approximately five or ten indicate a high recovery of solute is possible with the quantity of extract probably being less than the raffinate. Distribution coefficients less than one indicate the solute is incompletely extracted unless very large amounts of solvent are used. This affects the economics of the liquid-liquid extraction since recovery of the solute from the extract must always be taken into account and this will, more than likely, be more expensive with a larger amount of solvent.

Given the significance of the distribution coefficient, methods or rules-of-thumb for predicting it are very valuable for making preliminary determinations of the desirability of using liquid-liquid extraction versus other separation techniques. For dilute solutions, Henry's Law is applicable. Schultz and Randall (1970) found that there is a correlation between distribution coefficient and the number of carbon atoms in a molecule for similar species (Figures 2-2 and 2-3). It may be that this relationship holds for other species as well and, therefore, estimates of the distribution coefficient can be made for any solute if data for similar compounds are known. In the absence of distribution coefficient data, as is the case with liquid carbon dioxide systems in general, activity coefficients can provide some basis for estimating how well a compound might be extracted. Schultz and Randall (1970) found that a trend exists between the activity of an organic compound in water and the equilibrium distribution

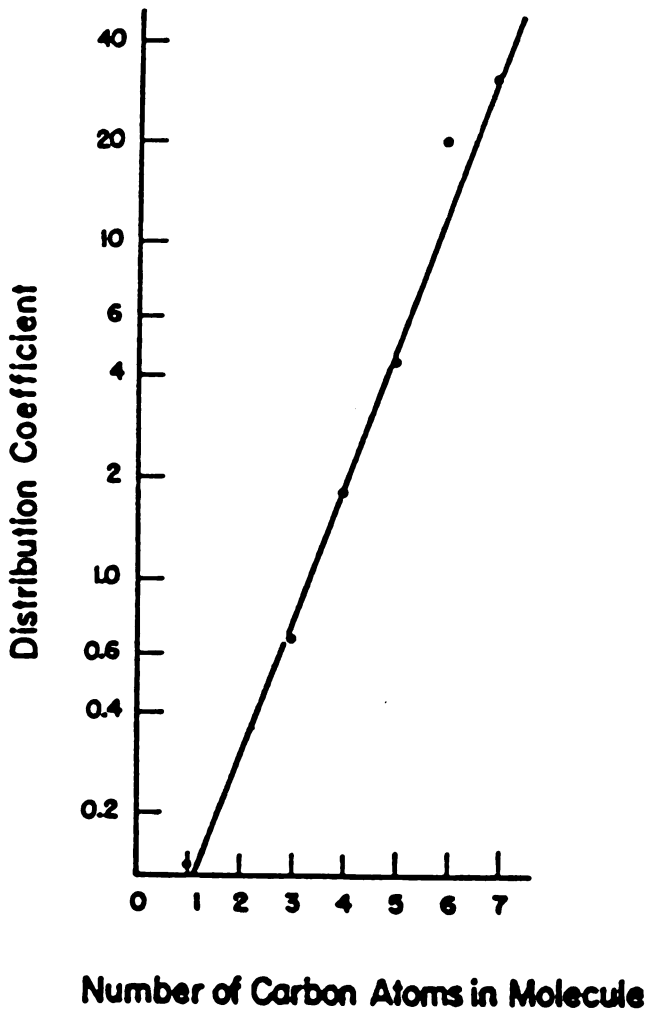

Figure 2-2. Distribution Coefficient versus Carbon Atoms for n-Primary Alcohols

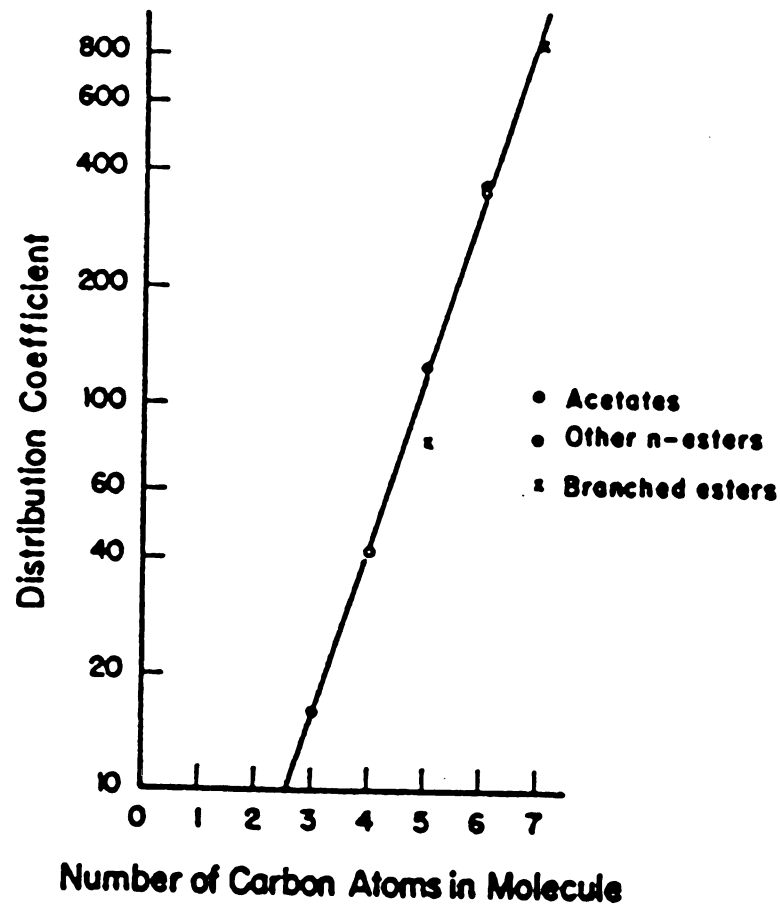

Figure 2-3. Distribution Coefficient versus Carbon Atoms for Selected Esters

of the compound between liquid carbon dioxide and water. See Table 2-2. Although no formal correlation was attempted by these authors for the alcohols and esters studied, in all cases large activity coefficients in water correspond to large distribution coefficients.

When working with liquid carbon dioxide it is advantageous to keep costs down by operating the extraction equipment at ambient temperature to eliminate the need for expensive low-temperature cooling capability even though decreasing the temperature of operation facilitates keeping the carbon dioxide in its liquid state. At ambient temperatures, however, the equipment must be designed to operate at a minimum pressure equal to the vapor pressure of carbon dioxide which is 882 psig at 22.4 °C. Once this criterion is met, the maximum operating pressure will normally be specified at approximately 1,500 psig or more to allow for fluctuations. When this is realized it is useful to note that the extraction equipment is able to operate above the critical point of carbon dioxide. This means that an examination of the advantages of performing a supercritical fluid (SCF) extraction versus a liquid carbon dioxide extraction is worthwhile and this was done for the separation of benzaldehyde from the hydrolysis broth under investigation in this project.

Supercritical Fluid Extraction

Over the last decade there has been substantial interest in the use of supercritical fluids. According to Akgerman et al. (1991) three factors have contributed to the recent attention: (1) the environmental problems associated with common industrial solvents (mostly chlorinated hydrocarbons), (2) the increasing cost of energy-intensive separation techniques (for example distillation), and (3) the inability of traditional techniques to provide the necessary separations needed for emerging new industries (microelectronics, biotechnology, etc.). In addition, more stringent pollution-control legislation and the availability of inexpensive, nontoxic supercritical solvents such as

Table 2-2. Distribution and Activity Coefficients for Alcohols and Esters

Compound	Distribution Coefficient[2], K 16 °C	γ_1° (experimental)[1] 25 °C	γ_1° (calculated)[1] 25 °C
Methanol	0.40	---	1.53
n-Propanol	0.66	11.7	11.40
n-Butanol	1.8	48.2	---
n-Pentanol	4.5	169.0	---
n-Hexanol	15.0	---	644.0
n-Heptanol	31.0	---	2740.0
i-Propanol	0.35	6.54	---
i-Butanol	1.7	---	44.3
t-Butanol	0.82	10.1	---
s-Butanol	1.23	---	31.2
i-Pentanol	5.0	---	157.0
Ethyl formate	16.0	52.0	---
Ethyl acetate	42.0	65.0	77.6
Isopropyl acetate	80.0	---	---
Methyl Butyrate	120.0	400.0	394.0
Butyl acetate	350.0	---	1270.0
Propyl propionate	370.0	1100.0	1210.0
Isoamyl acetate	850.0	---	5400 (est)

[1] Activity coefficients by Pierotti et al., 1959
2 Distribution coefficients by Schultz et al. Between water and liquid CO_2

carbon dioxide have prompted research into supercritical fluid extraction as a means of waste water treatment. The focus of supercritical fluid use as a clean-up technique has been in three major areas (Akgerman et al., 1977): 1) extraction of organic contaminants from water, 2) extraction of organics from contaminated soil, and 3) extraction of organics from adsorbents.

The critical point of a pure substance is defined as the highest temperature and pressure at which a substance can exist in vapor-liquid equilibrium. At temperatures and pressures above this point a single homogeneous fluid is formed and it is said to be supercritical. A schematic diagram of this behavior is shown in Figure 2-4. Table 2-3 lists the critical temperatures and pressures for a number of gases and liquids.

Supercritical fluids exhibit some physical properties that are intermediate between those of a gas and those of a liquid as shown in Table 2-4. It is this unique combination of physical properties, at least in part, that frequently garners attention to the use of supercritical fluids as extraction solvents. From a theoretical viewpoint, it would appear that the decreased viscosity and increased diffusion coefficient of supercritical fluids relative to liquids would indicate better mass transfer in supercritical fluids and, therefore, more efficient extraction. In addition, the solvent power of a supercritical fluid can be related to its density in the critical region. This statement can be clarified by considering the density behavior of a pure component as shown in Figure 2-5 (McHugh and Krukonis, 1986, p. 5). According to these authors, for a reduced temperature, T_R, in the range of 0.9 to 1.2 and at reduced pressures, P_R, greater than 1.0, the reduced density, ρ_R, of the solvent can change from a value of about 0.1, a gas-like density, to about 2.5, a liquid-like density. As the reduced density becomes liquid-like the supercritical fluid begins to act as a liquid solvent. This increase in density corresponds to an increase in the solvent power of the supercritical fluid. Conversely, a decrease in density accompanying a decrease in pressure results in a dramatic decrease in the solubility of the solute. This is particularly useful for

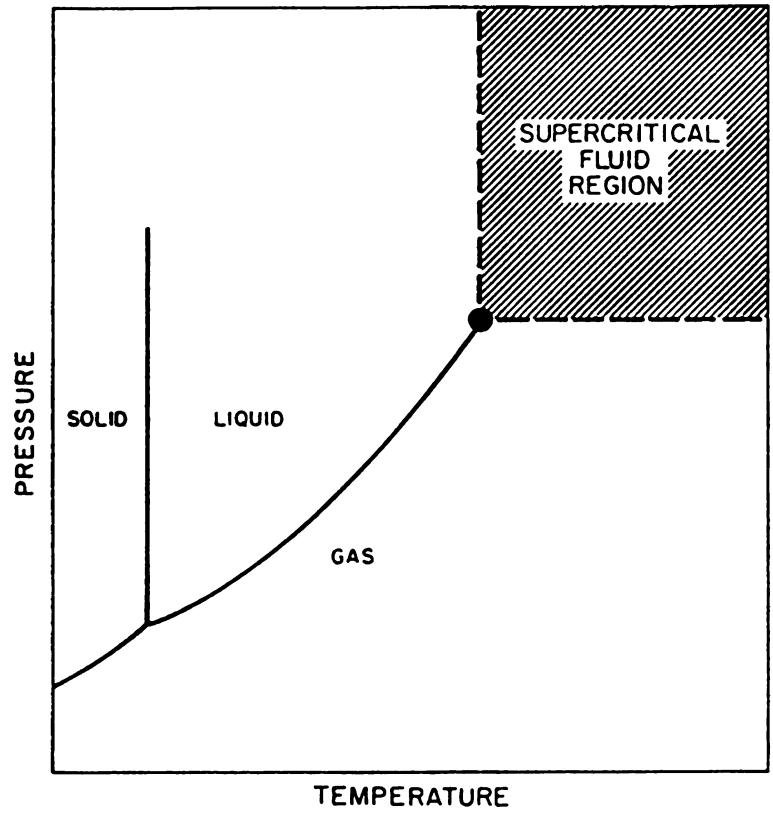

Figure 2-4. Pressure-Temperature Diagram for a Pure Component

Table 2-3. Critical Conditions for Various Solvents

Solvent	Critical Temperature (°C)	Critical Pressure (atm)
Nitrogen Dioxide	157.8	100
Nitrogen	-147	33.5
Oxygen	-118.4	50.1
Hydrogen	-239.9	12.8
Helium	-267.9	2.26
Carbon Dioxide	31.1	72.8
Ethane	32.3	48.2
Ethylene	9.3	49.7
Propane	96.7	41.9
Propylene	91.9	45.6
Cyclohexane	280.3	40.2
Isopropanol	235.2	47.0
Benzene	289.0	48.3
Toluene	318.6	40.6
p-Xylene	343.1	34.7
Chlorotrifluoromethane	28.9	38.7
Trichlorofluoromethane	198.1	43.5
Ammonia	132.5	111.3
Water	374.2	217.6
Weast, 1969-1970		

Table 2-4. Comparison of Properties for a Gas, SCF, and Liquid

Property	Gas	SCF	Liquid
Density (kg/m^3)	1	700	1000
Viscosity (ns/m^2)	10^{-5}	10^{-4}	10^{-3}
Diffusion Coefficient (cm^2/s)	10^{-1}	10^{-4}	10^{-5}

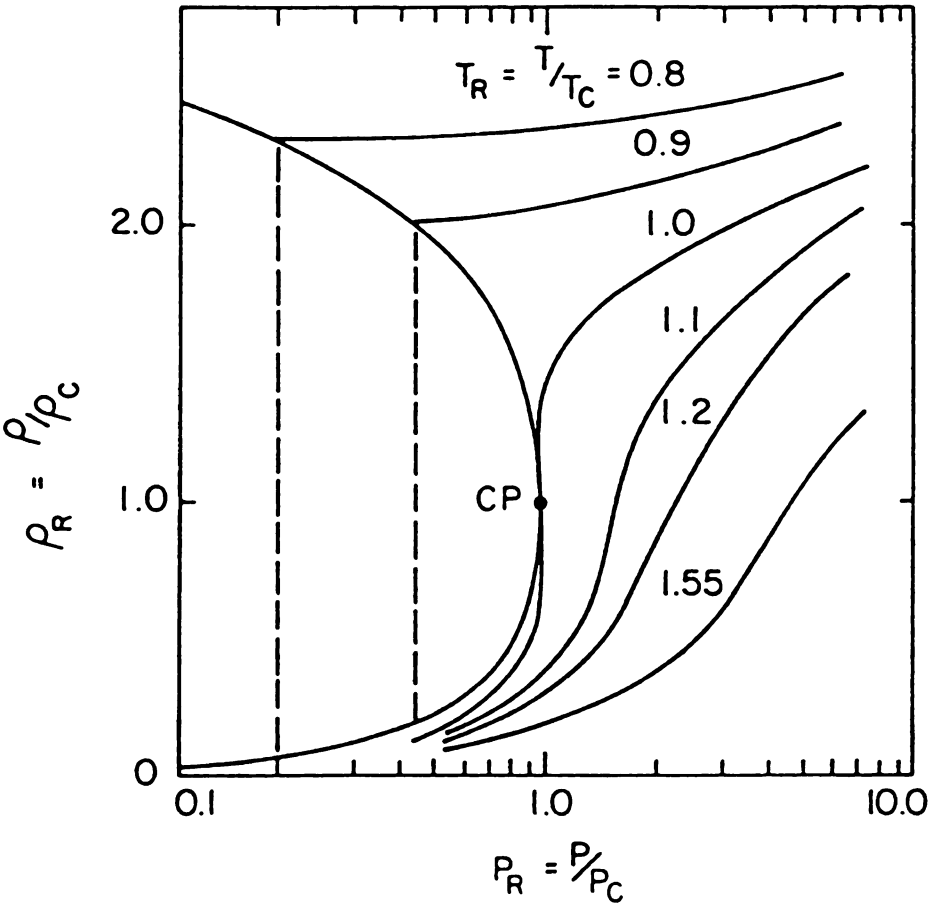

Figure 2-5. Reduced Density vs. Reduced Pressure Near the Critical Point

separation of the supercritical fluid and the solute after the actual extraction is accomplished.

The solvent power of supercritical fluids is typified by the solubility of solid naphthalene in supercritical ethylene as shown in Figure 2-6. At a temperature of 12 °C (T_R = 1.01) the solubility of naphthalene in supercritical ethylene increases quite dramatically as the pressure is increased to 50 atmospheres and higher. The solubility reaches a maximum of about 1.5 mole percent at pressures greater than 90 atmospheres. At pressures below 50 atmospheres the naphthalene solubility is quite low as would be expected for the solubility of a solid in a gas. The solubility behavior along the 12 °C isotherm can be interpreted by considering the reduced-density isotherm at 1.0 shown previously in Figure 2-5. Note that the naphthalene isotherm has the same general characteristic shape as the reduced-density isotherm at 1.0. From this example, it can readily be seen why the solvent behavior of a supercritical fluid is related (to a first approximation) to the solvent density behavior in the critical region (McHugh and Krukonis, 1986, p 5). Considering the 35 °C isotherm in Figure 2-6, it can be seen that the solubility behavior is not as sensitive to pressure in the region near 50 atmospheres as it was for the 12 °C isotherm. However, at pressures greater than 100 atmospheres where ethylene exhibits liquid-like densities, the 35 °C isotherm reaches a higher limiting solubility value of about 5 mole percent.

The properties of gas-like diffusivity and viscosity, zero surface tension, and liquid-like density combined with the pressure dependent solvent power of a supercritical fluid make its use as an extraction solvent very attractive. However, on occasion these properties may offer no advantage relative to conventional solvents. According to McHugh and Krukonis (1986, p 10), it is necessary to evaluate supercritical fluid technology on a case-by-case basis since the advantage gained by the mass transfer properties of a supercritical fluid are relative to the entire system under evaluation.

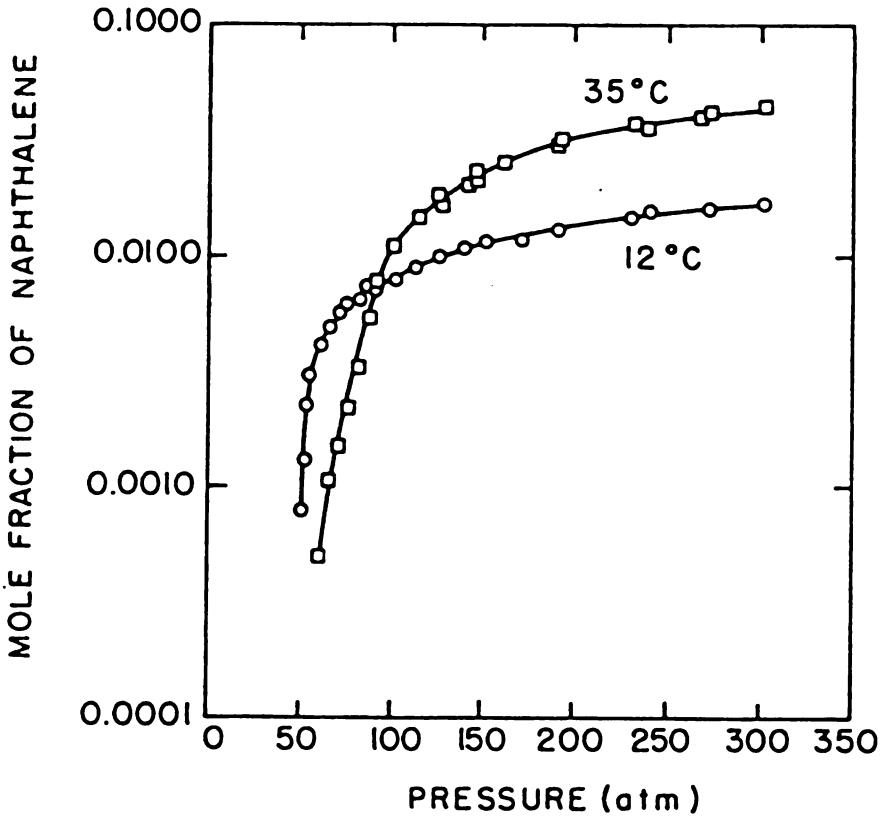

Figure 2-6. Solubility of Naphthalene in Ethylene

CHAPTER 3

LIQUID-LIQUID EXTRACTION

Liquid-Liquid extraction is the separation of the components of one liquid solution by contact with another insoluble liquid. Two liquid phases form after the two liquids are mixed together, therefore, the densities of the two phases must be different so that the phases will separate. The solution which is to be contacted is the *feed* and the liquid with which the feed is to be contacted is the *solvent.* The components dissolved in the feed are the *solutes.* The solvent-rich product of the extraction operation is the *extract* and the solute depleted feed is the *raffinate.* Ideally, the valuable components of the initial solution will preferentially partition into the solvent thus being extracted from the feed.

There are many types of liquid-liquid extraction devices. The various devices are generally classified into stage and continuous-contact (differential) types. The stage type includes mixer-settlers and sieve-tray (perforated plate) towers. The continuous contact type includes spray towers, packed towers, centrifugal extractors, and mechanically agitated, countercurrent extractors. The later type includes the rotating-disk contactor, Mixco Lightnin CM contactor, Scheibel extractor (Figure 3-1), and Karr column.

There are many factors involved in the selection and design of a liquid-liquid extraction device such as those described above. The following discussion examines these factors from both the operational and mass transfer points of view.

Solvent Selection

There are several important factors governing the selection of the solvent used for extraction. The following criteria are recommended by Treybal (Treybal, 1980, p 488):

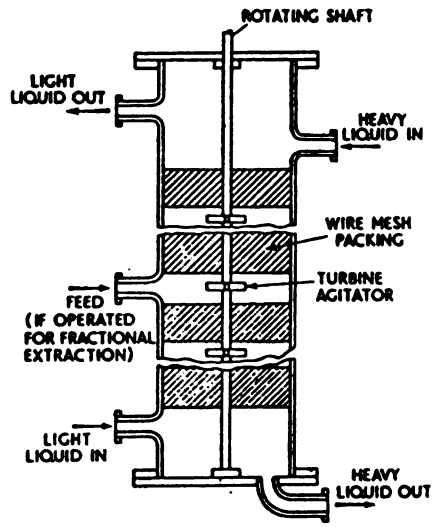

Figure 3-1. Scheibel Extractor

1. *Selectivity.* The effectiveness of solvent B for separating a solution of solvent A and solute C into its components is the selectivity, β. At equilibrium:

$$\beta = \frac{(\text{wt fraction A in R})}{(\text{wt fraction A in E})} \frac{(\text{wt fraction C in E})}{(\text{wt fraction C in R})} = \frac{(\text{wt fraction A in R})\, x_E^*}{(\text{wt fraction A in E})\, x_R} \qquad 3\text{-}1$$

where E is the extract stream

R is the raffinate stream

For useful extraction operations the selectivity must exceed unity. If the selectivity is unity, no separation is possible.

2. *Distribution Coefficient.* This is the ratio x_E^*/x_R in the above equation. While

it is not necessary for the distribution coefficient to be greater than unity, large values are desirable since less solvent will then be required for the extraction.

3. *Insolubility of solvent.* The extraction solvent should be as completely insoluble in the original solvent as possible. Ideally, the two solvents are completely immiscible. Immiscible solvents will have higher selectivities than solvents that exhibit partial solubility.

4. *Recoverability.* It is usually preferred to separate the solvent from the solute after the extraction and recover the solute for reuse. This is most often accomplished by distillation therefore the relative volatility of the solute and solvent should be considered. Whether it is the solvent or the solute, that substance which is present in the extract in the lesser quantity should be the most volatile. The cost of separating and recovering the solute can significantly influence the cost of the extraction operation.

5. *Density.* A difference in the saturated liquid densities is necessary for the phases to separate. The larger the difference the better. The density difference for equilibrium phases decreases with increasing solute concentration and this must be carefully considered during the solvent selection.

6. *Interfacial tension.* There exists an interfacial tension between two immiscible liquid phases. Quite often the interfacial tension between the two liquid solvents is altered markedly by the presence of the solute. While high values of interfacial tension tend to increase the difficulty of dispersing one phase in another, a large value of interfacial tension will promote the coalescence of the dispersed phase droplets. On the other hand, low values of interfacial tension may produce an emulsion of the dispersed phase. The tiny droplets of such an emulsion do not separate easily from the continuous phase which makes operation of the extractor difficult.

7. *Chemical Reactivity.* The solvent should be inert toward the other components of the system and towards the materials of construction.

8. *Viscosity.* If the solvent is the continuous phase, a high solvent viscosity will

decrease the rate of rise (or fall) of the dispersed phase for a given pressure drop. This increases the contact time between phases and the total mass of solute transferred. However, flooding correlations such as those of Crawford and Wilke (Crawford and Wilke, 1951) or Rao and Rao (Rao and Rao, 1958) and others show that a high viscosity continuous phase lowers the column capacity by lowering the flooding velocity. If the solvent is the dispersed phase, a high viscosity will result in a lower rate of mass transfer relative to a lower viscosity and the rate of solute diffusion will be reduced. However, it has been demonstrated that dispersed phase viscosity has little affect on column capacity (Breckenfeld, 1942).

9. *Vapor pressure and freezing point.* These should be as low as possible to promote ease of handling.

10. *Safety.* The solvent should be nontoxic and nonflammable.

Since no solvent meets all of the optimum criteria, the selectivity and distribution coefficient usually play a significant role in selecting the solvent used for a particular extraction. However, the recoverability of the solvent can have a high enough cost so as to make the choice of solvent favor the one with a lower selectivity or distribution coefficient. For pharmaceuticals and food applications, solvent toxicity may be the overriding criterion. Regardless of which solvent property is deemed the most important, the physical properties of the solvent will affect which type of extractor is selected.

Because the purpose of this research was to extract a food flavoring from a fermentation broth, the solvent toxicity was of primary importance. In addition, even for a solvent with acceptable toxicity, the solvent recoverability in terms of very low levels of residual solvent in the product was also important. Carbon dioxide met both of these criteria. The high cost of an extraction process designed to utilize liquid carbon dioxide was thought to be justified by the high value of the recovered cherry flavoring (benzaldehyde).

Once carbon dioxide was selected as the solvent, its properties in relation to the water/benzaldehyde feed mixture, the cost of operation, and the relative capital cost of each type of extractor were used to select the continuous, packed column as the type of extractor to use for this project.

Dispersed Phase

When extraction is carried out in a packed column, the more dense solvent is introduced near the top and the less dense solvent is introduced near the bottom. In order for mass transfer of the solute to occur, the phases must contact each other. This occurs in such a way that one phase is dispersed in the other in the form of droplets. The smaller the droplets the greater the interfacial surface area and the greater the rate of mass transfer. The phase which is not dispersed is the continuous phase. Either of the solvents can be the dispersed phase.

The choice of which phase is the continuous one and which is the dispersed one is based on mass transfer. Usually, the solvent with the higher mass transfer coefficient should be selected as the continuous phase since the path length for solute travel is larger in the continuous phase. Since the higher mass transfer coefficient is related to lower viscosity, the continuous phase should also be the phase with the lower viscosity.

For this research, carbon dioxide was selected as the continuous phase since it has a lower viscosity than water. With carbon dioxide as the continuous phase, water must be introduced at the top of the column because its density is greater than that of carbon dioxide.

Column Capacity

Extraction is often accomplished in a column filled with packing similar to the types used in distillation. During proper operation, the dispersed phase droplets fall (or rise) through the interstitial voids in the packing immersed in the continuous phase.

If the flow rate of the dispersed phase is increased, the droplets will occupy a larger fraction of the of the void space. Further increases in the dispersed phase flow will eventually result in the void space becoming filled with droplets that coalesce to completely fill the void space in the packing. This phenomenon is flooding and the superficial velocity at which flooding occurs is the flooding velocity. Flooding can also occur if the dispersed phase flow is held constant and the flow rate of the continuous phase is increased. Eventually, the continuous phase flow will reach a velocity sufficient to prevent the dispersed phase droplets from moving down (or up) the column. Thus, the flooding of the column is dependent upon the flow rates of both phases.

The physical properties of each of the solvents are also related to column flooding. Consider the following hypothetical experiments. The flow rates of both phases are held constant at those corresponding to normal operation of the column for each of the following experiments. The more dense, dispersed phase is assumed to be descending through the less dense continuous phase (the situation for this research):

1. If the density of the dispersed phase could be increased independently of any other properties, the terminal velocity of the droplets would increase and there would result a corresponding increase in the flooding velocity;

2. If the viscosity of the continuous phase were increased independently of any other properties, the rate of descent of the dispersed phase droplets would decrease and there would be a corresponding decrease in the flooding velocity;

3. If the surface tension of the dispersed phase were varied independently of any other properties, the droplet size would change resulting in a change in the rate of descent of the droplets thus changing the flooding velocity;

4. If the void space between the individual pieces of packing is decreased it will take fewer droplets to fill the smaller space. This would correspond to a lower flooding velocity.

Thus, it would appear that the flooding velocity is affected by density, viscosity, surface tension, and the packing free volume as well as the superficial velocity of both phases.

Investigations of the flooding rates in columns have been carried out and reported in the literature. Although very useful, many of these studies and the resulting correlations suffer from the deficiency of having observed only pure component, binary systems. The correlations resulting from three of these studies are presented below:

1. Modified Crawford-Wilke (Crawford, 1951) correlation:

$$\frac{\mu_C}{\Delta\rho}\left(\frac{\sigma}{\rho_C}\right)^{0.2}(F\varepsilon^2)^{1.5} \text{ versus } \frac{\rho_C}{a_p\mu_C}(V_D + V_C)^2 \qquad 3\text{-}2$$

where

	a_p	Surface area of packing (ft^2/ft^3)
	F	Packing factor, dimensionless
	V_C	Continuous phase superficial velocity (ft/hr)
	V_D	Distributed phase superficial velocity (ft/hr)
	ε	Void fraction of packing, dimensionless
	μ_C	Continuous phase viscosity (cps)
	ρ_C	Density of the continuous phase, (lb/ft^3)
	$\Delta\rho$	Density difference between phases (lb/ft^3)
	σ	Interfacial tension (dyne/cm)

Generally, values for the constants in the left-hand expression are known or are easily measurable. Calculating this value and locating its intercept with the curve in Figure 3-1 allows the value for the right-hand expression to be read from the curve. This value corresponds to the combined phase flow rates that will flood the column

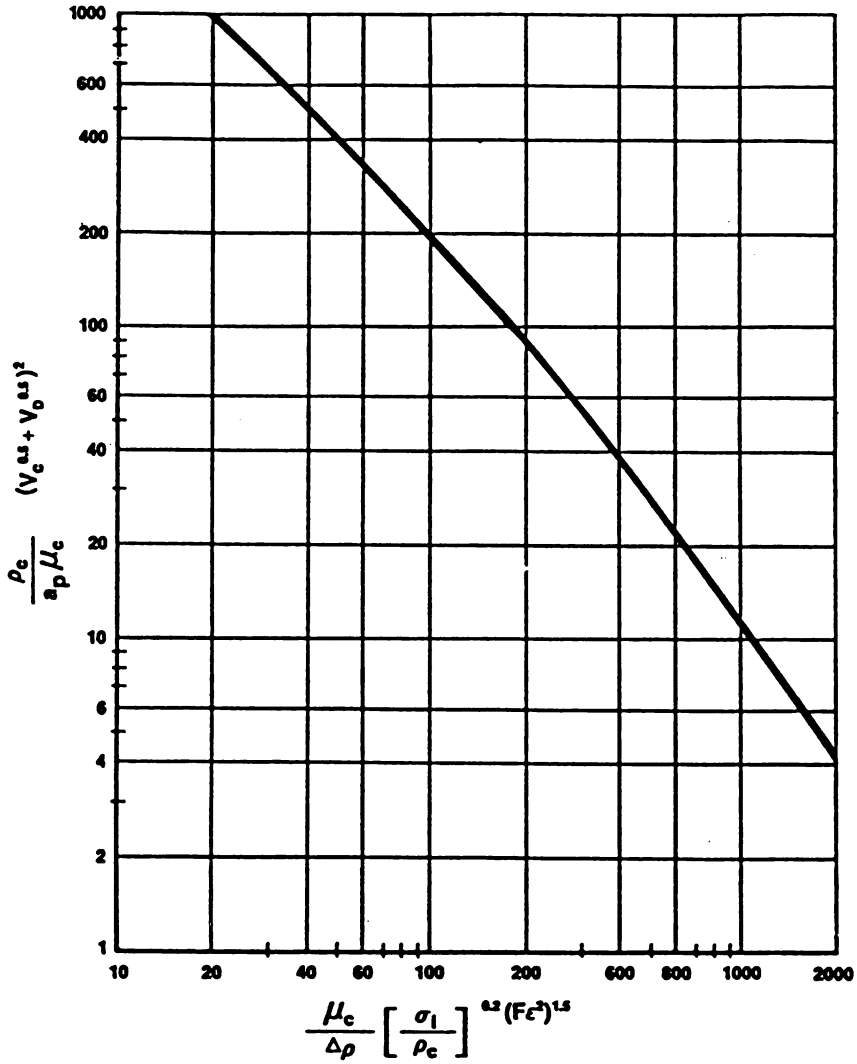

Figure 3-2. Crawford-Wilke Correlation

since the values for ρ_C, μ_C, and a_p have been determined previously. When the velocity of one phase is specified the other can be calculated so that the combined flows will be less than the combination which will result in flooding.

The original Crawford and Wilke correlation was based on eight different binary liquid systems. The properties varied as follows:

packing void fractions	maximum of 0.74
liquid viscosity	0.58 to 7.8 cps
liquid density difference	9.4 to 37.2 lb/ft^3
interfacial tension	8.9 to 44.8 dyne/cm

The modified correlation was based on data from six different tower packings with void fractions, ε, having values up to 0.94. All of these flooding data were based purely on hydraulic flow data with no mass transfer of solute occurring.

2. Rao and Rao (Rao, 1957) correlation:

$$1 + 0.835\left(\frac{\rho_D}{\rho_C}\right)^{0.25}\left(\frac{V_D}{V_C}\right)^{0.5} = C\left[\left(\frac{V_C^2 a_p}{g\varepsilon^3}\right)\left(\frac{\rho_C}{\Delta\rho}\right)\sigma^{0.25}\right]^n \qquad 3\text{-}3$$

where a_p Surface area of packing (ft^2/ft^3)

g Gravitational acceleration, ft/hr^2

V_C Continuous phase superficial velocity (ft/hr)

V_D Distributed phase superficial velocity (ft/hr)

ε Void fraction of packing, dimensionless

ρ_C Density of the continuous phase, (lb/ft^3)

ρ_D Density of the discontinuous phase, (lb/ft^3)

and

floc

con

neg

was

$$1 + 0.835\left(\frac{V_0}{V_\infty}\right)^{1/2}\left(\frac{\rho_0}{\rho_\infty}\right)^{1/2}$$

$\Delta\rho$ Density difference between phases (lb/ft^3)

σ Interfacial tension (dyne/cm)

C Curve-fit parameter

n Curve-fit parameter

The authors correlated their data from over 50 runs with different liquid systems and packings. Interfacial tensions ranged from 10 dyne/cm to 39 dyne/cm. Their flooding data were fitted by the dimensionless expression Equation 3-3 when the constant, C, and the value of the slope of the curve, n, were taken to be 0.66 and negative 0.25 respectively. The original development for the dimensionless equation was done by Dell and Pratt. Such a plot is shown in Figure 3-3.

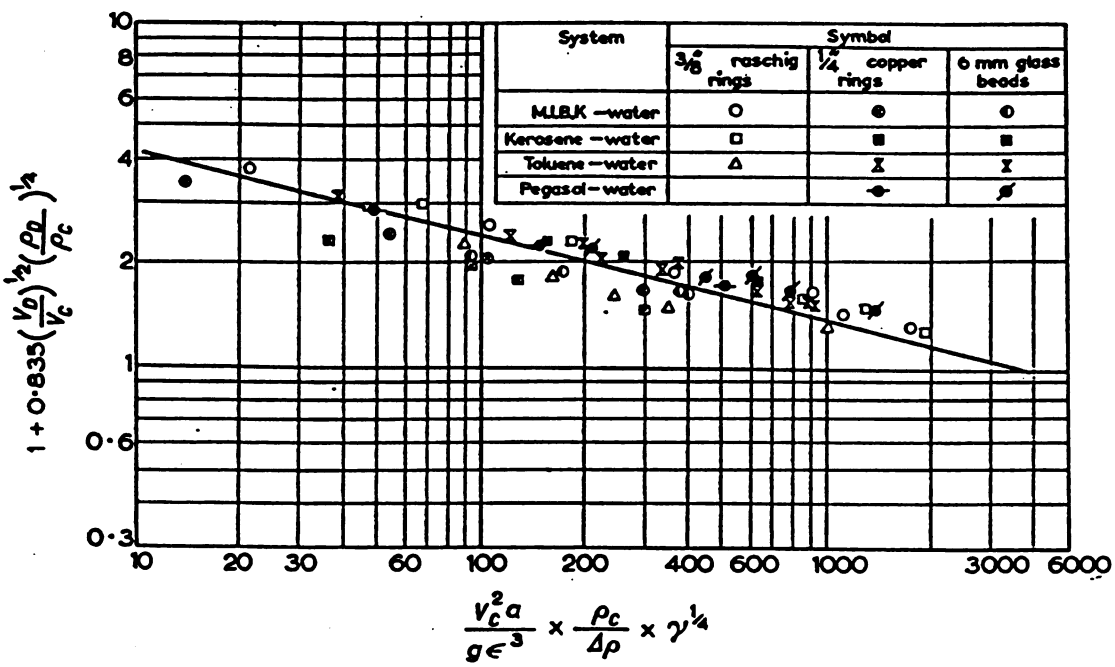

Figure 3-3. Flooding Correlation of Dell and Pratt

The solvent physical properties and packing parameters for any system under consideration are generally known. For a known continuous phase superficial velocity, V_C, the expression on the right-hand side of the expression can be calculated. Locating this value on the curve and reading the value for the left-hand expression and setting it equal to the left-hand expression allows a value for the dispersed phase superficial velocity, V_D, to be calculated. This dispersed phase velocity will result in a flooding condition in the column when combined with the previously specified continuous phase velocity.

3. Venkataraman and Laddha (Venkataraman, 1960) correlation:

$$\left[1+0.835\left(\frac{\rho_D}{\rho_C}\right)^{0.25}\left(\frac{V_D}{V_C}\right)^{0.5}\right]\left[\left(\frac{V_C^2 a_p}{g\varepsilon^3}\right)\left(\frac{\rho_C}{\Delta\rho}\right)\right]^{0.25} = C\left(\frac{a_p \varepsilon \gamma}{\rho_C V_C^2}\right)^n \qquad 3\text{-}4$$

where

	a_p	Surface area of packing (ft^2/ft^3)
	g	Gravitational acceleration, ft/hr^2
	V_C	Continuous phase superficial velocity (ft/hr)
	V_D	Distributed phase superficial velocity (ft/hr)
	ε	Void fraction of packing, dimensionless
	ρ_C	Density of the continuous phase, (lb/ft^3)
	ρ_D	Density of the discontinuous phase, (lb/ft^3)
	$\Delta\rho$	Density difference between phases (lb/ft^3)
	γ	Interfacial tension (lb/hr)
	C	Curve-fit parameter
	n	Curve-fit parameter

Table 3-1. Curve-Fit Parameters for the Correlation of Rao and Rao

Type of Packing	C	n	Average Deviation %
Raschig rings	0.894	-0.078	7.6
Berl saddles	0.882	-0.052	8.8
Lessing rings	0.853	-0.046	3.7
Spheres	0.839	-0.029	5.0

The parameters C and n were obtained by the method of least squares for the packings given in Table 3-1.

The parameter n varies significantly with packing type. The authors found that after a statistical analysis of their experimental data and those reported by others, with all the types and sizes of packing, different tower diameters, and different liquid systems taken into account, the values of C and n as a general correlation are found to be 0.812 and negative 0.048 respectively. With these values of C and n the average deviation of all the points is 12.6%, and the maximum deviations are +32% and -29% from those predicted by the correlation. The accuracy for the specific values of C and n for a particular packing are significantly better than those for the general correlation.

These three correlations were selected for review primarily because their scope encompassed the range of variables encountered in this study (i.e. packing size, surface tension, and density). All three of these correlations claim to predict flooding in packed columns with the qualification that the operating velocity should be approximately one half the flooding velocity.

Inter

pack

inter

easil

emul

can c

value

is no

corre

transf

calcu

again

solute

liquid

The T

estima

King

pressu

σ

where

Interfacial Tension

The interfacial tension between the two liquid phases affects the operation of a packed column by determining the size of the dispersed phase droplets. If the interfacial tension is very low, tiny droplets will be formed which will not separate easily from the continuous phase. If the interfacial tension is sufficiently low, an emulsion of the dispersed phase could be formed. High values of interfacial tension can cause difficulty in dispersing one phase in the other while. On the other hand, high values of interfacial tension promote coalescence of the dispersed phase for separation.

That interfacial tension is important in liquid extraction is rather obvious. What is not obvious is how to calculate interfacial tension values for use in the above correlations for column capacity or to estimate the interfacial surface area for mass transfer calculations. The interfacial tension between the two liquid phases cannot be calculated as the difference between the individual phase surface tensions measured against air. Since the interfacial tension is strongly dependent on the concentration of solute present in a ternary system, values of the surface tension for a variety of binary liquid systems reported in the literature can provide only useful approximations at best. The Treybal correlation for interfacial tension shown in Figure 3-4 is useful for estimating interfacial tension in the absence of pure component, binary data.

Another useful method for estimating interfacial tension is that of Massoudi and King (1974). For pure water with various gases the interfacial tension as a function of pressure is given by:

$$\sigma = \sigma_o + BP + CP^2 + DP^3 \qquad 3\text{-}5$$

where σ_0 is the interfacial tension of water with the gas at atmospheric pressure.

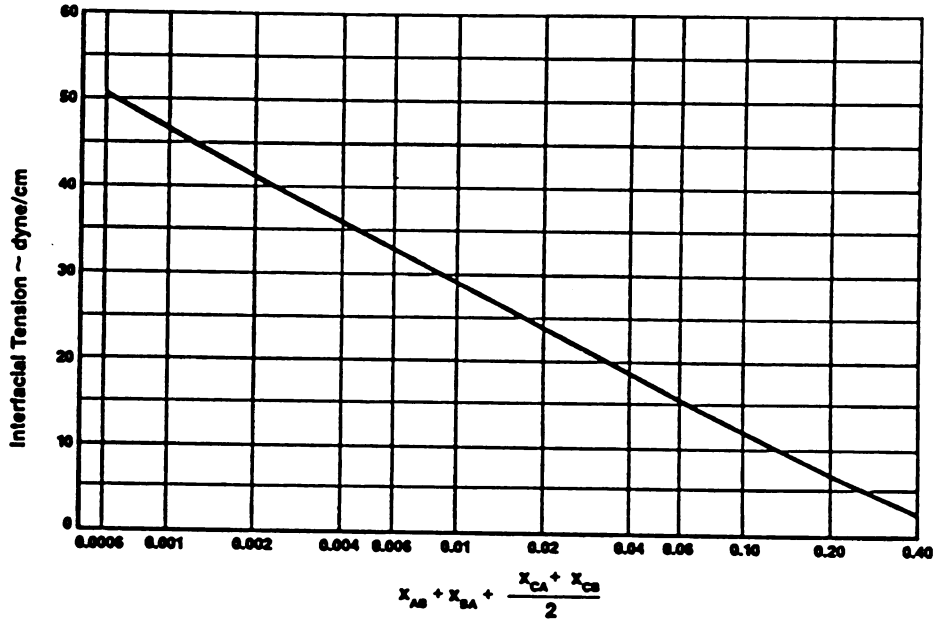

where x_{AB} is the mole fraction of solvent A dissolved in solvent B,

x_{BA} is the mole fraction of solvent B dissolved in solvent A,

x_{CA} is the mole fraction of solute C dissolved in solvent A, and

x_{CB} is the mole fraction of solute C dissolved in solvent B.

Figure 3-4. Treybal Interfacial Tension

Va

exp

Pa

con

giv

pac

sec

for

Values for the coefficients determined by fitting the polynomial equation to experimental data are given in Table 3-2.

Packing

Packing performs four important functions in continuous extractors:

1. Increases the flow path length for the dispersed phase. This increases the contact time between the phases producing a greater amount of solute transfer. For a given steady state flow rate, the relationship between increased path length and packing void volume is the holdup;

2. Maintains a uniform distribution of flow of both phases across the entire cross section of the column;

3. Distorts the dispersed phase droplets which increases the surface area available for mass transfer and also causes mixing within the droplet again increasing mass

Table 3-2. Interfacial Tension for Pure Water with Various Gases

Gas	B dyn/cm atm	C dyn/cm atm^2	D dyn/cm atm^3
O_2	-0.0779	0.000104	
N_2	-0.0835	0.000194	
Ar	-0.0840	0.000194	
CO	-0.1041	0.000239	
CH_4	-0.1547	0.000456	
C_2H_4	-0.6353	0.003160	
C_2H_6	-0.4376	-0.001570	
C_3H_8	-0.9681	-0.0589	
N_2O	-0.6231	0.00287	-0.000040
CO_2	-0.7789	0.00543	-0.000042

tran

the

pac

the

for

for

pac

pac

cap

Be

are

are

ch

pa

th

(C

transfer. This droplet distortion also occurs as continuous coalescence and breakup of the drops (Coulson and Richardson, 1978);

4. Prevents back mixing of the phases.

The role of packing in liquid-liquid extraction is somewhat different than for packing in gas-liquid contacting (distillation or absorption). In gas-liquid contacting, the liquid must wet the packing so as to provide the maximum possible interfacial area for mass transfer. In liquid-liquid extraction however, interfacial area occurs in the form of dispersed phase droplets and it is undesirable for the dispersed phase to wet the packing since this generally results in the dispersed phase running in rivulets down the packing if it is the more dense phase or an increase in holdup and decreased column capacity if the dispersed phase is the less dense phase.

Packings for liquid-liquid extraction are almost exclusively randomly packed. Berl saddles, Rashig rings, Pall rings, Intalox saddles, and Lessing rings, among others, are used. A wide variety of materials of construction for these manufactured packings are used including different metals, ceramics and polymers.

Packing size selection should follow two guidelines:

1. The packing should not be larger than 1/8 times the column diameter to avoid channeling and to reduce dispersed phase contacting at the wall. For this research, the packing selected was 1/8 inch, perforated-316 SS squares;

2. The minimum packing size should be such that the mean void height is not less than the mean drop diameter. This critical packing size for a pair of liquids is given by (Gayler, Roberts, and Pratt, 1953):

$$d_{crit} = 2.42\left[\frac{\sigma}{\Delta\rho g}\right]^{0.5} \qquad 3\text{-}6$$

where σ interfacial surface tension, M/T^2

$\Delta\rho$ density difference between the two phases, M/L^3

g acceleration due to gravity, L/T^2

Extractor Internals

Although the most common manner of operating an extractor is with the light phase dispersed, the following discussion of the extractor internals assumes that the light phase is the continuous phase since this is the desirable method for this project. Nevertheless, the description of the internals applies to the dispersion of either phase. (If the light phase is the dispersed phase, then the following equipment item descriptions will be valid if they are exchanged end-for-end in the column where appropriate.)

At the top of the column it is necessary to disperse the heavy phase. For small columns, an arrangement of nozzles utilizing the discharge pressure of the feed pump is used to introduce dispersed phase streams through orifices typically 0.125-0.25 inches in diameter. For this research, the feed nozzle orifice diameter was 1/32 inches. The exact diameter is chosen to cause the formation of small droplets with the intent of maximizing the interfacial surface area for mass transfer. For larger columns, a disperser plate is used. In this case, a sparger is used to fill the disperser plate with the heavy phase. The difference in density between the two phases causes the heavy phase to fall through downcomers in the plate arranged to distribute the heavy phase as uniformly as possible across the cross section of the column. The less dense continuous phase rises up to the bottom of the disperser plate and passes through holes arranged uniformly across the cross section of the plate.

The light phase is introduced into the side of the column near the bottom through a standard side fitting. The distance of the light phase injection point from the

bot

bot

usu

the

bot

pha

int

Ex

sol

the

Kn

for

ind

Usu

cor

con

the

colu

stag

sett

extr

num

colle

bottom is sufficient to allow room for the separation of the two phases in the very bottom of the column.

At the bottom of the bed it is necessary to separate the two phases. This is usually done by a flow control valve which regulates the flow of the heavy phase out the bottom of the column while maintaining a small level of the heavy phase in the bottom of the column. This small level of the heavy phase insures that none of the light phase escapes out the bottom opening. The control valve is adjusted to maintain the interface between the two phases at the desired level.

Extraction Column Sizing

As previously discussed, flooding curves have been developed correlating the solvent physical properties and physical characteristics of the column and packing to the maximum phase velocities which result in a flooding condition in the column. Knowledge of the flooding velocities is used to calculate the required column diameter for a given throughput. This is done by adjusting the column diameter to give the individual phase velocities which correspond to 50% of the flooding velocities. Usually, it is necessary to build a pilot scale column and run it to determine which correlation(s) fit the data or to generate a flooding curve unique to the system under consideration. The second criteria required for the sizing of an extraction column is the column's height. Several methods used to predict the height of an extraction column are described below.

1. One way to calculate column height is to estimate the number of theoretical stages (NTS) required for a given separation. Each stage can be viewed as a mixer/ settler in which the two phases are well contacted and then separated cleanly into extract and raffinate streams. Material balances can be done for each stage and the number of theoretical stages calculated. The NTS can be determined from data collected from a pilot column giving a measurable separation with a known height of

packing. The Height Equivalent of a Theoretical Stage (HETS) is the height of the packing for the experimental column divided by the NTS required for the separation. This procedure can be done graphically by plotting the ratio of the solvent flows as a line on rectangular plot of the raffinate composition (abscissa) versus the extract composition (ordinate). This line is called the operating line. The number of equilibrium stages is determined by connecting the operating line with the equilibrium curve for the system by a series of steps as shown in Figure 3-5.

2. A second method for determining the height of an extraction column is to view the solute concentration in each phase as changing differentially with height. This method is based on the diffusion of solutes across a thin film at the interface separating the two bulk phases. The value for the number of transfer units (NTU) when multiplied by the height of a transfer unit, HTU, gives the height of the tower:

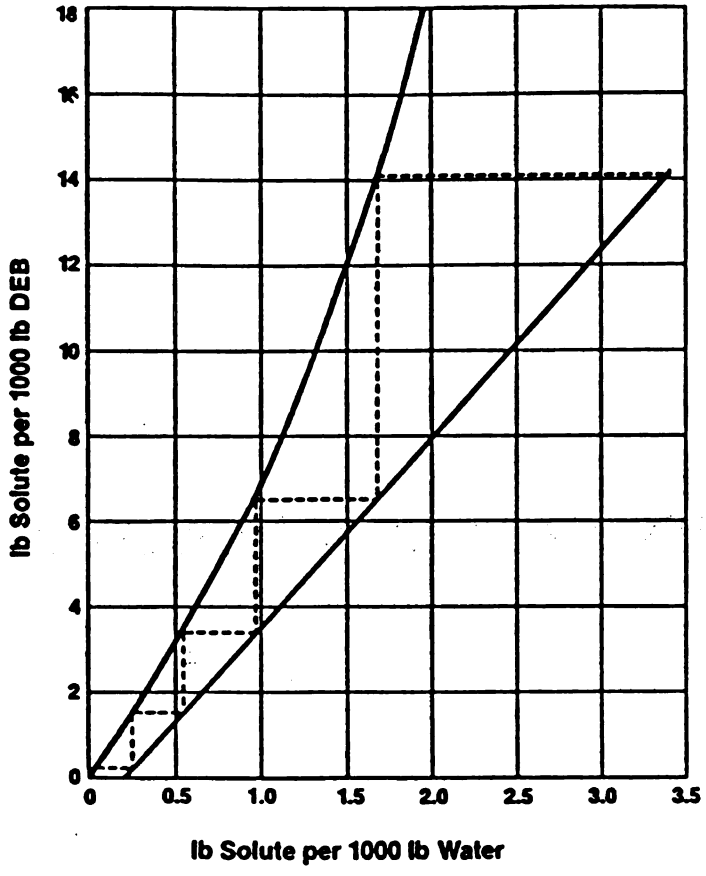

Figure 3-5. Graphical Representation of Extraction Column Stages

$$H = NTU \times HTU \qquad 3\text{-}7$$

3. A third method for calculating the column height for the special case when the two solvents are mutually insoluble and the distribution coefficient is independent of concentration relies on the extraction factor, U, first described by Kremser (1930). The extraction factor is related to the number of theoretical stages required for a specified separation and to the column height. Whereas the previous two methods rely on experimental column testing, the Kremser extraction factor method does not and can be used as a predictive method.

Each of the three methods is described in detail below.

Determination of the Number of Transfer Stages (NTS)

The concept of the number of transfer stages required for a given extraction may be visualized by considering the development of a graphical method for determining the number of transfer stages required for a series of discrete mixing and separating vessels. These vessels are arranged for countercurrent contacting utilizing two completely immiscible solvents. The conditions for this type of flow can be represented as shown in Figure 3-6. Each circle represents a mixer and a separator. The initial solution F of the solute B dissolved in solvent A is fed to the first unit and leaves as raffinate R_1. This stream passes through the units and leaves from the nth unit as stream R_n. Fresh solvent enters the nth unit and passes in the reverse direction through the units, leaving as extract E_1. Since the two solvents are immiscible, the original solvent in the raffinate streams remains constant at A units and the added fresh solvent in the extract streams also remains constant at S units.

Material balances for the solute can be written in several ways. For the first stage as:

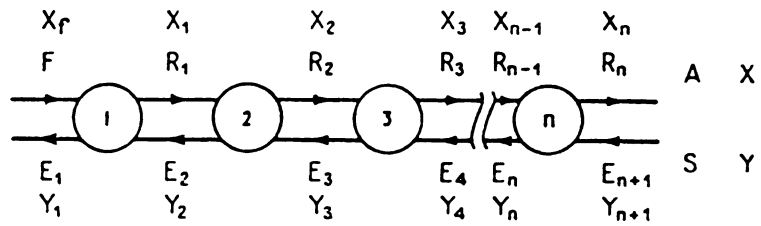

Figure 3-6. Countercurrent, Stagewise Extraction Schematic

$$AX_f + SY_2 = AX_1 + SY_1 \qquad 3\text{-}8$$

where solute concentrations in the raffinate and extract streams, X and Y, are expressed as mass units per unit of solvent. Material balances for the solute for the nth stage can be expressed as:

$$AX_{n-1} + SY_{n+1} = AX_n + SY_n \qquad 3\text{-}9$$

And for the whole unit as:

$$AX_f + SY_{n+1} = AX_n + SY_1 \qquad 3\text{-}10$$

$$Y_{n+1} = \frac{A}{S}(X_n - X_f) + Y_1 \qquad 3\text{-}11$$

Equation 3-11 is in the form of an equation for a straight line of slope A/S. It is known as the operating line and is shown in Figure 3-5. It is seen to pass through the points (X_f, Y_1) and (X_n, Y_{n+1}). Also drawn in Figure 3-5 is the equilibrium relation Y_n versus X_n. The number of stages required to pass from X_f to X_n is found by drawing in steps between the operating line and the equilibrium line; in Figure 3-5 four stages are required and (X_n, Y_{n+1}) corresponds to (X_4, Y_5). It should be noted that the operating line connects the compositions of the raffinate stream leaving each unit and the solvent stream entering each unit.

This graphical development of the number of stages required for an extraction is frequently used to estimate the number of stages required for a continuous extraction because of its ease of use. In most cases, the data necessary to generate the equilibrium curve can be generated in the laboratory. Consider the following example (Treybal, 1951):

> An aqueous process effluent contains 3.4 lb of a valuable organic compound per 1,000 lb of water. Since the organic material has a boiling point only slightly higher than water, an extraction of this organic appears to be the least expensive method for recovery of the solute. This organic is highly soluble in aromatic solvents that are almost immiscible in water. Therefore, p-diethyl benzene (DEB) will be used as the solvent. Tests of mixtures prepared in the laboratory give the distribution coefficients shown in Table 3-3.
>
> The data from Table 3-3 can easily be used to construct an equilibrium diagram on rectangular coordinates as in Figure 3-5. To recover 95% of the solute would give a concentration of 0.17 lb of solute

Table 3-3. Equilibrium Data

Solute in Water lb/1,000 lb	Solute in DEB lb/1,000 lb	m
2.1	21.1	10.05
1.7	14.2	8.35
1.2	8.7	7.25
0.7	4.3	6.14
0.2	1.2	6.00

per 1,000 lb of water in the raffinate. Assuming the DEB is solute free means that the concentration at the bottom of the extractor can be established. This concentration will lie on the X-axis of the diagram.

Since DEB and water are almost immiscible and the amount of solute transferred is small compared to the total mass flow rates of the solvents, the operating line of this column will be essentially a straight line. Next, the slope of the operating line can be fixed by choosing the DEB flow rate so as to avoid a pinch against the equilibrium curve. Further, since a packed column has been selected, the DEB flow rate will be selected so that no more than five theoretical stages of mass transfer are required. The equilibrium stages are stepped off and are shown as the dashed line in Figure 3-5. For this extraction, 4.3 theoretical stages are necessary for 95% recovery.

Deter

can be

liquid

drivin

diffus

the ph

1924)

conce

solute

extrac

the si

condit

Determination of the Number of Film Transfer Units

The transfer of solute in liquid-liquid extraction in a continuous packed column can be explained by applying the two-film theory of diffusion. For the two immiscible liquids in contact, there will exist concentration gradients in both phases which act as driving forces for the transfer of solute from one phase to the other. The resistance to diffusion can be represented by an effective film thickness near the interface between the phases. Assuming that equilibrium is established at the interface, (Whitman, p 147, 1924) the transfer of solute on the raffinate side of the interface is driven by the concentration difference $C_R - C_{Ri}$ where the subscript i refers to the concentration of solute that exists at the interface between the two phases. The transfer of solute on the extract side is driven by the concentration difference $C_{Ei} - C_E$. Figure 3-7 represents the situation just described (Coulson and Richardson, 1968). Under steady-state conditions, the rate of transfer of solute through the extract phase equals the rate of

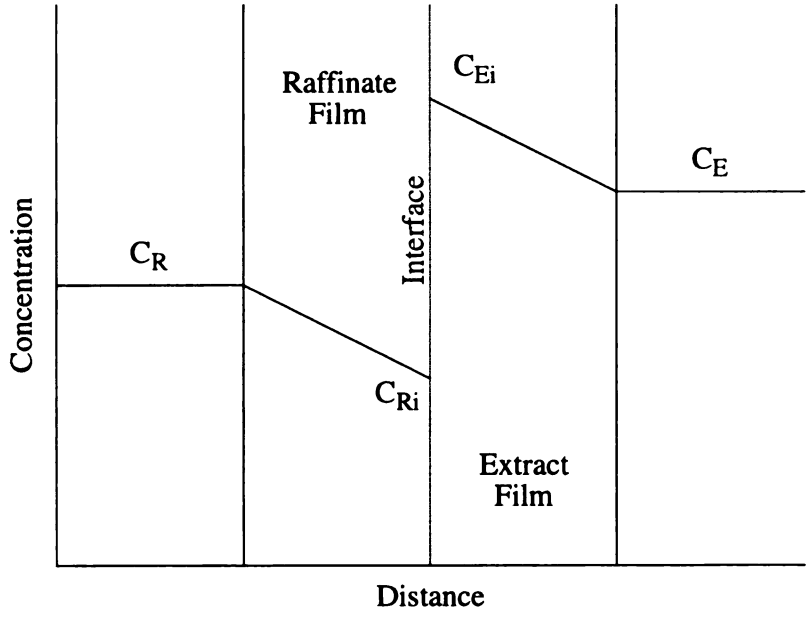

Figure 3-7. Concentration Profile Near a Liquid-Liquid Interface

transfer

express

$N =$

where

transfer,

dN

or

dN

transfer through the raffinate phase. The rate of transfer across these films, N, can be expressed in the following way:

$$N = k_R S (C_R - C_{Ri}) = k_E S (C_{Ei} - C_E) \qquad 3\text{-}12$$

where C_R, C_E are the concentrations of solute in the raffinate and extract phases, $gmol/cm^3$

C_{Ri}, C_{Ei} are the concentrations of solute in the raffinate and extract at the interface between the phases, $gmol/cm^3$

k_R, k_E are the transfer coefficients for raffinate and extract films, $\frac{gmol}{sec \cdot cm^2 \cdot gmol/cm^3}$

S cross-sectional area perpendicular to the direction of mass transfer, cm^2

N rate of mass transfer, $gmol/sec$

For continuous extraction, it is useful to consider the differential rate of mass transfer, dN, which will occur through a differential area, dS (Treybal, 1951). Then:

$$dN = k_R dS (C_R - C_{Ri}) = k_E dS (C_{Ei} - C_E) \qquad 3\text{-}13$$

or

$$dN = k_R dS \Delta C_R = k_E dS \Delta C_E \qquad 3\text{-}14$$

point

equilil

3-8.

contin

$d($

where

At ste

theory

Treyba

averag

dN

where

The equilibrium distribution curve will contain the point (C_{Ei}, C_{Ri}) and the point represented by the main body concentrations (C_E,C_R) will be below the equilibrium curve (Treybal, 1951, p 119). These concentrations are shown in Figure 3-8.

A solute balance over the differential height dH for the extraction with continuous countercurrent contact shown in Figure 3-9 (Treybal, 1951, p 242) is:

$$d(Rx_R) = d(Ex_E) \qquad 3\text{-}15$$

where R is the raffinate phase flow rate, gmol/sec

E is the extract phase flow rate, gmol/sec

x_R is the solute mole fraction in the raffinate

x_E is the solute mole fraction in the extract

At steady state, the solute from the raffinate was previously described by the two-film theory to be transferred across the interface between the two phases (Equation 3-13). Treybal (1951, p 242) defines the average solute concentration, C_{RM} gmol/sec, as the average of the values of C_R and C_{Ri}. Substitution into Equation 3-13 yields:

$$dN = k_R dS C_{RM} (x_R - x_{Ri}) \qquad 3\text{-}16$$

where x_R is the mole fraction of solute in the raffinate

x_{Ri} is the mole fraction of solute in the raffinate interfacial film

$C_{RM} = \dfrac{(C_R - C_{Ri})}{2}$ where C_R refers to the total concentration of all substances present.

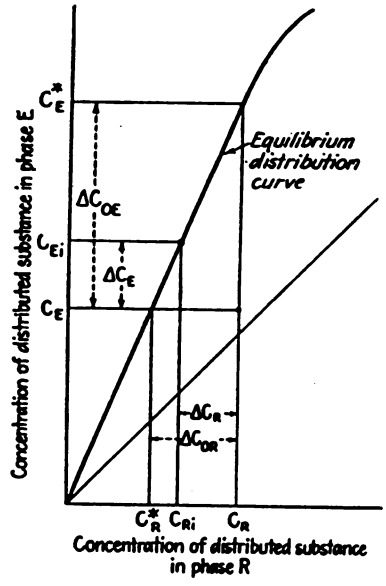

Figure 3-8. Over-all and Individual Film Driving Forces

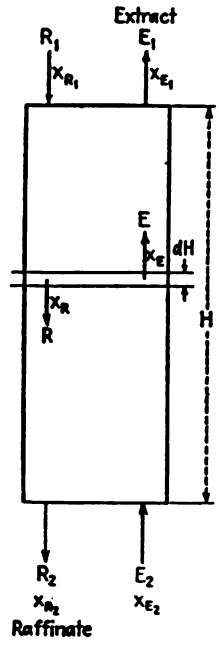

Figure 3-9. Extraction with Continuous Countercurrent Contact

Combining Equations 3-15 and 3-16 for the raffinate phase:

$$dN = d(Rx_R) = k_R dS C_{RM} (x_R - x_{Ri}) \qquad 3\text{-}17$$

Use of this equation is limited to cases where the solvents are completely immiscible or to dilute solutions since the diffusion upon which Equation 3-13 is based includes only that of the solute and not the solvents.

The total raffinate R varies from one end of the tower to the other but the solute-free raffinate, $R(1 - x_R)$, remains constant. Consequently,

$$d(Rx_R) = R(1 - x_R) d\left(\frac{x_R}{1 - x_R}\right) = \frac{R dx_R}{1 - x_R} \qquad 3\text{-}18$$

The mass transfer coefficient k_R includes a term $(1 - x_R)_{iM}$ which varies throughout the tower. The quantity $k_R (1 - x_R)_{iM}$ is more likely to be constant (Treybal, 1951, p 243). Because it is difficult to quantify the interfacial area for mass transfer, S cm^2, it is convenient to define the interfacial area per unit of tower volume, a cm^2/cm^3, so that $dS = aA dH$ where A is the tower cross-sectional area and H is the tower height. The interfacial transfer area, a, is usually combined with the film-transfer coefficient k_R or k_E and treated as one entity being either $k_R a$ or $k_E a$. Incorporating these terms in Equation 3-17 yields:

$$\frac{(1 - x_R)_{iM} R dx_R}{(1 - x_R)} = k_R a (1 - x_R)_{iM} A C_{RM} (x_R - x_{Ri}) dH \qquad 3\text{-}19$$

wher

1951

chan

chan

integ

this i

phase

HTU

N

migh

N

$$\frac{(1-x_R)_{iM}\,dx_R}{(1-x_R)\,(x_R-x_{Ri})} = \frac{k_R a\,(1-x_R)_{iM} AC_{RM}\,dH}{R} \qquad 3\text{-}20$$

where $(1-x_R)_{iM} = \dfrac{(1-x_{Ri})-(1-x_R)}{\ln\left[(1-x_{Ri})/(1-x_R)\right]}$

A tower cross-sectional area, cm^2

Since the terms $(1-x_R)_{iM}$ and $(1-x_R)$ are usually nearly unity (Treybal, 1951, p 243), the left-hand portion of Equation 3-20 is essentially the concentration change dx_R experienced per unit of concentration difference $(x_R - x_{Ri})$ causing the change and represents a measure of the difficulty of the extraction. When solved by integrating over the change in concentration from the bottom of the tower to the top, this is designated as the number of transfer units based on mass transfer in the raffinate phase, NTU_R. When the NTU_R's is multiplied by the experimentally determined factor HTU, the height of a transfer unit, the result is the height of the tower, H:

$$NTU_R = \int_{x_{R_2}}^{x_{R_1}} \frac{(1-x_R)_{iM}\,dx_R}{(1-x_R)\,(x_R-x_{Ri})} = \int_0^H \frac{dH}{HTU_R} = \frac{H}{HTU_R} \qquad 3\text{-}21$$

In similar fashion, the concentration differences in terms of the extract phase might have been used which would have resulted in:

$$NTU_E = \int_{x_{E_2}}^{x_{E_1}} \frac{(1-x_E)_{iM}\,dx_E}{(1-x_E)\,(x_E-x_{Ei})} = \int_0^H \frac{dH}{HTU_E} = \frac{H}{HTU_E} \qquad 3\text{-}22$$

Height of a Film Transfer Unit

Consideration of the right-hand side of Equation 3-20 and Equation 3-21 shows that HTU_R and the mass transfer coefficient are related:

$$HTU_R = \frac{R}{k_R a (1 - x_R)_{iM} A C_{R_{av}}} \qquad 3\text{-}23$$

where $C_{R_{av}} = \frac{(C_{RM_1} - C_{RM_2})}{2}$. The subscripts 1 and 2 refer to the concentrations of all substances present at the raffinate (feed) inlet and outlet respectively.

In similar fashion, the height of a transfer unit, HTU_E, based on the concentration difference between the bulk extract and the extract interfacial concentration is:

$$HTU_E = \frac{E}{k_E a (1 - x_E)_{iM} A C_{E_{av}}} \qquad 3\text{-}24$$

Number of Overall Film Transfer Units

In most practical situations, it is impossible to determine the interfacial concentrations accurately. Therefore, true film driving forces, ΔC_R and ΔC_E (Equation 3-14), can not be obtained. If the equilibrium-distribution curve is a straight line so that at all concentrations encountered C_{Ei} is proportional to C_{Ri} then:

$$C_{Ei} = mC_{Ri} \qquad 3\text{-}25$$

where m is the distribution coefficient (slope of the equilibrium line) expressed in the same units as the concentrations.

extr

Sim

If th

n

mann

N

where

and

N

Further, a concentration C_E^* can be defined as the concentration of solute in the extract that would be in equilibrium with C_R:

$$C_E^* = mC_R \qquad 3\text{-}26$$

Similarly C_R^* is defined as a concentration in equilibrium with C_E:

$$C_E = mC_R^* \qquad 3\text{-}27$$

If the solute concentrations are expressed in mole fractions, then:

$$m = \frac{x_{Ei}}{x_{Ri}} = \frac{x_E^*}{x_R} = \frac{x_E}{x_R^*} \qquad 3\text{-}28$$

The complete mass-transfer process in both phases can now be represented in a manner analogous to Equation 3-13 and Equation 3-16:

$$N = K_E a\,(C_E^* - C_E) = K_E a \Delta C_{OE} \qquad 3\text{-}29$$

where K_E is an over-all mass transfer coefficient based on an over-all concentration gradient in the extract phase.

and

$$N = K_R a\,(C_R - C_R^*) = K_R a \Delta C_{OR} \qquad 3\text{-}30$$

wher

are (

whe

relat

base

where K_R is an over-all mass transfer coefficient based on an over-all concentration gradient in the raffinate phase.

The number of film transfer units based on the over-all concentration gradients are (Treybal, 1951):

$$NTU_{OR} = \int_{x_{R_2}}^{x_{R_1}} \frac{(1-x_R)_{OM}\, dx_R}{(1-x_R)\,(x-x_R^*)} \qquad 3\text{-}31$$

$$= \int_{x_{R_2}}^{x_{R_1}} \frac{dx_R}{(1-x_R)\ln\left[\dfrac{(1-x_R^*)}{(1-x_R)}\right]} = \frac{H}{HTU_{OR}}$$

where $$(1-x_R)_{OM} = \frac{(1-x_R^*)-(1-x_R)}{\ln\left[(1-x_R^*)/(1-x_R)\right]}$$

The height of a transfer unit based on the over-all concentration gradient is related to the over-all mass transfer coefficient:

$$HTU_{OR} = \frac{R}{K_R a\,(1-x_R)_{OM} C_{R_{av}} A} \qquad 3\text{-}32$$

The equations for the number of transfer units and the height of a transfer unit based on the over-all concentration gradient in the extract phase are:

$$NTU_{OE} = \int_{x_{E_2}}^{x_{E_1}} \frac{(1-x_E)_{OM}\, dx_E}{(1-x_E)\,(x-x_E^*)} \qquad 3\text{-}33$$

$$= \int_{x_{E_2}}^{x_{E_1}} \frac{dx_E}{(1-x_E)\ln\left[\dfrac{(1-x_E^*)}{(1-x_E)}\right]} = \frac{H}{HTU_{OE}}$$

$$HTU_{OE} = \frac{R}{K_E a\,(1-x_R)_{OM} C_{E_{av}} A} \qquad 3\text{-}34$$

In cases where the principal resistance to diffusion lies in the raffinate phase (m large), Equation 3-31 is used for the extraction column design. In cases where the principal resistance is in the extract phase (m small), Equation 3-33 is used for the design. To evaluate NTU_{OR} either the quantity $\dfrac{(1-x_R)_{OM}}{(1-x_R)\,(x-x_R^*)}$ or $\dfrac{1}{(1-x_R)\ln\left[\dfrac{(1-x_R^*)}{(1-x_R)}\right]}$ is calculated and plotted against x_R. The area under the resulting curve between the limits x_{R_1} and x_{R_2} is the required value.

It should be kept in mind that, in general, the mass-transfer coefficients depend on complex functions of diffusivity, viscosity, density, interfacial tension, and turbulence. Similarly, the mass-transfer area of the droplets depends on complex functions of viscosity, interfacial tension, density difference, extractor geometry, agitation intensity, agitator design, flow rates, and interfacial rag deposits. Only limited success has been achieved in correlating extractor performance with these basic

princ

Simp

aver

than

Sub

sub

the

Sub

principles (Perry and Green, Eds., 1984).

Simplified Integration

If $(1 - x_R^*)$ and $(1 - x_R)$ differ by no more than a factor of two, an arithmetic average rather than a logarithmic average for $(1 - x_R)_{OM}$ incurs an error of no more than 1.5% (Wiegand, p 679, 1940). Thus,

$$(1 - x_R)_{OM} = \frac{(1 - x_R^*) + (1 - x_R)}{2} \qquad 3\text{-}35$$

Substitution into Equation 3-31 leads to:

$$NTU_{OR} = \int_{x_{R_2}}^{x_{R_1}} \frac{dx_R}{(x - x_R^*)} + \frac{1}{2} \ln \frac{1 - x_{R_2}}{1 - x_{R_1}} \qquad 3\text{-}36$$

For dilute solutions, $(1 - x_R)$ and $(1 - x_E)$ are nearly unity and R and E are substantially constant (Treybal, 1950). A material balance over the lower portion of the tower in Figure 3-9 (p 3-48) then becomes approximately:

$$R\,(x_R - x_{R_2}) = E\,(x_E - x_{E_2}) \qquad 3\text{-}37$$

Substitution of $m x_R^*$ for x_E and rearrangement leads to:

$$x_R^* = \frac{R}{mE}(x_R - x_{R_2}) + \frac{x_{E_2}}{m} \qquad 3\text{-}38$$

This ma

(Treyba

$$x_{R_1}$$

$$\int$$

$$x_{R_2}$$

In a si

$$x_E$$

$$\int$$

$$x_I$$

Extr

extr

fact

the

wh

fe

co

This may be substituted into the integral of Equation 3-36 and the integral evaluated (Treybal, 1950, p 246):

$$\int_{x_{R_2}}^{x_{R_1}} \frac{dx_R}{(x_R - x_R^*)} = \frac{1}{1 - \frac{R}{mE}} \ln \left[\left(1 - \frac{R}{mE}\right) \left(\frac{x_{R_1} - \frac{x_{E_2}}{m}}{x_{R_2} - \frac{x_{E_2}}{m}} \right) + \frac{R}{mE} \right] \qquad 3\text{-}39$$

In a similar manner,

$$\int_{x_{E_2}}^{x_{E_1}} \frac{dx_E}{(x_E^* - x_E)} = \frac{1}{1 - \frac{mE}{R}} \ln \left[\left(1 - \frac{mE}{R}\right) \left(\frac{x_{E_1} - m x_{R_2}}{x_{E_2} - m x_{R_2}} \right) + \frac{mE}{R} \right] \qquad 3\text{-}40$$

Extraction Factor

A predictive method for determining the number of stages required for an extraction tower was developed by Kremser (1930). Kremser defined the *extraction factor,* U, as the slope of the equilibrium line (distribution coefficient), m, divided by the slope of the operating line, R/E:

$$U = m\left(\frac{E}{R}\right) \qquad 3\text{-}41$$

where E is the fresh solvent rate to the column and R is the rate of solvent flow in the feed. Both E and R must be expressed in the same units used for expressing the solute concentrations in the distribution coefficient.

The height of the extraction column, H, and the number of theoretical stages, n,

can

(Co

and

whe

and

are

sol

inc

can be calculated using one of the Kremser equations, Equation 3-43 or Equation 3-44 (Coulson, 1968):

$$H = \frac{x_0 - x_n}{x_0 - \frac{y_{n+1}}{m}} = \frac{U^{n+1} - U}{U^{n+1} - 1} \qquad 3\text{-}42$$

and

$$n = \frac{\log\left[\frac{1}{1-H}\left(1 - \frac{1}{U}\right) + \frac{1}{U}\right]}{\log U} \qquad 3\text{-}43$$

where x_0 mole fraction of solute in the feed

x_n mole fraction of solute in the raffinate leaving stage n

y_{y+1} mole fraction of solute in the extract

In order to apply the Kremser formulae, the equilibrium line must be straight and its intercept zero, and the operating line must also be straight. These restrictions are met when the two solvents selected for the process are mutually insoluble and the solute concentrations are dilute enough so that the distribution coefficient is independent of concentration, respectively.

sepa
com
limi
be s
carb
wate
spec
low
diox
phas

at e
to th
m, f

r

the c
the d
as th
of s
conc

CHAPTER 4

BENZALDEHYDE DISTRIBUTION COEFFICIENT MEASUREMENT

In liquid-liquid extractions, at least one component in the original mixture to be separated must have a higher selectivity in the extraction solvent than the other components. The two solvents should be mutually immiscible or exhibit only a very limited mutual solubility. However, the transferred component, or solute, which is to be separated is soluble in both liquid phases. For the ternary system benzaldehyde/ carbon dioxide/water the solute, benzaldehyde, is soluble in both carbon dioxide and water. If the solute has a different solubility in each of the solvents at the conditions specified then a partitioning of the solute will occur. Since the two solvents exhibit a low mutual solubility at temperatures and pressures near the critical point of carbon dioxide, a two phase mixture will exist with a different concentration of solute in each phase.

There exists a definite concentration relationship between the two liquid phases at equilibrium. The ratio of the concentration of benzaldehyde in carbon dioxide x_E to the concentration of benzaldehyde in water x_R is called the distribution coefficient, m, for this temperature:

$$m = \frac{x_E}{x_R} \qquad 4\text{-}1$$

Solubility in a normal liquid increases with increasing temperature; however, the change in solubility with temperature may not be the same in both solvents. Thus, the distribution coefficient for a solute between two solvents may increase or decrease as the temperature rises. The distribution coefficient also depends on the total amount of solute present in a given amount of both solvents. As shown in Figure 4-1, the concentration of solute in the extract phase can be plotted against the concentration of

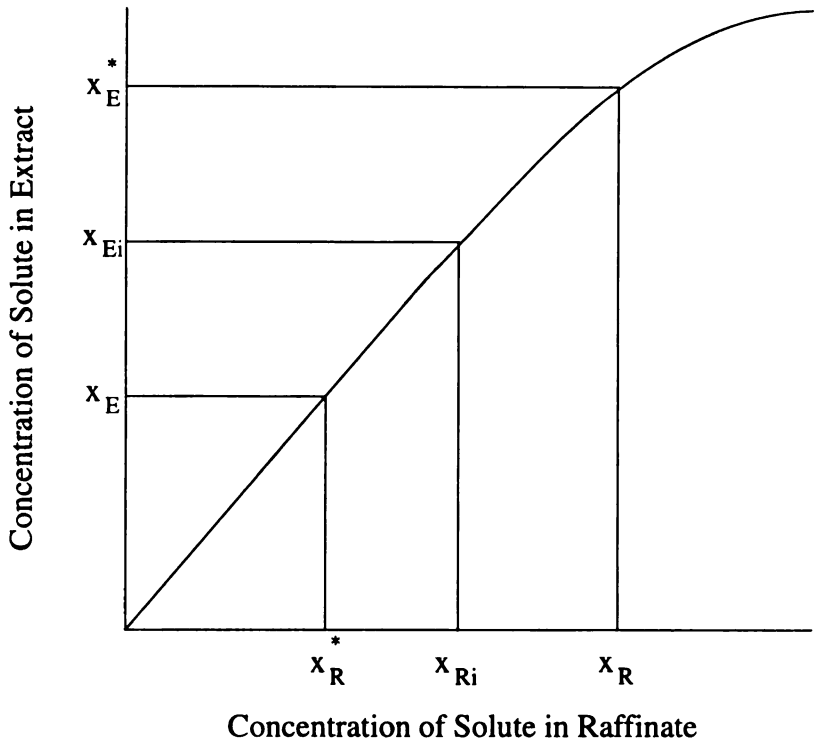

Figure 4-1. Equilibrium Relationship

solute in the raffinate phase. The resulting line is the equilibrium line and its slope is represented by the distribution coefficient, m. At low solute concentrations the slope of the equilibrium curve is essentially constant and, hence, the distribution coefficient is constant.

Prediction of Distribution

In the discussion that follows, B is considered the extracting solvent for removing a distributed substance C from A-C solutions. Provided that the same standard state is chosen for each substance, the activities of the substance in each phase at equilibrium are equal (Treybal, 1951):

$$a_{CA} = a_{CB} \qquad a_{AA} = a_{AB} \qquad a_{BA} = a_{BB} \tag{4-2}$$

where subscript CA refers to the activity of solute C in the C-A binary

subscript CB refers to the activity of solute C in the C-B binary

and so on.

From the definition of the activity coefficient:

$$a_{CA} = \gamma_{CA} x_{CA} \qquad a_{CB} = \gamma_{CB} x_{CB} \qquad a_{AA} = \gamma_{AA} x_{AA} \qquad \text{etc.} \qquad 4\text{-}3$$

where γ_{CA} is the activity coefficient of C in the C-A binary and γ_{CB} is the activity of C in the C-B binary.

Substituting the appropriate expressions from Equation 4-3 into Equation 4-2 and rearranging provides an alternate definition for the distribution coefficient:

$$m = \frac{\gamma_{CA}}{\gamma_{CB}} \qquad 4\text{-}4$$

This relationship between the distribution coefficient and the activity coefficients is useful for predicting values of the distribution coefficient from literature values for activity coefficients and vapor-liquid equilibrium data as well as from integrated forms of the Gibbs-Duhem equation such as the Margules and van Laar equations.

Activity constants for binary systems can be estimated fairly accurately with the van Laar equations (Perry, 5th ed., p 13-9):

$$\ln \gamma_1 = \frac{A_{12}}{\left[1 + \frac{A_{12} x_1}{A_{21} x_2}\right]^2} \qquad 4\text{-}5$$

and

$$\ln \gamma_2 = \frac{A_{21}}{\left[1 + \frac{A_{21}x_2}{A_{12}x_1}\right]^2} \qquad 4\text{-}6$$

These two-suffix equations have been extended to cover the ternary systems such as those found in liquid-liquid extraction (Wohl, 1946):

$$\log\gamma_A = \frac{x_B^2 A_{AB}\left(\frac{A_{BA}}{A_{AB}}\right)^2 + x_C^2 A_{AC}\left(\frac{A_{CA}}{A_{AC}}\right)^2 + x_B x_C\left(\frac{A_{BA}}{A_{AB}}\right)\left(\frac{A_{CA}}{A_{AC}}\right)\left[A_{AB} + A_{AC} - A_{CB}\left(\frac{A_{AC}}{A_{CA}}\right)\right]}{\left[x_A + x_B\left(\frac{A_{BA}}{A_{AB}}\right) + x_C\left(\frac{A_{CA}}{A_{AC}}\right)\right]^2} \qquad 4\text{-}7$$

The expression for $\log\gamma_B$ can be obtained by substituting subscripts B for A, C for B, and A for C throughout the equation. Thus in the equation for $\log\gamma_B$, x_B in Equation 4-8 is changed to x_C, A_{AB} to A_{BC}, A_{AC} to A_{BA}, etc. Similarly, in that for $\log\gamma_C$, x_C in Equation 4-8 is changed to x_B, A_{BA} to A_{AC}, etc. Wohl has shown that these equations are limited to those cases where:

$$\frac{A_{CB}}{A_{BC}} = \left(\frac{A_{CA}}{A_{AC}}\right)\left(\frac{A_{AB}}{A_{BA}}\right) \qquad 4\text{-}8$$

In the absence of published values for the van Laar constants, reasonable estimates for them can be made using mutual solubility data following the procedure of Treybal (1951, p 60).

Unfortunately, values for the van Laar or Margules constants for the binaries benzaldehyde-water, benzaldehyde-carbon dioxide, and carbon dioxide-water could not be found in the literature. Mutual solubility data was unavailable as well. Therefore, it was undertaken to experimentally determine the value of the distribution

coefficient for benzaldehyde in the carbon dioxide-water system.

Equipment Design

The process equipment for the measurement of the benzaldehyde distribution coefficient consists of three sections: the pumping or feed section, the equilibrating section, and the sampling section. The equipment schematic for the entire process is shown in Figure 4-2.

In the feed section the carbon dioxide and aqueous feed containing benzaldehyde were metered into the phase separating cell. A 50 pound cylinder equipped with a drop tube was used as the source of liquefied carbon dioxide. The carbon dioxide was passed through a 1/4" FPT check valve to prevent contamination of the cylinder and a 1/4" FPT, 1 micron filter to prevent contaminants from fouling the downstream metering pump. The check valve and filter were supplied by Forberg Scientific with part numbers 4F-C4L-1/3-SF and 4F-F4L-1-SS respectively. The carbon dioxide was then passed through a 3.5' long piece of 1/8" stainless steel tubing shaped into a coil approximately 3" in diameter. The coil was placed in an ice water bath to lower the vapor pressure of the carbon dioxide to prevent cavitation at the pump inlet. The 1/8" coil was connected as closely as possible to the suction side of one head of a LCD Analytical duplex pump model 2396 having a capacity of 49 to 920 ml/hr. The pump flow rate was controlled by a micrometer type adjustment on each head. For the aqueous feed, a 1 liter glass flask with an outlet tangential to the bottom was placed on top of a Mettler PM 4600 Deltrange weigh scale with a capacity of 4 kg. A short piece of flexible plastic tubing connected the feed flask to a length of 1/8" stainless steel tubing fastened to the second head of the duplex pump to allow accurate weighing of the feed on a continuous basis. The outlets of both pump heads were connected to 1/16" stainless steel tubing joined together by a cross (not shown in Figure 4-2). The third port of the cross (again, not shown in Figure 4-2) was connected to a High

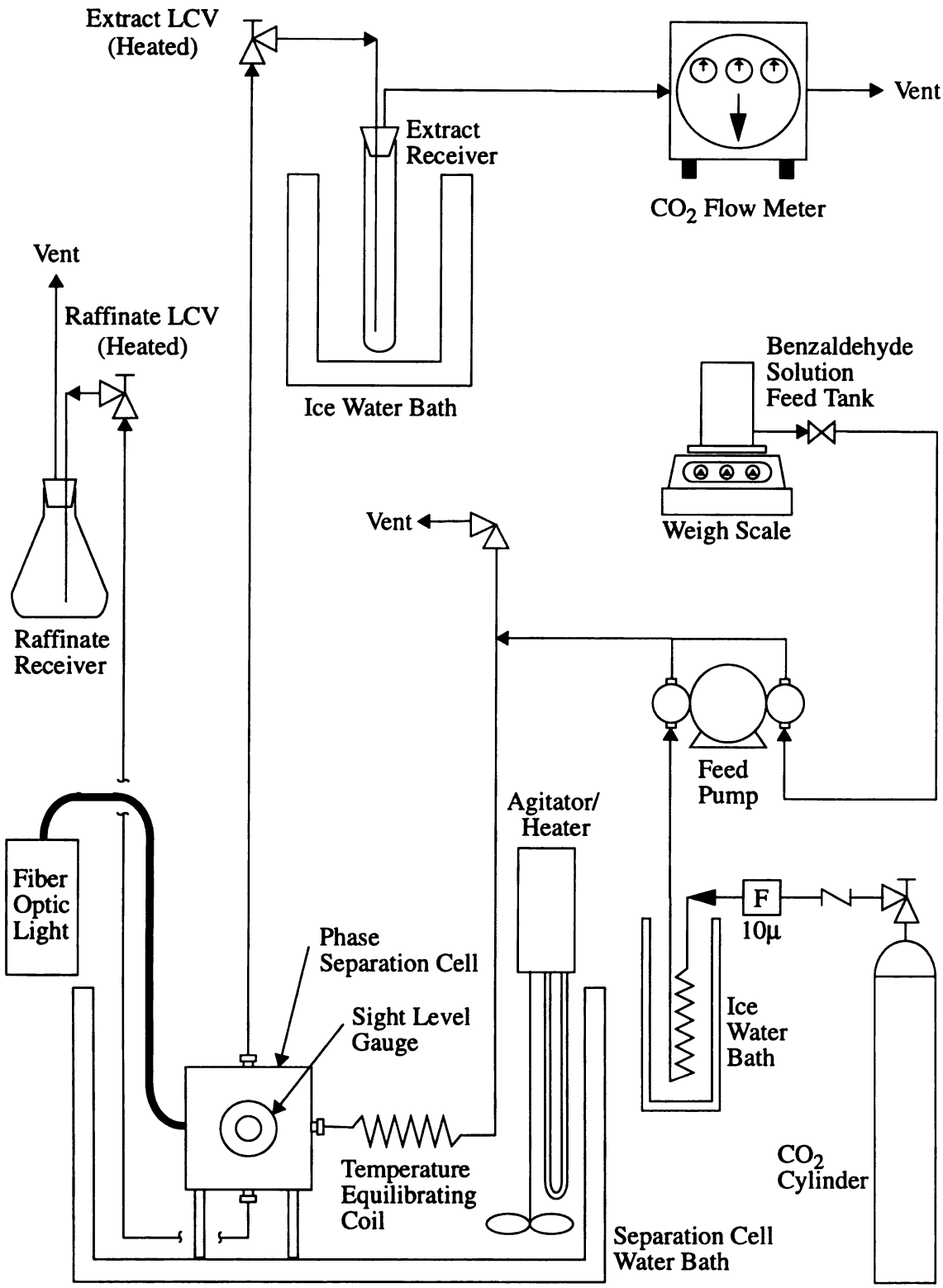

Figure 4-2. Benzaldehyde Distribution Coefficient Measurement Schematic

Pressure Equipment Company rupture disk housing model 15-63AF1 containing an OSECO, Inc. 1/4A, standard, 316 stainless steel frangible with a burst pressure of 3,000 psig at 72 °F.

The equilibrium section of the distribution coefficient measurement equipment begins with the fourth port of the above cross connected to a short length of 1/16" SS tubing. This leads to a 20' length of 1/8" SS tubing coiled to fit on the bottom of a 24"L x 18"W x 16"H fiberglass water bath. The 1/8" coil served as an equilibrating chamber for both temperature and mass transfer. Water temperature in the bath was maintained by an Isotemp Immersion Circulator model 730 from Fisher Scientific Company. The equilibrating coil is connected to a separating cell rated for 5,000 psig made by the Michigan State University machine shop. The internal volume was measured to be 65 ml by taring the empty cell on a balance, filling it with room temperature water and reweighing it to determine the weight of water added. The separating cell has a side port for introduction of the two-phase feed mixture, a bottom port for discharge of the aqueous phase and a top port for discharge of the carbon dioxide phase. In addition, two 1/2" diameter sight glasses were part of the separating cell. One was located on the side and was used to introduce light into the cell via a fiber optic cable that could be immersed in water without harm. The other sight glass served as a sight level gauge so that the interface between the two phases could be controlled at a point roughly in the middle of the cell. The fiber optic light was a model 9745-00 from Cole-Parmer Instrument Company.

The sampling section consisted of a short length of 1/8" tubing running from the bottom port of the separating cell, out of the water bath and terminating in a 1/8" SS flow control valve series 10VRMM2812 manufactured by Autoclave Engineers. This two-way angle valve has a micrometering valve stem with a C_v of 0.004 and an orifice diameter of 0.062". The valve was heated to prevent freezing caused by the sudden decrease in solubility and rapid expansion of the carbon dioxide dissolved in the water

resulting from the pressure drop across the valve. The heater was made by sandwiching the valve body between two 3/4" thick aluminum blocks roughly cut to the same height and width as the valve. The top of each block was drilled with a hole of the correct diameter and depth to allow the insertion of a Vulcan Electric Company T. B. cartridge heater. The two cartridges were electrically wired in parallel and one was inserted into each block. The wires connecting the cartridges terminated in a standard 120V two-prong plug inserted into a Staco Energy Products Company model 3PN1010 variable transformer. The discharge of the raffinate (water phase) valve was connected to 1/8" SS tubing inserted into the opening of a 500 ml Erlenmeyer flask which served as the raffinate receiver. The inlet tubing extended through the top opening to about half the depth of the flask. The top port of the separating cell was connected to a 1/8" SS tubing tee. One of the two remaining ports of the tee was connected to a Heise model 901A digital electronic pressure gauge with a range of 0-10,000 psig and the other to the inlet side of a 1/8" Autoclave Engineers micrometering valve identical to the raffinate valve. It was fitted with a cartridge heater of the same design as described above. The discharge of the heated extract valve (carbon dioxide phase) was connected to 1/8" SS tubing inserted into a rubber stopper fitted into the opening of the extract receiver. The extract receiver was a 20 mm O.D. x 14" L glass tube with a 7 mm glass side arm vent extending radially from the side and positioned 2" from the top. The 1/8" SS tubing from the separating cell extended through the stopper to within approximately 1/2 " of the bottom of the test tube. The test tube was filled with approximately 75 ml of dehydrated, 200-proof ethanol to trap the benzaldehyde as it emerged from the end of the drop line carried by the carbon dioxide. The ethanol trap was immersed in an ice water bath to lower the temperature of the ethanol to minimize evaporation losses. Plastic tubing connected the side arm vent to a Precision Scientific Wet Test Meter model number 63126 to measure the flow of carbon dioxide. The wet test meter was filled with Amoco 5-NF light weight mineral oil instead of water to reduce error caused

by the solubility of carbon dioxide in the water normally used in the meter.

Experimental Procedure

1. The aqueous feed mixture was prepared by mixing weighed quantities of benzaldehyde and water in a 1 liter glass flask with a side arm outlet port located so as to be flush with the bottom of the flask to allow complete drainage. The clean, dry flask was tared on a Mettler PM 4600 Deltarange balance having a maximum capacity of 4 kg. To this was added approximately 500 ml of room temperature, reverse osmosis purified water and the weight recorded. Approximately 1 gram of reagent grade benzaldehyde from Aldrich was pipetted into the 1 liter flask and the weight recorded. A magnetic stirrer was added, the flask stoppered and the mixture stirred for 12-18 hours at room temperature. All of the feed mixtures had concentrations of 2000 ± 200 ppm benzaldehyde.

2. After the aqueous phase was finished mixing, the water bath circulating pump and temperature controller were turned on and allowed to reach steady state. The carbon dioxide and the extract trap ice baths were filled with ice and water and allowed to cool. The discharge valve heaters were also turned on to a low setting and allowed to heat up.

3. While waiting for the various temperature controlled devices to reach steady state, the feed mixture was analyzed to verify the concentration of benzaldehyde present. The gas chromatographic method is described fully in Appendix B. The benzaldehyde concentrations varied markedly from the prepared concentrations. The consistent decrease in concentration was thought to be due to the reaction of benzaldehyde and oxygen to form benzoic acid. Two or three injections of the feed mixture were made and the average of the analyses used for the actual feed concentration.

4. The aqueous phase 1 liter flask was placed on the weigh scale, the weight

recorded and the plastic tubing between the flask and the metering pump was connected taking care to eliminate any entrapped air.

5. The carbon dioxide flow meter reading was noted and recorded.

6. After checking the raffinate and extract discharge valves to be sure that both were closed, the micrometer adjustments on both heads of the feed pump were adjusted to give roughly equivalent flows of each phase and the carbon dioxide cylinder valve was opened. It is important to note that the carbon dioxide phase began to rapidly fill the separation cell as soon as the cylinder valve was opened since the pressure in the cell was atmospheric pressure versus the 838 psig equilibrium vapor pressure of the carbon dioxide in the room temperature cylinder. However, the small volume of the separating cell reached equilibrium with the cylinder pressure very quickly.

7. The feed pump was started allowing both the aqueous and carbon dioxide phases to flow into the separating cell.

8. The feed into the cell was allowed to continue uninterrupted until either the pressure reached 1500 ± 100 psig or the water level reached the midpoint of the sight level glass. If the pressure reached the desired value first, the extract valve was opened very slowly to control the pressure in the desired range. When the aqueous phase level reached the middle of the sight glass, the raffinate valve was slowly opened to maintain the level as closely as possible to that point. If the aqueous phase level reached the middle of the sight glass first, the raffinate valve was opened and then when the pressure reached the desired setpoint the extract valve was opened.

9. The flow of each phase was continued for approximately two hours. This corresponded to 6-8 turnovers of the cell contents of each phase. After this number of turnovers it was assumed that a steady state for mass transfer had been reached. Both the extract and raffinate receivers were changed over to clean, empty ones and the experiment continued as before.

10. After another 1.5-2 hours the experiment was terminated by shutting off the

feed metering pump and closing both the raffinate and extract valves as quickly as possible. Samples of both the raffinate and extract were taken and prepared for analysis.

11. The carbon dioxide cylinder valve was closed.

12. The raffinate valve was opened slightly and the remainder of the aqueous phase allowed to collect in the raffinate receiver. As soon as all of the raffinate was drained from the cell, the raffinate valve was closed carefully to avoid damaging the valve stem.

13. The extract valve was opened to allow the remainder of the carbon dioxide to bubble through the ethanol trap.

14. The final weight of the aqueous feed flask was noted and recorded. A sample of the final feed mixture was taken and prepared for analysis. The flask was disconnected from the feed pump and the unused feed discarded.

15. Shutdown of the experiment was completed by emptying the ice baths, shutting off the valve heaters, and shutting off the water bath circulating pump and heater.

Results and Discussion

A summary of the experimental results found in this investigation are shown in Table 4-1 shown on the following pages. Runs 1-3 can be neglected because the analytical method used to determine the concentration of benzaldehyde in water was found to have an unacceptable level of error which resulted in unreliable mass balance calculations. After run 3 the analytical techniques used to determine benzaldehyde in both water and the ethanol solutions were changed to the internal standard methods described in Appendix B. In addition, material balance calculations after run 3 used an average value for the benzaldehyde concentration in the aqueous feed. This was done because the benzaldehyde concentration in the aqueous feed decreased significantly with time due to oxidation. To complicate things further, the low solubility of benzaldehyde in water made it difficult to determine when a feed mixture had achieved

Table 4-1. Distribution Coefficient Measurement Data

Run Number	Run Time, minutes	Feed Conc., ppm Benz.	Benz. Recovery, %	Water Recovery,%	Distribution Coefficient[1]
1	108	3170	69.8	-	15.0
2	108	3626	66.5	96.7	15.8
3	184	3650	62.6	101.8	12.6
4	165	1854	83.9	97.3	11.7
5*	150	1878	96.0	102.4	19.2
6	180	1908	96.3	100.3	11.9
7	185	1868	90.0	99.0	14.9
8	151	1947	90.0	102.0	7.2
9	154	1869	99.4	100.9	9.4
10	150	1917	91.0	96.2	12.2
11	150	1883	94.0	94.7	11.2
12	406	1837	97.6	102.8	16.7
13	242	1716	97.7	100.2	26.2
14*	250	1757	83.0	100.0	19.2
15	272	1932	95.9	100.7	21.5
16	240	1982	96.6	100.3	20.5
17	243	2149	92.3	101.9	19.0
18	191	2630	93.2	100.3	30.2
19	197	1911	94.1	100.0	23.9
20	226	1924	90.1	100.0	20.0
21	253	1952	91.3	99.6	21.6
22	255	2052	98.8	99.4	21.1
23	241	2019	93.1	99.3	21.3
24	242	2080	99.5	99.9	28.2
25	240	2025	96.0	97.6	28.3

1 Weight Distribution Coefficient
* Ethyl Acetate solute

Table 4-1. (Continued)

Run Number	Distribution Coefficient[2]	Temperature °C	CO_2/Water gm/gm	Feed Rate gm/min	Water Turnovers
1	36.7	30	.712	3.606	
2	38.3	"	.678	3.770	
3	30.9	"	.974	1.831	
4	28.7	"	.477	3.322	
5*	47.0	"	.602	3.557	
6	29.1	"	1.232	3.108	
7	36.4	"	1.186	2.956	
8	17.5	24	1.386	3.277	
9	23.0	37	1.267	3.190	
10	29.7	"	1.285	3.147	
11	27.3	25	1.029	2.891	
12	40.9	"	.897	.952	
13	64.0	"	1.082	2.834	5.79
14*	46.8	35	1.319	3.136	6.22
15	52.7	"	.991	2.716	5.52
16	50.2	"	1.015	1.858	4.82
17	46.5	"	.951	4.073	3.40
18	73.8	"	1.016	4.763	7.21
19	58.3	"	.787	4.413	10.0
20	49.1	"	.662	4.026	10.7
21	52.9	"	1.241	4.413	8.35
22	51.5	"	1.165	3.865	8.54
23	52.0	"	.897	3.408	7.40
24	68.9	20	1.508	4.507	7.52
25	69.2	21	1.406	4.440	8.14

2 Molar Distribution Coefficient
* Ethyl Acetate solute

equilibrium and the benzaldehyde was completely dissolved. In order to minimize these two problems, a sample of the feed was taken at the beginning and end of each run and the average of the two analysis used in the mass balance calculations and, therefore, to determine the percentage of benzaldehyde recovery shown in Table 4-1.

Run 5 differed from the previous runs in a very important respect. The solute was changed from benzaldehyde to ethyl acetate so that a calibration of the experimental apparatus and method could be made. For the liquid carbon dioxide extraction of ethyl acetate from water at room temperature and 918 psig Schultz (1970) reported a distribution coefficient of 42. Although the conditions used for run 5 were different at 30 °C and 2,000 psi the experimentally determined value of 47 agreed well with Schultz's value.

Given the fairly good agreement of the experimentally determined distribution coefficient with the literature value, the experiments to determine the benzaldehyde distribution coefficient were continued as before. Runs 6 and 7 were conducted under identical conditions but produced a distribution coefficients of 29.1 and 36.4 respectively. Although this was not unusually bad agreement, it was decided that the two values should be reproducible to at least within ten percent and preferably within five percent. Experiments 9 and 10 were run at identical conditions as were experiments 11 and 12. The only difference between these two pairs of experiments was that they were run at 37 °C and 25 °C respectively. Again, the deviation between the distribution coefficients for each of these pairs was found to be greater than the acceptable upper limit of ten percent.

After reviewing the experimental procedure it was concluded that the run times were too short to allow equilibrium to be reached. The method was modified to change both the raffinate and extract receivers after an amount equal to 7-10 cell volumes for each phase had been pumped through the separating cell. It was felt that after this approximate volume of material had been pumped through the cell that the mass

transfer would be at equilibrium and, perhaps more importantly, the cell contents of each phase would be of a uniform composition equal to the equilibrium concentration.

Run 14 used the modified method but again used ethyl acetate as the solute. The distribution coefficient was determined to be 47, again showing the good agreement with the literature value of 42 as before.

Runs 15-18 were conducted at the same conditions except for the total feed rate of the combined aqueous feed and carbon dioxide. The combined flows were varied to determine if there was a corresponding change in the distribution coefficient. It was felt that if the system was at equilibrium an increase or decrease in total flow rate to the separating cell should not have resulted in a change in the distribution coefficient. However, changing the total flow into the cell did result in an unacceptable change in the distribution coefficient.

Prior to run 21 it was decided that the lack of mixing in the separating cell was still the problem causing the lack of a reproducible distribution coefficient. A small agitator was finally built that was not only small enough to fit in the separating cell but that would not get "hung up" and stop spinning. A 1/32" hole was drilled through the teflon coating of a small magnetic stirring bar. A piece of wire in the shape of a "t" was inserted into the hole in the stirring bar so the top of the tee would be near the top of the separating cell and would contact only the top (carbon dioxide) phase. A water proof magnetic stirrer was immersed in the water bath and the separating cell placed on top of it. The speed of rotation was kept at approximately 40-60 rpm. At these low speeds the stirring bar itself caused agitation in the bottom (aqueous) phase and the cross bar of the t-shaped wire caused agitation in the top phase with only a slight upset of the interface between the two phases. Thus, each phase of the cell was now well mixed and the two phases separated cleanly.

Runs 21-23 were run at identical conditions and were the first series of three consecutive runs to produce essentially the same value for the distribution coefficient

at 52.9, 51.5, and 52.0 respectively. The maximum deviation between them is 2.7%.

The temperature for runs 24 and 25 was decreased from 35 °C to 20 °C (room temperature) and the same conditions as for runs 21-23 were repeated. The runs gave virtually identical values of 68.9 and 69.2 respectively.

The work to determine the distribution coefficient was terminated at the end of run 25. It was decided that the value of the distribution coefficient for benzaldehyde in the benzaldehyde/carbon dioxide/water ternary was 52 at 35 °C and 69 at 20 °C. For subsequent work using these values of the distribution coefficient it was assumed that these distribution coefficients would remain constant in the benzaldehyde concentration range of 0-2,000 ppm.

CHAPTER 5

BENZALDEHYDE EXTRACTION EQUIPMENT DESIGN

The benzaldehyde extraction equipment description is divided into three segments; the pumping or feed section, the extraction column, and the receiver section. Schematic drawings for each section are shown in Figures 5-1, 5-2, and 5-3 respectively. A flow schematic for the entire process is shown in Figure 5-4.

Feed Section (Figure 5-1)

In this section the aqueous feed and the carbon dioxide solvent are introduced into the system. A 20 liter Nalgene tank served as the aqueous feed vessel. It was equipped with a Lightnin Mixing Company Labmaster TSM 2510 agitator for mixing the benzaldehyde/water feed solution. The bottom outlet of the feed tank was connected to the inlets of both heads of a LDC Analytical model 2396 metering pump. The LDC 2396 is capable of delivering 49-920 ml/hr against a maximum discharge pressure of 6,000 psig. Separate micrometer-type adjusters control the delivery of each head independently. The discharge nozzles of each head were joined together by a 1/16" tubing cross. The third port of the cross was connected to a High Pressure Equipment Company model 15-63AF1 rupture disk housing. An OSECO, Inc. 1/4A, standard, 316 SS rupture disk with a burst pressure rating of 3,000 psig at 72 °F was installed in the rupture disk housing to protect the apparatus from exceeding its maximum pressure rating. The fourth port was connected to the top feed port isolating valve on the extraction column.

Carbon dioxide was supplied to the system from a 50 pound cylinder equipped with a siphon tube. From the cylinder valve the carbon dioxide flowed through a check valve (part number 4F-C4L-1/3-SS) to prevent backflow into the cylinder and a 1 micron filter (part number 4F-F4L-1-SS) to remove small particulates from the line to

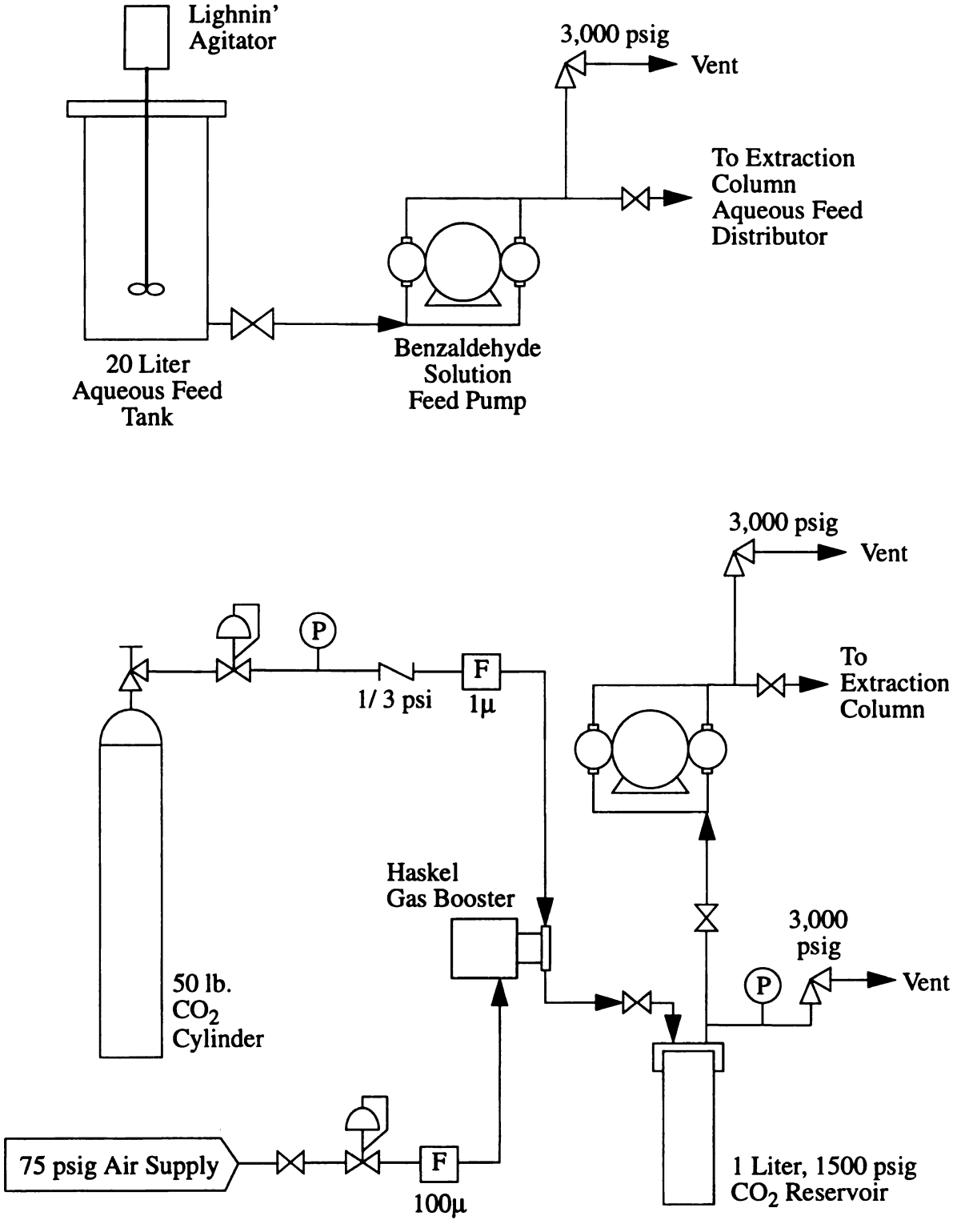

Figure 5-1. Benzaldehyde Extraction Column Feed Section Schematic

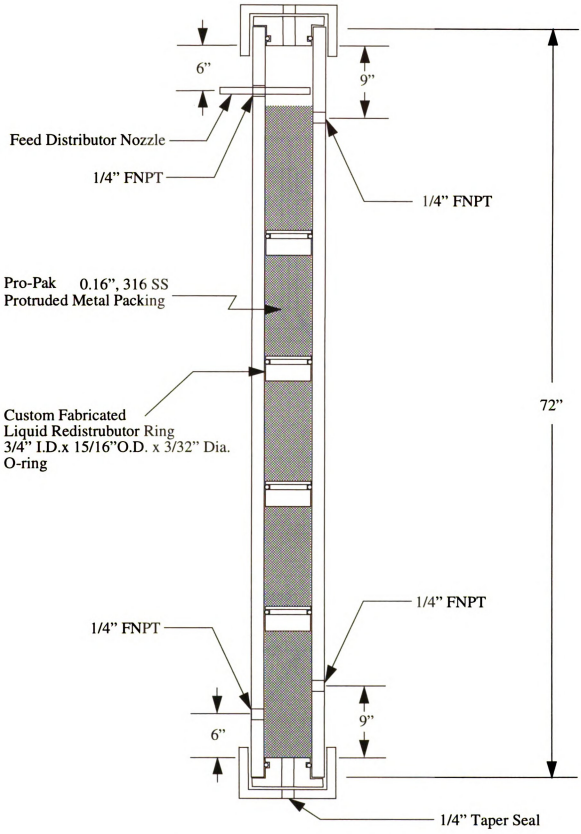

Figure 5-2. Extraction Column Detail

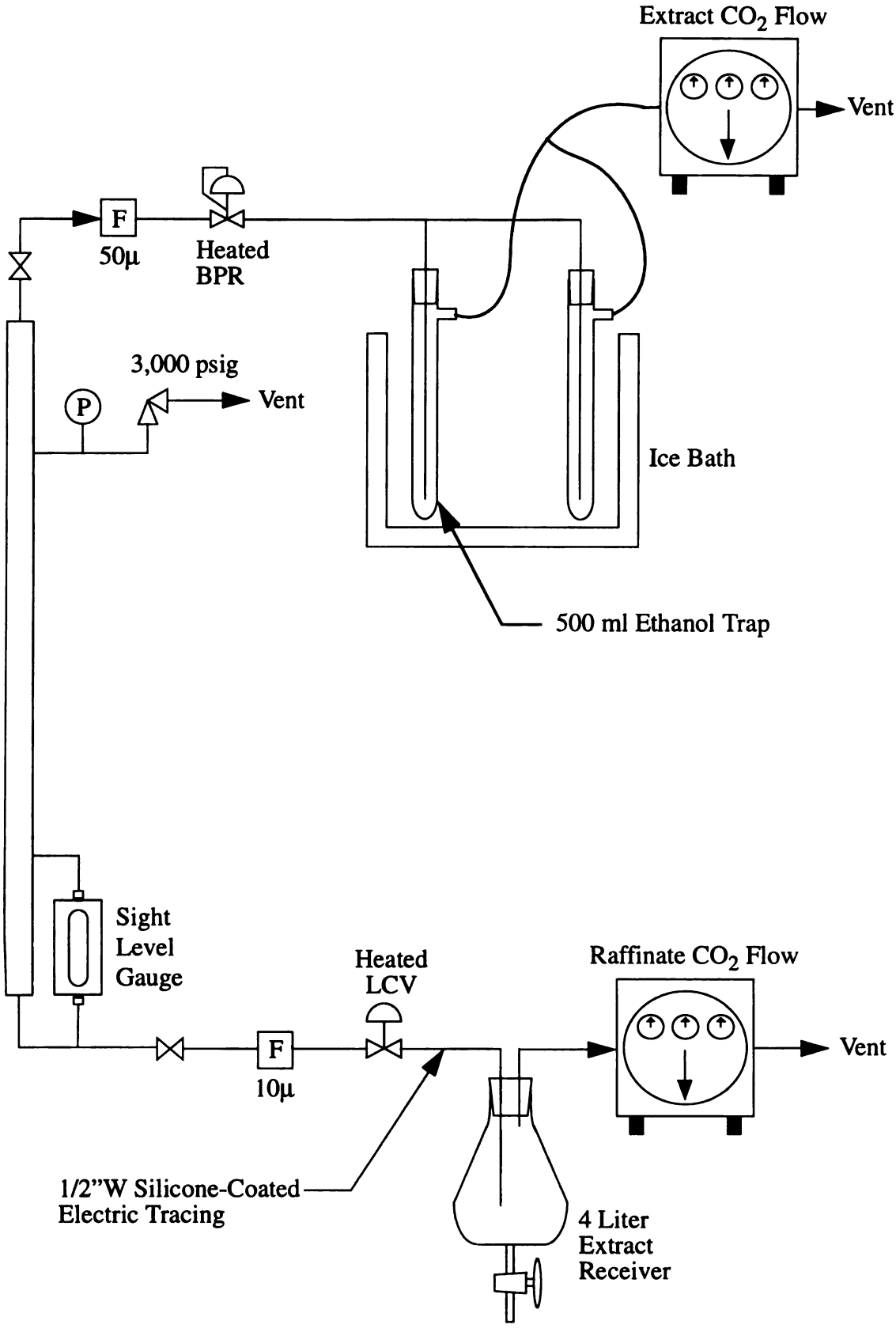

Figure 5-3. Extraction Column Receiver Section Detail

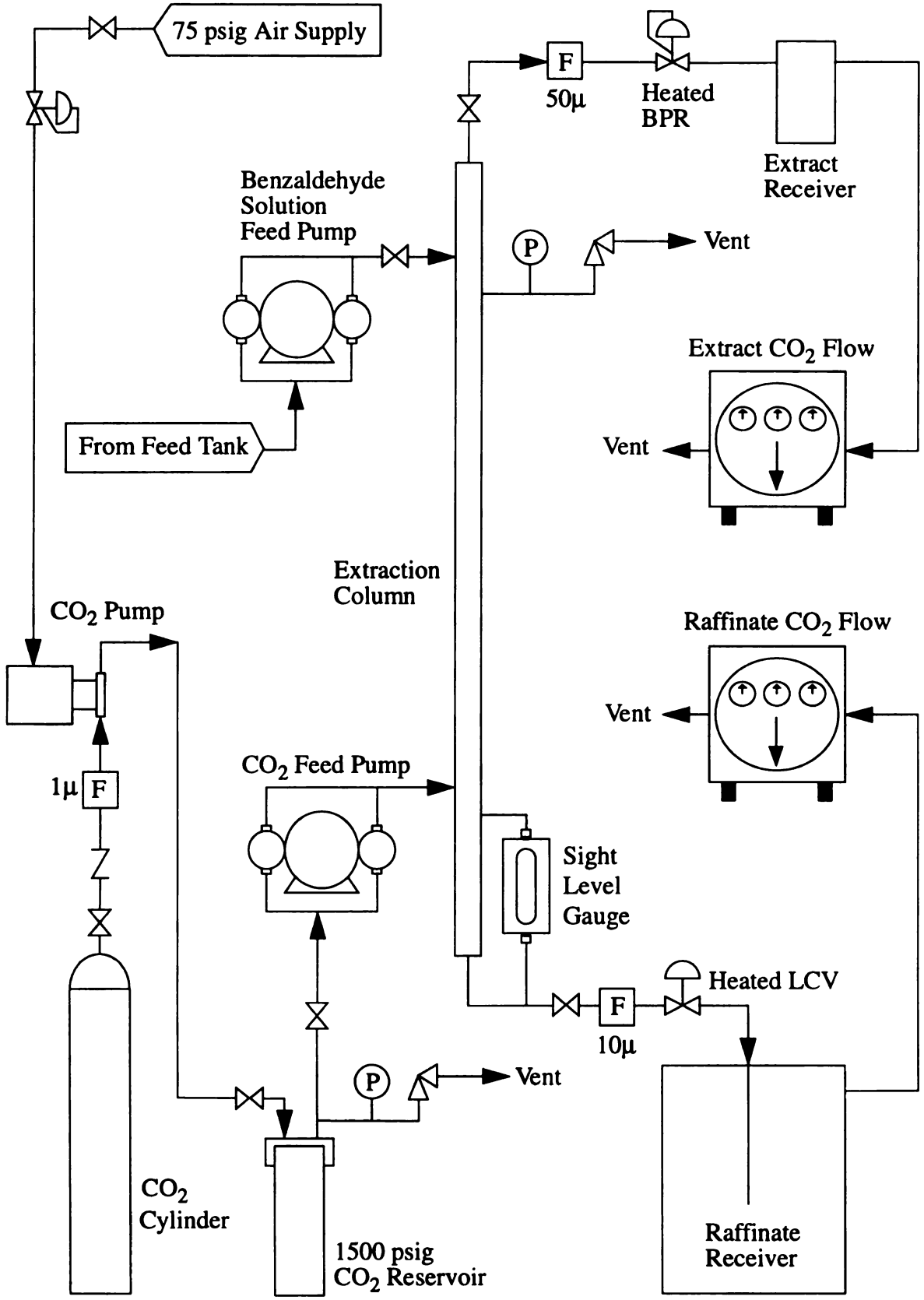

Figure 5-4. Benzaldehyde Extraction Column Flow Schematic

protect the pumps downstream. Both the check valve and the filter were supplied by Forberg Scientific, Inc. The downstream side of the filter was connected by 1/4" SS tubing to the suction side of a Haskel, Inc. Gas Booster model AG-152. This pump was used to maintain a reservoir of carbon dioxide at between 1,300-1,500 psig.

The reservoir was a 1 liter, 316 SS vessel, model number OC-11 manufactured by High Pressure Equipment Company. The reservoir supplied liquid carbon dioxide to the suction side of an LDC Analytical model 2396 metering pump at a sufficient pressure to prevent cavitation and insure accurate, reproducible delivery of carbon dioxide into the system. The inlet and outlet ports of the reservoir were connected by short lengths of 1/4" SS tubing to 1/4" block valves manufactured by High Pressure Equipment Company (model 10-11AF4). A pressure gauge was connected between the outlet of the reservoir and the block valve to monitor the pressure. In a configuration similar to that of the aqueous phase feed pump discharge, the discharge nozzles of the carbon dioxide metering pump were connected to two ports of a 1/16" cross. The third port of the cross was connected to a rupture disk assembly identical to the one protecting the aqueous phase metering pump. The fourth port of the cross was connected to the isolating valve on the lower feed port of the extraction column.

Extraction Column (Figure 5-2)

A model TOC-72, 316 SS Tubular Series Reactor with standard AF4 taper seal connections at each end was purchased from High Pressure Equipment Company and modified to serve as an extraction column by adding four 1/4" FPT connections. Two of the additional ports are located on the same side of the column 6" from each end and are used for the top and bottom solvent feeds. The 6" measurement is taken from the end of the O-ring plug that fits into the end of the column and not the end of the column itself or the end of the end caps. In this way, the 6" dimension is the actual height of the separating section for the two phases. The remaining two ports are on the side of

the column directly opposite of the feed ports and are 6" from each end. These ports were used to connect a sight level gauge at either the top or bottom of the column to monitor the interface between the two phases in the column. In other words, the additional ports added to the column are located in a symmetrical fashion about the axial middle of the column so as to allow the column to be run with either phase as the continuous phase. The column is 72"L with a 1" I.D. and a 2" O.D. The end connections with the 1/4" female (AF4) taper seal fittings use Buna N O-rings (part number B-113) for a pressure seal.

The external configuration of the column included a Jergusen 12-R-32 reflex sight level gauge with a maximum pressure rating of 4,000 psig at 72 °F. The height of the view port of this cell is approximately 5". The sight gauge was mounted at the bottom of the column to measure the interface between the continuous (carbon dioxide) phase and the dispersed (water) phase. The gauge was mounted so that the bottom of the view port aligned with the bottom of the column so as to monitor the interface level in the bottom 5" of the column.

Both of the column solvent feed ports and the top and bottom outlet ports were connected by stainless steel tubing to High Pressure Equipment Company block valves which could be used to isolate the contents of the column and prevent the loss of the liquid carbon dioxide between successive runs. The top solvent feed port used for the aqueous feed and both of the outlet valves were 1/4" SS model 10-11AF4 valves. The bottom solvent feed port used for the carbon dioxide feed was a 1/8" SS model 15-11AF2 valve. The remaining top port was connected by 1/16" SS tubing to a Heise digital pressure indicator model 901A with a range of 0-10,000 psig and to a High Pressure Equipment Company 1/4" rupture disk holder model 15-61AF1 containing an OSECO 1/4A, standard rupture disk with a burst pressure of 3,000 psig at 72 °F.

Three items made up the extraction column internals; the column packing, the liquid redistributors, and the aqueous feed distributor. The packing was 0.16"L, 316

SS Pro-Pak protruded metal packing purchased from Scientific Development Company. The packing was added to the column dry by slowly pouring the packing through a funnel inserted into the top of the column with the column in the vertical position. Four liquid redistributing rings were installed in the column spaced 16" apart and beginning 16" from the bottom of the column. The design of the redistributing rings is shown in Figure 5-5. The redistributors were made from aluminum while the O-ring seals were Buna N rubber. The aqueous feed distributor was a 4" long piece of 1/4" SS tubing plugged at one end by a TIG weld. A 1/8" diameter hole was drilled into one side of the tube centered exactly 1/2" from the plugged end to serve as the spray nozzle. The liquid redistributing rings and the feed distributor were fabricated in the Michigan State University engineering machine shops. The distributor tube was installed in the column by inserting it through a Swagelock 1/4" tube x 1/4" MPT adapter fitting that had been bored out so that the feed distributor would slide

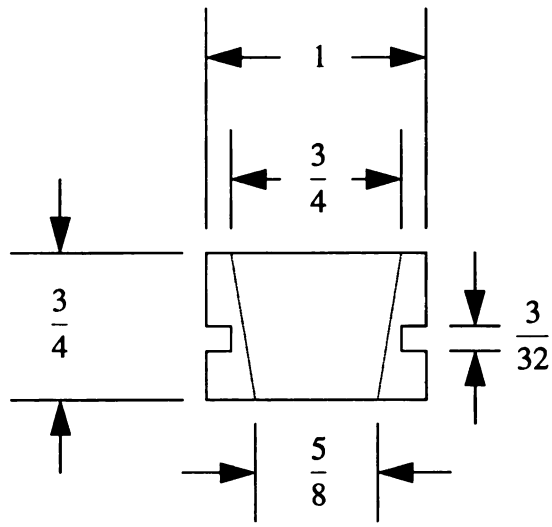

Figure 5-5. Liquid Redistributing Rings.

completely through it. After the modified fitting had been tightened into the top feed port, the distributor tube was marked at the end that would remain outside the column so that the discharge nozzle location could be verified after installation. Care was taken to be sure that the discharge nozzle pointed straight downward and that the distributor tube was pushed through the modified adapter fitting until the plugged end came to rest against the far wall of the extraction column. By doing this, the precise distance of the nozzle from the plugged end of the tube insured that the nozzle was in the exact center of the column.

Receiver Section (Figure 5-3)

The carbon dioxide phase flowed out the top of the extraction column through the isolating valve and then through a 50 micron model 4Z-F4L-50-SS filter purchased from Forberg Scientific. The filter discharge was connected by 1/4" SS tubing to a Tescom Corporation model 26-1724-24 back pressure regulator to control the operating pressure in the extraction column. Because of the cooling caused by the Joule-Thomson expansion of the carbon dioxide across the back pressure regulator, an aluminum-block heater was designed to heat the regulator. Two holes sized to fit a Vulcan Electric Company T.B. cartridge heater (approximately 1/4" O.D. x 2"L) were drilled into the side of a 3"W x 3-3/4"L x 3/4"D aluminum block to a depth sufficient to allow the cartridges to center on the centerline of the block. Fiberglass insulation was packed into the holes behind the cartridges to hold them in place. The cartridges were electrically wired in parallel to a standard 120V, two-prong plug. The heaters were plugged into a Staco Energy Products variable autotransformer type 3PN1010 to regulate the temperature of the aluminum block. The back pressure regulator was placed on top of the aluminum block and covered with fiberglass insulation. An Omega type K thermocouple connected to an Omega CN9000A temperature indicating controller was placed underneath the aluminum block heater to monitor temperature.

The flow of carbon dioxide vapor discharged from the back pressure regulator was split into two streams by a 1/4" plastic "Y". Both branches of the "Y" went to identical ethanol traps to collect the benzaldehyde extract. The ethanol traps were test tubes 14"L with an outer diameter of 2-1/8". A 7 mm O.D. side arm was located 2" from the top to provide a vent for the carbon dioxide bubbling through the trap. An ACE Glass Company gas sparger was extended to 18" in length and inserted into a hole bored through a number 10½ rubber stopper. The stopper was pressed into the end of the test tube to provide a leak free seal. The glass frit at the end of the sparger was adjusted to be 1/2-1" from the bottom of the test tube. Approximately 500 ml of dry ethanol was poured into the test tube to trap the benzaldehyde. The entire trap was then immersed in an ice water bath to minimize evaporation of the ethanol during the run. The vents from the two traps were connected together and the combined flow was then directed into a Precision Scientific Wet Test Flow meter catalog number 63126. The Wet Test Meter was vented to the atmosphere.

The bottom isolating valve of the column was connected by 1/4" SS tubing to a 10 micron Parker 4F-F4L-10-SS filter. The raffinate then flowed through 1/8" SS tubing to a control valve to control the interface level between the two phases in the bottom of the column. The flow control valve was a series 10VRMM2812 manufactured by Autoclave Engineers. This two-way angle valve has a micrometering valve stem with a C_v of 0.004 and an orifice diameter of 0.062". Because of cooling caused by the expansion of carbon dioxide dissolved in the raffinate, an aluminum block heater was used to heat the valve to prevent freezing. The heater consisted of two 3/4" thick aluminum blocks slightly larger than the valve body. Two holes sized to fit Vulcan T.B. cartridge heaters were drilled into the top of the blocks. Mounting holes were drilled into the sides of both blocks at one top corner and at the bottom corner diagonally opposite to the top hole. The blocks were placed on either side of the flow control valve with threaded rod inserted through the corner holes and then secured with

hex nuts. As before, the cartridge heaters were wired in parallel and plugged into a Staco Energy Products model 3PN1010 variable autotransformer. The flow control valve discharge was connected by 1/4" SS tubing inserted through a hole bored into a rubber stopper. The stopper was forced into the top of a 4 L Erlynmeyer flask which served as the raffinate receiver. The raffinate tubing extended about half way into the flask to allow separation of the raffinate and carbon dioxide. The Erlenmeyer flask was modified by adding a glass stopcock to the bottom so that the entire contents of the flask could be drained without holdup. Carbon dioxide was vented out the top of the flask through a vent connected by Tygon tubing to a wet test meter identical to the one described above. The meter was vented to the atmosphere.

CHAPTER 6

BENZALDEHYDE EXTRACTION EXPERIMENTAL METHOD

Prior to the first run of the extraction column an estimate of the carbon dioxide feed rate required to extract benzaldehyde from a dilute aqueous solution was made. This estimate was used as the initial carbon dioxide feed flow to the column. The approach used was to assume that there were either one or two equilibrium stages in the column and perform a material balance around each stage. The benzaldehyde concentration in the feed was taken as 200 ppm and it was desired to recover 50% of the benzaldehyde from the feed. This would result in a decrease in the benzaldehyde concentration from 200 ppm to 100 ppm in the raffinate. A schematic diagram of the single stage model is shown in Figure 6-1. The material balance for the single equilibrium stage is:

$$x_0 Q_W^{IN} + y_0 Q_{CO2}^{IN} = x_1 Q_W^{OUT} + y_1 Q_{CO2}^{OUT} \qquad 6\text{-}1$$

In order to simplify the material balance, it was assumed that carbon dioxide and water are mutually insoluble. This is a reasonable assumption considering that Wiebe (1977) determined that at 25°C and 125 atmospheres of pressure the equilibrium solubility of

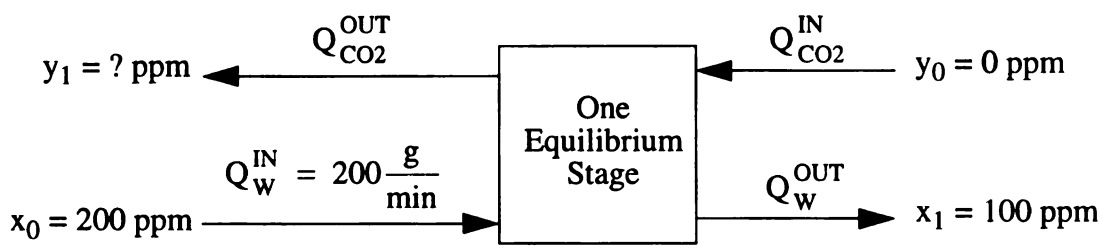

Figure 6-1. One Equilibrium Stage Flow Simulation

carbon dioxide in water is close to 6.3% by weight while the solubility of water in carbon dioxide is very low at only 0.14% by weight. This mutual insolubility combined with the dilute concentrations of benzaldehyde mean that the flow of both phases is constant:

$$Q_W^{IN} = Q_W^{OUT} \qquad \text{and} \qquad Q_{CO2}^{IN} = Q_{CO2}^{OUT} \tag{6-2}$$

Substituting into Equation 6-1, noting that the concentration of benzaldehyde in the fresh solvent stream, y_0, is zero, and rearranging yields:

$$(x_0 - x_1)\, Q_W = y_1 Q_{CO2} \tag{6-3}$$

Since there are two unknowns, y_1 and Q_{CO2}, remaining in the above expression another relationship must be found before Equation 6-3 can be solved. The equilibrium distribution coefficient for the ternary system benzaldehyde/carbon dioxide/water relates the concentration of benzaldehyde in the raffinate, x_1, to the concentration of benzaldehyde in the extract, y_1. The distribution coefficient reported previously was 52. Therefore, $y_1 = 52x_1$ and equation 6-3 becomes

$$\frac{(x_0 - x_1)\, Q_W}{52x_1} = Q_{CO2} \tag{6-4}$$

Solving this equation for the flow rate of carbon dioxide given the values shown in Figure 6-1 yields a value of 3.8 g CO_2/min.

The same technique can be used to estimate an initial carbon dioxide flow rate assuming that there are two equilibrium stages in the column as shown in Figure 6-2. Again making the assumption that the two phases are completely immiscible and the solute concentration is dilute enough so that the flow of each phase is constant, an

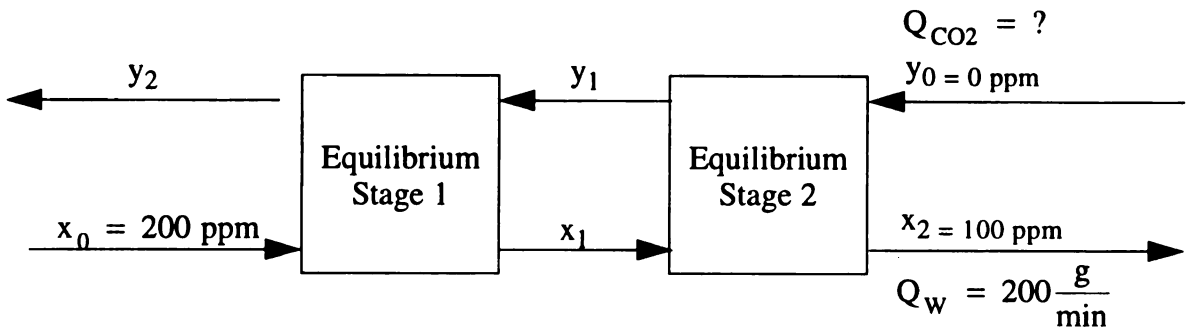

Figure 6-2. Two Equilibrium Stage Flow Simulation

overall material balance is given by:

$$y_2 Q_{CO2} = (x_0 - x_2) Q_W \qquad 6\text{-}5$$

The distribution coefficient provides a relationship between the streams leaving the second equilibrium stage:

$$y_2 = m x_1 \qquad 6\text{-}6$$

Substituting Equation 6-6 into Equation 6-5 yields:

$$x_1 m Q_{CO2} = (x_1 - x_2) Q_W \qquad 6\text{-}7$$

A material balance around the first equilibrium stage is given by:

$$(x_1 - x_2) Q_W = y_1 Q_{CO2} \qquad 6\text{-}8$$

Again, the distribution coefficient can be used to eliminate an unknown variable:

$$y_1 = m x_2 \qquad 6\text{-}9$$

Substituting this expression into Equation 6-8 gives:

$$(x_1 - x_2)\, Q_W = x_2 m Q_{CO2} \qquad 6\text{-}10$$

Solving for x_1:

$$x_1 = \frac{Q_{CO2} m x_2}{Q_W} + x_2 \qquad 6\text{-}11$$

Finally, Equation 6-11 can be substituted into Equation 6-7 for x_1 yielding an equation with only one unknown variable:

$$Q_{CO2} m \left[\frac{Q_{CO2} m x_2}{Q_W} + x_2 \right] = (x_0 - x_2)\, Q_W \qquad 6\text{-}12$$

Rearranging:

$$\frac{Q_{CO2}^2 m^2 x_2}{Q_W} + Q_{CO2} m x_2 - (x_0 - x_2)\, Q_W = 0 \qquad 6\text{-}13$$

Substituting the known values from Figure 6-2 for the appropriate variables, Q_W = 200 g/min, x_0 = 200 ppm and x_2 = 100 ppm, and recalling that the distribution coefficient, m, is 52 and solving the quadratic expression yields a value for the carbon dioxide flow rate, Q_{CO2}, of 2.4 g CO_2/min.

The estimated initial carbon dioxide flow rate of 3.8 g CO_2/min. or 2.4 g CO_2/ min. using the assumption of one or two equilibrium stages respectively were found to be within the CO_2 pump capacity of 0-15 g CO_2/min. at 1,500 psig.

The next step in preparing to run the extraction column was to examine the

estimated flow rates of both the feed (200 g/min) and the solvent (2.4-3.8 g/min) with the flooding correlations of Crawford and Wilke, Rao and Rao, and Venkataraman and Laddha to insure that these conditions would not flood the column. A summary of the calculations is shown in Table 6-1.

It is apparent from Table 6-1 that there is disagreement between the three correlations as to what total flow rate results in column flooding. For design purposes, the authors recommend that 50% of the calculated flooding value should not be exceeded. Since the packing used in the benzaldehyde project was different from any of those used in the published flooding correlations this conservative approach seemed appropriate. Accordingly, the initial values for the carbon dioxide and aqueous feed flow rates were chosen to be in the range of 4.0-5.0 g/min. and 10-15 g/min. respectively.

Selecting the carbon dioxide flow rate in the 4.0-5.0 g/min. range corresponds to a continuous phase retention time of 2.9-2.3 hours. Since it was assumed that a minimum of three complete turnovers of the carbon dioxide were necessary to achieve steady-state operation this range of retention times corresponds to a minimum operating time of 8.6-6.9 hours.

Preparation

1. Between 10-15 liters of aqueous feed solution were prepared prior to starting a run of the extraction column. The benzaldehyde and water were allowed to mix with gentle stirring overnight to insure that the benzaldehyde was completely dissolved.

2. About 1-2 hours prior to each run, the gas chromatograph used to analyze for benzaldehyde in ethanol was turned on and allowed to equilibrate.

3. The ultraviolet-visible light spectrophotometer used for determining the concentration of benzaldehyde in the feed and raffinate streams was turned on and allowed to equilibrate.

Table 6-1. Flooding Correlation For Prestart-up Conditions

Continuous Phase Flow Rate g/min	Discontinuous Phase Flow Rate g/min	CO2 Retention Time hr	% Flooding		
			C&W	R&R	V&L
2.4	200	4.77	70	91	127
"	150	"	54	80	113
"	100	"	38	67	95
"	75	"	30	60	84
"	50	"	21	51	71
"	25	"	12	39	55
"	10	"	7	29	40
3.8	200	3.02	74	93	126
"	150	"	58	83	112
"	100	"	41	70	95
"	75	"	33	62	84
"	50	"	24	54	72
"	25	"	14	42	56
"	10	"	8	31	42

C&W = Crawford and Wilke (1951)

R&R = Rao and Rao (1958)

V&L = Venkataraman and Laddha (1960)

The following values for the correlation parameters were used:

ρ_C = 62.4 lb/ft3 ε = 094

ρ_D = 53.78 lb/ft3 F = 693

ϕ = 1.0 in γ = 21.6 dyne/cm

μ_C = 0.068 cps RST = 0.3

Table 6-1. Continued

Continuous Phase Flow Rate g/min	Discontinuous Phase Flow Rate g/min	CO2 Retention Time hr	% Flooding		
			C&W	R&R	V&L
7.5	200	1.53	82	99	125
"	150	"	65	88	112
"	100	"	47	76	96
"	75	"	38	68	86
"	50	"	28	59	75
"	25	"	18	47	60
"	10	"	11	37	47
15.0	200	0.76	87	107	136
"	150	"	68	95	121
"	100	"	56	84	98
"	75	"	46	76	90
"	50	"	35	67	79
"	25	"	24	55	65
"	10	"	15	45	53

C&W = Crawford and Wilke (1951)
R&R = Rao and Rao (1958)
V&L = Venkataraman and Laddha (1960)

4. The variable power controller used to supply electric current to the heating cartridges in the extraction column backpressure regulator heating block was turned on at a setting of approximately 55% and allowed to equilibrate for about an hour prior to running the extraction column. The thermocouple measuring the bottom surface of the backpressure regulator was not allowed to exceed 120°C to prevent damage to the regulator.

5. The variable power controller used to supply power to the silicone-coated electric tracing on the metal tubing between the raffinate level control valve and the raffinate receiver was turned on an hour before running the column to preheat.

6. The variable power controller used to supply power to the electric heating cartridges on the water phase level control valve was turned on and allowed to equilibrate for an hour prior to column start-up. Preheating this valve was found to be very important in preventing freezing of the raffinate line early during the run.

7. The two ethanol traps were rinsed clean, filled with fresh ethanol, and installed on the discharge of the continuous phase backpressure regulator in series.

8. The current readings of the carbon dioxide flow meters were recorded.

Operating Procedure

Refer to Figure 6-3 in reference to the following discussion. The valve numbers described below are shown in Figure 6-3 as circled numbers next to the appropriate valve.

1. The carbon dioxide cylinder pressure was checked to be sure that there was sufficient carbon dioxide for the run. The final carbon dioxide inlet block valve into the column was checked to be sure that it was closed. The cylinder valve was opened to supply liquid carbon dioxide through the cylinder dip-tube into the Haskel gas booster pump.

2. The blockvalve (1) supplying air to the Haskel gas booster was opened. The air

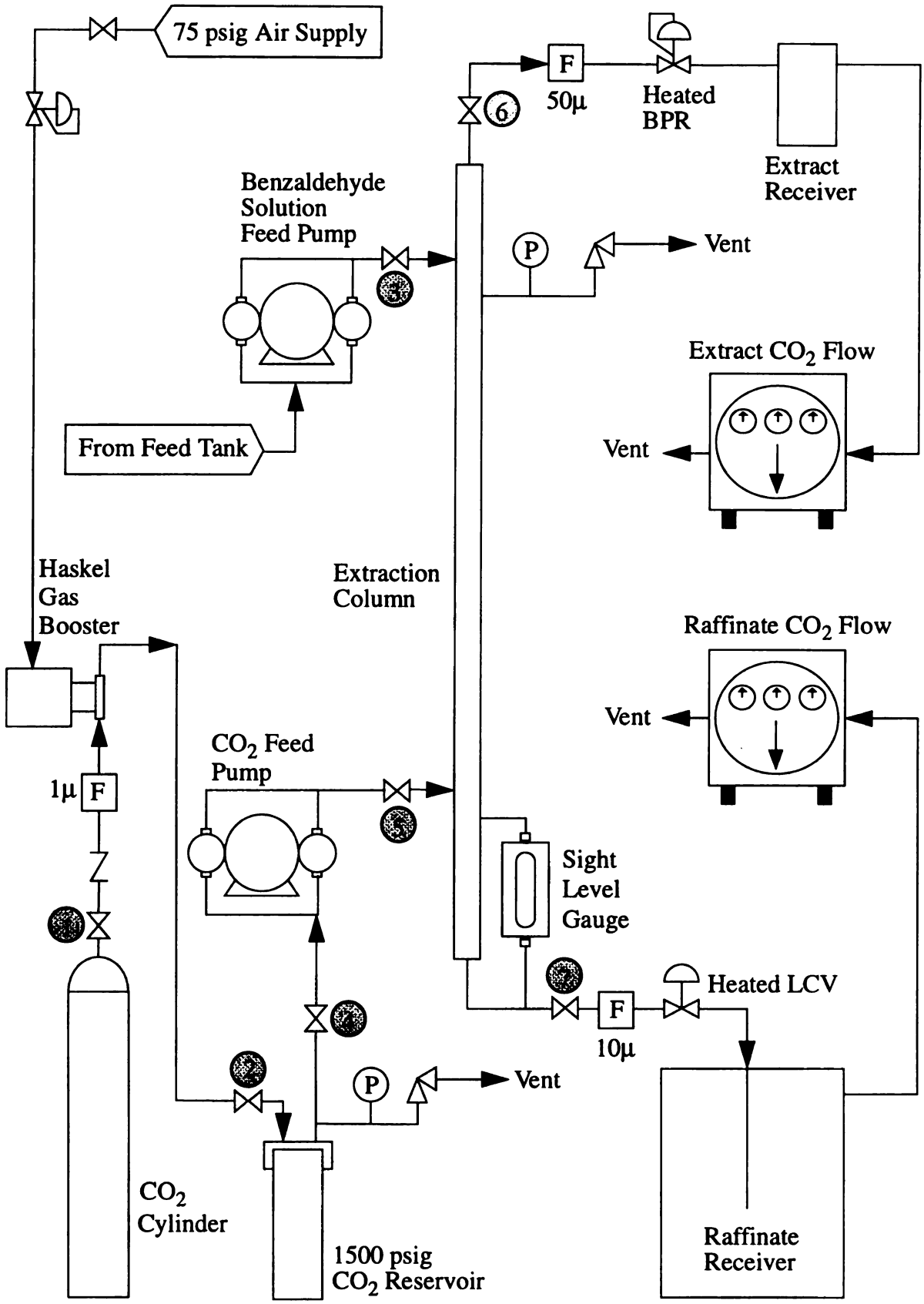

Figure 6-3. Benzaldehyde Extraction Column Flow Schematic

supply pressure was 75 psig.

3. The blockvalve (2) between the discharge of the Haskel gas booster and the high pressure carbon dioxide reservoir was opened. The reservoir pressure was maintained at 1,500 psig to provide a continuous, uninterrupted flow of liquid carbon dioxide into the metering pump.

4. The raffinate phase level in the sight level gauge was checked to determine if there was a level visible. The level was maintained at 1/2 to 2/3 the height of the glass.

5. The aqueous phase feed tank was connected to the suction side of the feed metering pump. The manual valves between the feed pump and the suction of the feed metering pump were opened. The micrometering adjusters on the pump were set to the desired percentage of maximum flow.

6. The blockvalve (3) between the aqueous feed tank and the column was opened. The internal check valves in the pump heads were relied upon to prevent backflow from the column into the pump.

7. The pressure in the carbon dioxide reservoir was monitored. When it reached 1,500 psig the blockvalve (4) between the reservoir and the carbon dioxide feed metering pump was opened.

8. The blockvalve (5) supplying carbon dioxide to the column was opened. The reservoir has sufficient capacity to fill the column and will do so when the reservoir pressure is maintained at 1,500 psig.

9. The discharge blockvalve (6) on the top of the column was opened *slowly.* Opening this valve to quickly with the column pressure regulator not set properly will result in a sudden discharge of carbon dioxide through the regulator. This sudden depressurization of the column could be sufficient to blow the ethanol out of the cold traps into the wet test flow meters.

10. The raffinate level control valve was checked to be sure that it was closed. The blockvalve between the bottom of the column and the heated level control valve was

opened.

11. The micrometering adjustments on the carbon dioxide pump were set at the desired settings. The pump was turned on.

12. The aqueous phase feed pump was turned on.

13. The raffinate level in the sight glass was monitored. The level control valve was adjusted to maintain the level in the sight gauge.

14. The column pressure was monitored and small adjustments were made to the backpressure regulator to maintain the column pressure at the desired setpoint. The regulator is oversized by a small amount so that when it opened the column pressure decreased by 50-80 psig. The rate of carbon dioxide flow into the column was slow enough so that the pressure took about 10-15 minutes to recover enough for the regulator to open again.

Chemical Analysis

In order to be able to perform a material balance around the column it was necessary to analyze three of the column steams for benzaldehyde; 1) the aqueous feed, 2) the raffinate, and 3) the extract. The solvent feed was cylinder carbon dioxide and did not contain any benzaldehyde. The analytical methods used for these analysis are described below:

1. The aqueous feed was analyzed for benzaldehyde using Ultraviolet Spectrophotometry (u.v.). Benzaldehyde exhibits a strong absorption in the ultraviolet region of the electromagnetic spectrum at 241 nanometers. Concentrations in the range of 1-10 ppm could be measured. Calibration curves and other details of the u.v. method are presented in Appendix D.

For the assay of the column aqueous feed, serial dilutions of ten volumes of reverse-osmosis purified water to one volume of sample were done to dilute the benzaldehyde to give an on-scale reading on the u.v. spectrophotometer. Since the feed

solution was prepared to give benzaldehyde concentrations in the range of 100-700 ppm only one dilution was required to decease the concentration to a level which would yield an absorption readable on the u.v.

The feed tank was sampled three or four times during the course of a run to monitor the decrease in the benzaldehyde concentration due mostly to oxidation to benzoic acid and also partly due to evaporation. The benzaldehyde concentration did decrease by as much as much as 10% during the runs.

2. The raffinate streams were also analyzed for benzaldehyde by ultraviolet spectrophotometry. Dilutions of 1:1 or 2:1 were used.

3. Atmospheric pressure on the downstream side of the backpressure regulator controlling the column pressure resulted in vaporization of the carbon dioxide. This gas stream was bubbled through ethanol to trap the entrained benzaldehyde. In order to be able to perform a material balance around the column, the ethanol trap contents were analyzed to determine the amount of benzaldehyde dissolved therein. Gas chromatography using a Perkin-Elmer model 8500 equipped with a flame ionization detector was used for the gas chromatography. The column was an Alltech Associates, Inc. Econo-Cap capillary column, catalog number 19653, 10 m long x 0.53 mm ϕ, with a 1.2 μm thick carbowax stationary phase.

Isopentyl alcohol (IPA) was used as an internal standard. Because the benzaldehyde concentration was less than one percent, the ethanol peak coming off the column had a long shoulder extending to more than five minutes although the baseline was quite close to being re-established at this time. The IPA peak eluted at very close to five minutes. In the sample chromatogram shown in Figure 6-4, the IPA peak eluted at 4.96 minutes. The benzaldehyde peak appears at 7.6 minutes. Further details about the ethanol phase chromatography are described in Appendix B.

Material Balance Calculations

Material balance calculations were performed for each of the extraction column

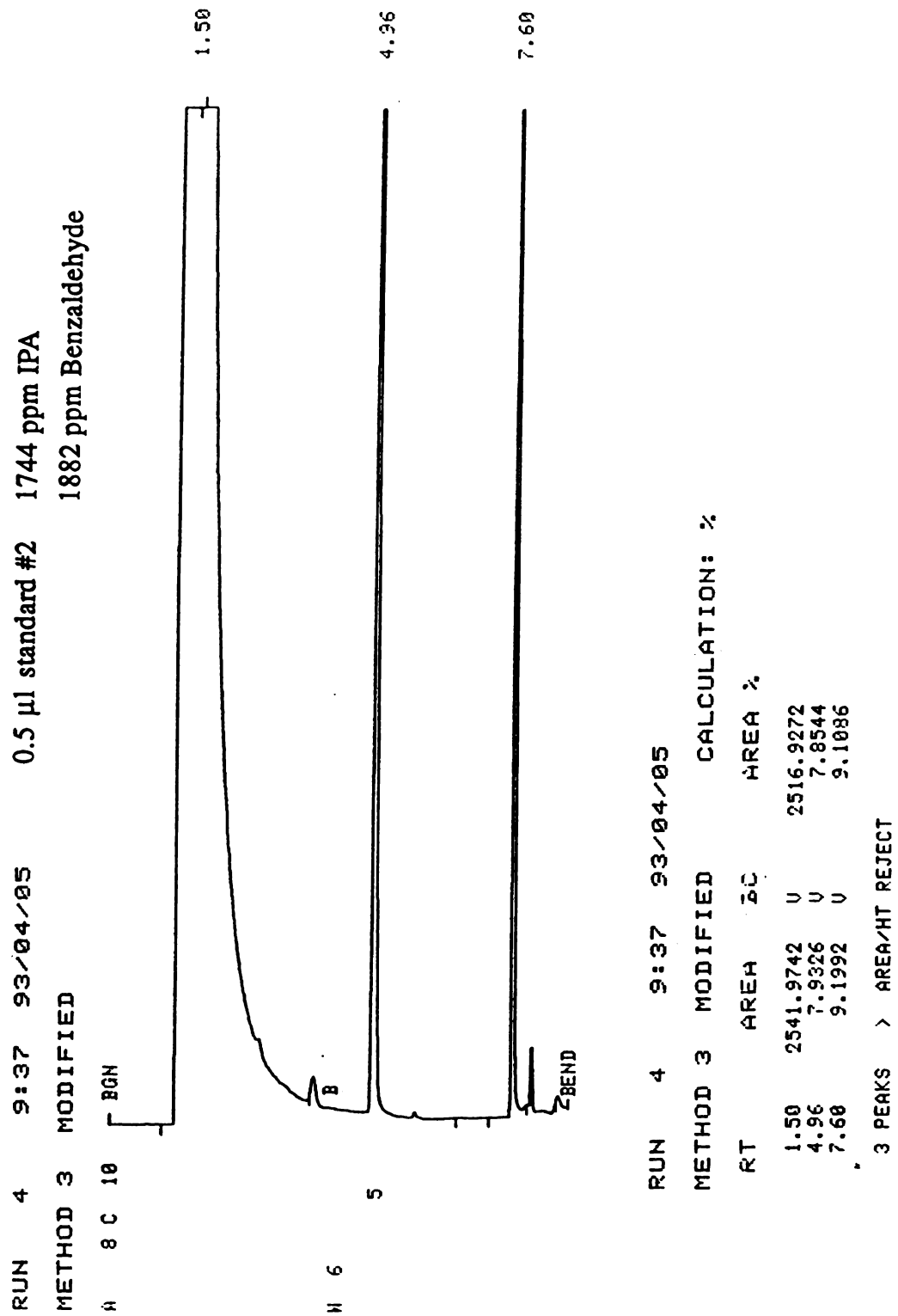

Figure 6-4. Sample Chromatagram for Ethanol Phase.

runs. The amount of benzaldehyde fed to the column was compared to the amount of benzaldehyde that left the column in the raffinate and extract streams and the amount remaining in the column when the run was terminated. The amount of benzaldehyde fed into the column over the course of the run was calculated by analyzing the feed several times during the run. An average of the feed concentrations was then multiplied by the decrease in weight of the feed vessel. The benzaldehyde leaving the extraction column in the raffinate was calculated by averaging the concentrations of benzaldehyde in samples taken at regular intervals throughout the run and multiplying the average times the total amount of raffinate collected. The benzaldehyde in the extract stream was determined by analyzing a single, representative sample of the ethanol cold-trap solution for the concentration of benzaldehyde and multiplying this value times the amount of ethanol remaining in the trap at the end of the run. Finally, the benzaldehyde remaining in the column at the end of the run was estimated by multiplying the carbon dioxide volume remaining in the column times the extract benzaldehyde concentration. The amount of benzaldehyde in the raffinate remaining in the column at the end of the run was assumed to be negligible.

The complete material balance calculations for Run 3 are given below. The measured parameters are shown in Figure 6-5:

1. The carbon dioxide flow rates for the extract and raffinate streams were measured with wet test flow meters. For Run 3 the flows were 1032.2 L and 277.6 L respectively. The volumetric rates were converted to mass flows according to the following equations;

$$1032.2\ \text{L CO2}\left(\frac{\text{gmol K}}{0.08205\ \text{atm L}}\right)\left(\frac{1\ \text{atm}}{293\ \text{K}}\right)\left(\frac{44\ \text{g CO2}}{\text{gmol}}\right) = 1845.1\ \text{g CO2} \qquad 6\text{-}14$$

$$277.6\ \text{L}\left(\frac{\text{gmol K}}{0.08205\ \text{atm L}}\right)\left(\frac{1\ \text{atm}}{293\ \text{K}}\right)\left(\frac{44\ \text{g CO2}}{\text{gmol}}\right) = 496.1\ \text{g CO2} \qquad 6\text{-}15$$

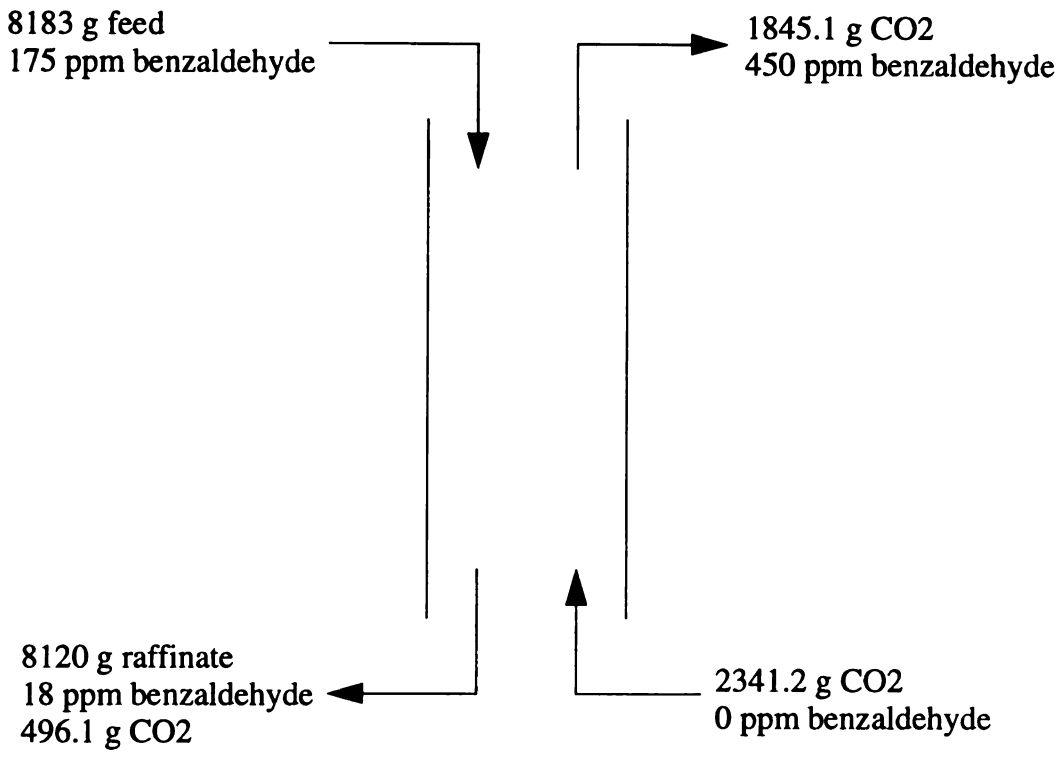

Figure 6-5. Run 3 Material Balance Diagram

The total carbon dioxide fed to the column was 1309.8 L (2341.2 g);

2. Benzaldehyde fed to the column;

$$8183\text{g feed}\left(\frac{175\text{ g benz.}}{\text{g feed}}\right) = 1.432\text{ g benz.} \qquad 6\text{-}16$$

3. Benzaldehyde leaving the column in the raffinate;

$$8120\text{ g raffinate}\left(\frac{18\text{ g benz.}}{10^6\text{ g raffinate}}\right) = 0.15\text{ g benz.} \qquad 6\text{-}17$$

4. The amount of benzaldehyde in the extract stream was determined by first by

analyzing the ethanol trap solution for benzaldehyde. For Run 3 this value was 1800 g benz./10^6 g ethanol. The total amount of trap solution was 460.74 g and the benzaldehyde leaving the column in the extract was;

$$460.74 \text{ g extract} \left(\frac{1800 \text{ g benz.}}{10^6 \text{ g extract}} \right) = 0.83 \text{ g benz.} \qquad 6\text{-}18$$

5. The amount of carbon dioxide remaining in the column at the end of each run was 840 ml. The concentration of benzaldehyde in this holdup was estimated to be the same as the average benzaldehyde concentration in the extract;

$$\frac{0.83 \text{ g benz.}}{1845.1 \text{ g CO2}} = \frac{450 \text{ g benz.}}{10^6 \text{ g CO2}} \qquad 6\text{-}19$$

and the accumulation of benzaldehyde in the carbon dioxide holdup;

$$840 \text{ ml} \left(\frac{0.85 \text{ g CO2}}{\text{ml}} \right) \left(\frac{450 \text{ g benz.}}{10^6 \text{ g CO2}} \right) = 0.33 \text{ g benz.} \qquad 6\text{-}20$$

6. The benzaldehyde balance is given by;

$$\text{in} = \text{out} + \text{accumulation} \qquad 6\text{-}21$$

7. For Run 3 Equation 6-22 becomes;

$$1.432 \text{ g benz.} = 0.15 \text{ g benz.} + 0.83 \text{ g benz.} + 0.33 \text{ g benz.} = 1.31 \text{ g benz.} \qquad 6\text{-}22$$

The benzaldehyde recovery is then

$$\left(\frac{1.31 \text{ g benz.}}{1.432 \text{ g benz.}} \right) 100 = 91\% \qquad 6\text{-}23$$

The carbon dioxide solubility in the raffinate was also calculated to determine if the experimental values were close to the 6.3% at 25 C and 125 atm (1837 psi) predicted by Wiebe (1977, p 476):

$$\left(\frac{496.1 \text{ g CO2}}{8120 \text{ g raffinate}}\right)100 = 6.1\% \qquad 6\text{-}24$$

which is reasonably good agreement.

CHAPTER 7

BENZALDEHYDE EXTRACTION EXPERIMENTAL RESULTS

The extraction column was run a total of seven times. Run 1 and Run 2 were test runs to check the operation of the equipment and the results for these runs are not reported.

The operating conditions for Runs 3 and 4 were kept identical to check the reproducibility of the entire system. The results of these runs were, in fact, identical within reasonable limits.

For Run 5, the operating parameters were kept the same as for the previous two experiments except that the feed concentration was increased by a factor of two. There was no significant change in the concentration of benzaldehyde (solute) in the raffinate although the concentration of benzaldehyde in the extract did increase as expected.

For Run 6, the concentration of benzaldehyde in the feed was again increased by a factor of two over the previous run with all other parameters held the same.

For the last run in this project, Run 7, the aqueous feed rate was decreased and the carbon dioxide feed rate was increased such that the total feed to the column was essentially the same as for all of the previous runs. This decrease in the solvent ratio (i.e. decrease in slope of the operating line) was also a decrease in the carbon dioxide retention time.

Table 7-1 focuses on the extraction column benzaldehyde material balances. Considering the very low concentrations of benzaldehyde used for these experiments, the benzaldehyde recoveries were very good with four of the five runs having 95% or greater recovery.

Table 7-2 examines the column fluid mechanics that are an important part of the information required for scale-up. The percent of flooding as predicted by the correlations of Venkataraman and Laddha, Rao and Rao, and Crawford and Wilke are

Table 7-1. Extraction Column Material Balances

Run No.	Feed Solution		CO_2 Feed		Slope of Operating Line F/CO_2	Total Benz. Fed g	Benz. in Extract g	Benz. in Raffinate g	Benz. in CO_2 Holdup	Benz. Recovered %
	Total Feed g	Rate g/min	Total g	Rate g/min						
3	8183	17.05	2341	4.88	3.50	1.432	.829	.155	.383	95.5
4	8210	17.10	2458	5.12	3.34	1.314	.905	.148	.335	105.6
5	8162	17.00	2469	5.14	3.31	2.408	1.524	.18	.560	94.0
6	8141	16.96	2484	5.18	3.28	5.780	3.060	.529	1.116	81.4
7	6136	12.78	2996	6.24	2.05	3.964	2.814	.387	.774	100.3

Table 7-2. Extraction Column Fluid Mechanics

Run Number	Water Holdup ml	Percent of Flooding			CO_2 Retention hr.	CO_2 Turnovers	CO_2 in Raffinate %
		C&W	R&R	V&L			
3	63	11.9	38.8	51.1	2.35	3.41	6.07
4	35	12.1	39.2	51.4	2.24	3.57	6.42
5	32	12.1	39.1	51.3	2.23	3.59	6.41
6	41	12.1	39.2	51.3	2.21	3.62	6.44
7	36	11.0	37.7	48.5	1.84	4.37	6.49

C&W = Extraction Column Flooding Correlation of Crawford and Wilke, (1960).

R&R = Extraction Column Flooding Correlation of Rao and Rao, (1958).

V&L = Extraction Column Flooding Correlation of Venkataraman and Laddha, (1951).

Physical parameters used for the flooding correlations are the same as those used for Table 6-1.

of particular interest. Conservative flow rates for both phases were used for the initial column runs to avoid flooding. No evidence of flooding was observed since the column could be run for extended periods of time without difficulty. Further runs at higher total flow rates are required in order to determine which of the correlations is the most accurate. The carbon dioxide retention time and turnovers are also included in Table 7-2. The turnovers in particular were important since this parameter was used as a rough prediction of when the column would reach equilibrium. It was believed that a minimum of 2-3 turnovers were required before the system was at equilibrium. In practice, samples of raffinate taken at fifteen minute intervals after the start of the run showed that the raffinate benzaldehyde concentration reached a constant value within a half hour or within less than one turnover. The concentration of carbon dioxide in the raffinate phase was also recorded. This value is between 6.0-6.5%(wt) for all of the runs which agrees very well with the 6.3% (wt) value for carbon dioxide solubility in water at the same temperature and pressure (25°C and 1,500 psig) determined by Wiebe (1977).

Number of Stages and the Height of a Transfer Unit

Calculations were performed for the three methods described in Chapter 3, p 39 for determining the number of stages in the column: 1) the number of theoretical stages, NTS, which compares the continuous column to a staged contactor, 2) the number of transfer units, NTU, which is based on film-transfer theory, and 3) the method of Kremser;

1. Table 7-3 first lists the feed, extract and raffinate concentrations as measured for Runs 3-7. Next a material balance is performed for one equilibrium stage (Equation 3-8) using the inlet concentrations for the feed and carbon dioxide streams actually used in each experiment. The extract stream concentration calculated in this manner is listed in the last column. It can be seen that for all of the runs except Run 5, the actual

Table 7-3. Equilibrium Stage Comparison

Run Number	Average Solute Concentration, ppm			One Theoretical Stage Extract Concentration
	Feed	Extract	Raffinate	
3	167	450	18	522
4	149	469	18	522
5	294	783	22	638
6	709	1561	65	1885
7	646	1083	63	1827

benzaldehyde concentration in the extract is slightly less than that calculated for the case where one equilibrium stage was assumed (column five). The implication is that in the 5 ft high experimental column there is close to one theoretical stage.

A graphical determination of the number of transfer stages performed following the discussion in Chapter 3 is shown in Figure 7-1. Because of the steep slope of the equilibrium curve it is somewhat difficult to see, but there is less than one stage for all of the runs except Run 5 which has very close to one stage. The dashed lines in Figure 7-1 show the step representing an equilibrium stage for Run 5 and Run 6;

2. Table 7-4 displays the values for the number of transfer units, NTU, and the height of a transfer unit, HTU, based on film-transfer theory. Since the principal resistance to diffusion was in the raffinate phase (large distribution coefficient), Equation 3-31, was used to calculate the NTU values. Further, since the benzaldehyde concentrations were dilute and the mutual solubilities of water and carbon dioxide are low, the integral of Equation 3-31 was evaluated using Equation 3-40. Examples of

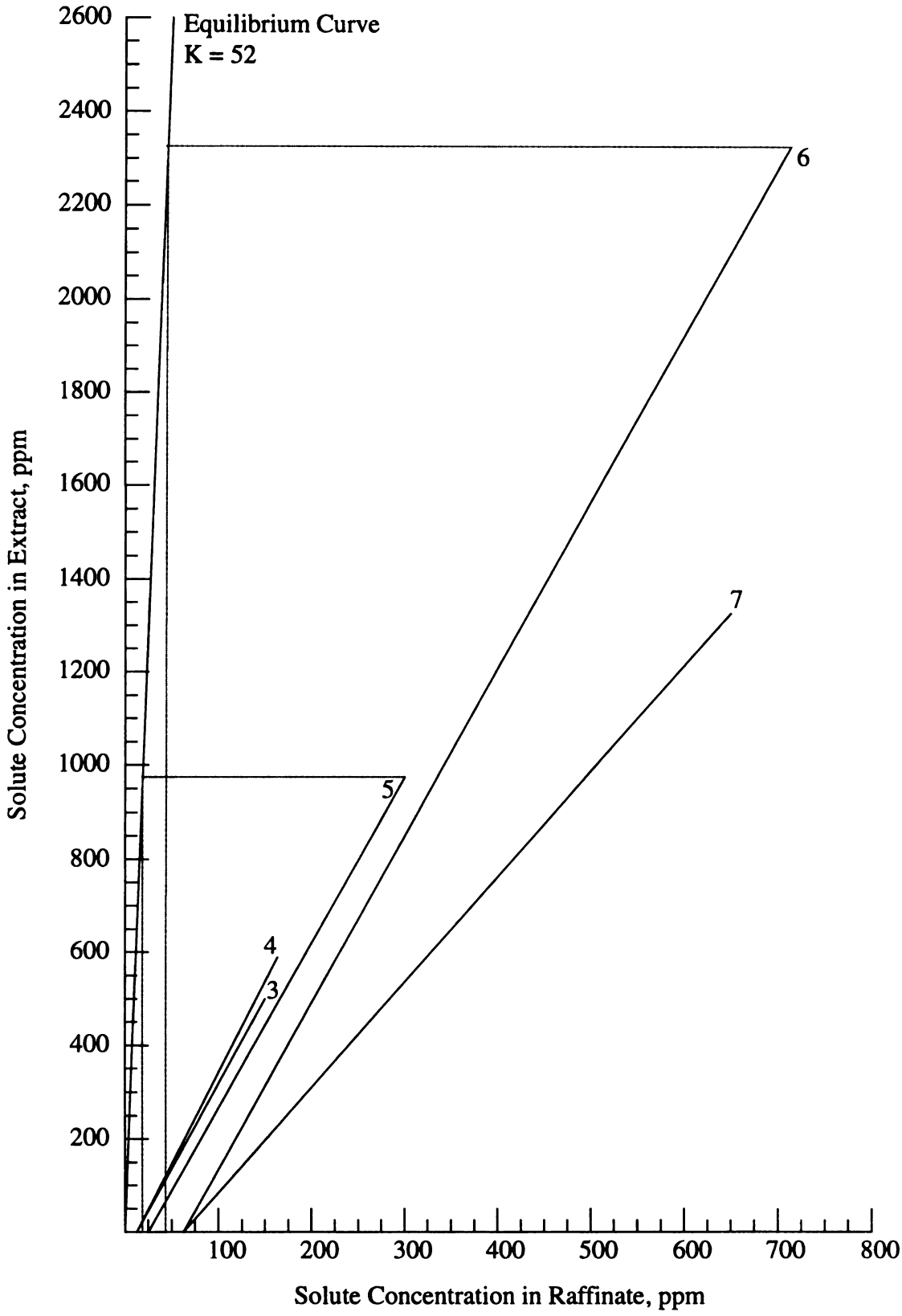

Figure 7-1. Graphical Determination of Equilibrium Stages

Table 7-4. NTU and HTU Based on Film-Transfer Theory

Run Number	NTU	HTU ft
3	2.52	1.98
4	2.38	2.10
5	2.90	1.72
6	2.68	1.87
7	2.48	2.02

these calculations are shown in Appendix E. The height of a transfer unit was calculated by dividing the height of the experimental column, 5 ft, by the number of transfer units;

3. A determination of the extraction factor and the number of stages using the Kremser method is shown in Table 7-5. Examples of these calculations are also shown in Appendix E.

Table 7-5. Equilibrium Stages Calculated by the Kremser Method

Run Number	Extraction Factor U	Number of Stages n
3	14.9	1.08
4	15.6	0.95
5	15.7	1.45
6	15.9	1.17
7	25.4	0.84

CHAPTER 8

CONCLUSIONS AND RECOMMENDATIONS

Conclusions

The flooding correlation of Venkataraman and Laddha appears to be to conservative for the benzaldehyde/carbon dioxide/water system. More runs are required to determine if the correlations of Rao and Rao or Crawford and Wilke are suitable for use in predicting flooding with this system. This is a very important information required for any scale-up.

The limited number of runs conducted so far all used low values for the ratio of the aqueous phase flow to the carbon dioxide phase flow (i.e. the slope of the operating lines, R/E) ranging from 2.05-3.5. These initial values were conservative because the equipment was new and unproven with respect to where flooding would occur. The very high distribution coefficient of 52 indicates that much higher ratios of the two solvents can be used.

As the ratio of aqueous phase to carbon dioxide is increased, the 6.5% (wt) solubility of carbon dioxide in water must be compensated for. The carbon dioxide flows in Runs 3-7 were greater than 5 g/min because at an aqueous feed of about 17 g/ min. such as those used in Runs 3-6, the weight of carbon dioxide in the raffinate will be approximately 1.2 g/min which is almost 25% of the carbon dioxide feed. There is a practical aspect of using carbon dioxide flows less than 5 g/min that must also be considered. The backpressure regulator which controls the column pressure by regulating the flow of carbon dioxide is slightly oversized. When operating, it would open too far and allow the column pressure to decrease by approximately 80 psig. It would take about 15 minutes for the pressure to recover before the valve opened again. Lower carbon dioxide flows will make this problem worse. If possible, a smaller backpressure regulator should be purchased and installed.

The material balance for one equilibrium stage for Runs 3-7 clearly indicate there is close to one stage in the 5 ft high column (Table 7-3) as does the Kremser method (Table 7-5). Film-transfer theory yields a different value of about 2.5 transfer units. However, the film-transfer theory calculations are suspect in regards to accuracy. The integral in the defining equation for the number of transfer units, Equation 3-31, was simplified so that it could be solved analytically, Equation 3-40. This simplification assumes that the two solvents are insoluble. Although the solubility of carbon dioxide in water is relatively low (6.5% wt) it may still not be low enough for the simplification to be used. The integral should be solved numerically to determine if the number of transfer units is closer to one as suggested by the other methods.

Recommendations

The following work and/or changes to continue this project are as follows:

1. Install a weigh cell or scale to monitor the flow of carbon dioxide. Currently, only the benzaldehyde and water flows can be monitored and used for material balance calculations.

2. Make more runs of the column to investigate where flooding occurs to determine whether or not one of the correlations by Rao and Rao or Crawford and Wilke is applicable. This is necessary to provide information for scale-up of the column to commercial size.

3. Make more runs with different ratios of aqueous feed to carbon dioxide. Compare the number of theoretical stages, the number of transfer units, and the Kremser method stages calculated with this additional data to the numbers already obtained to verify their accuracy.

4. Make additional runs using different feed distributor designs to determine if a more efficient design is possible.

5. Consider purchasing a smaller backpressure regulator to control the column pressure and regulate the carbon dioxide flow out the top of the column. The existing regulator is slightly oversized.

APPENDIX A

PHYSICAL PROPERTIES

Table A-1. Physical Properties of Carbon Dioxide

	U.S. Units[1]	Metric Units[1]
International Symbol	CO_2	CO_2
Molecular Weight	44.01	44.01
Vapor Pressure		
at 70 F (21.1 C)	838 psig	5778 kPa, gage
at 32 F (21.1 C)	491 psig	3385 kPa
at 2 F (-16.7 C)	302 psig	2082 kPa
at -20 F (-28.9 C)	200 psig	1379 kPa
at -69.9 F (-56.6 C)	60.4 psig	416 kPa
at -109.3 F (-78.5 C)	0 psig	0 kPa
Density of the gas		
at 70 F (21.1 C)	0.1144 lb/ft^3	1.833 kg/m^3
at 32 F (0 C)	0.1234 lb/ft^3	1.977 kg/m^3
Specific gravity of the gas		
at 70 F (21.1 C), 1 atm (air = 1)	1.522	1.522
at 32 F (0 C), 1 atm	1.524	1.524
Specific Volume of the gas		
at 70 F (21.1 C), 1 atm (air = 1)	8.741 ft^3/lb	0.5457 m^3/kg
at 32 F (0 C), 1 atm	8.104 ft^3/lb	0.5059 m^3/kg
Density of liquid, saturated		
at 70 F (21.1 C)	47.6 lb/ft^3	762 kg/m^3
at 32 F (21.1 C)	58.0 lb/ft^3	929 kg/m^3
at 2 F (-16.7 C)	63.3 lb/ft^3	1014 kg/m^3
at -20 F (-28.9 C)	66.8 lb/ft^3	1070 kg/m^3
at -69.9 F (-56.6 C)	73.5 lb/ft^3	1177 kg/m^3
Critical temperature (1 atm)	87.9 F	31.1 C
Critical pressure	1070.6 psia	7382 kPa, abs

Table A-1. Continued

	U.S. Units[1]	Metric Units[1]
Critical density	29.2 lb/ft^3	468 kg/m^3
Latent heat of vaporization		
at 32 F (21.1 C)	100.8 Btu/lb	234.5 kJ/kg
at 2 F (-16.7 C)	119.0 Btu/lb	276.8 kJ/kg
at -20 F (-28.9 C)	129.6 Btu/lb	301.4 kJ/kg
Specific heat of gas		
at 77 F (25 C)		
C_p	0.203 Btu/lb F	0.850 kJ/kg C
C_v	0.157 Btu/lb F	0.657 kJ/kg C
Ratio of specific heats	1.304	1.304
Solubility in water, vol/vol		
at 68 F (20 C)	0.90	0.90
Solubility in water, (wt/wt)[2]		
at 25 C, 125 atm	0.063	0.063
Viscosity of saturated liquid		
at 2 F (-16.7 C)	0.287 lb/ft hr	0.119 g/cm sec

[1] Above values from: Compressed Gas Association, Handbook of Compressed Gases

[2] Wiebe, 1977

Table A-2. Physical Properties of Water

	U.S. Units	Metric Units
Solubility in carbon dioxide at 25 C, 125 atm[2]	0.0014	0.0014
[2]Wiebe, 1977		

Table A-3. Physical Properties of Benzaldehyde

	U.S. Units[3]	Metric Units[3]
Formula C_7H_6O		
M. W.	106.13	106.13
Viscosity of liquid at 25 C		1.39 g/cm sec
Boiling Point		178 C
Specific gravity	$1.045^{10/4}$	$1.045^{10/4}$
[3] Weast, 1970		

Table A-4. Physical Properties of Isopentyl Alcohol (Isoamyl Alcohol)

	U.S. Units[3]	Metric Units[3]
Formula $C_5H_{12}O$		
M. W.	88.15	88.15
Viscosity of liquid at 10 C		6.20 g/cm sec
Boiling Point		128.5 C
Specific gravity	0.8092	0.8092
[3]Weast, 1970		

Table A-5. Physical Properties of n-Propanol

	U.S. Units[3]	Metric Units[3]
Formula C_3H_8O		
M. W.	60.11	60.11
Viscosity of liquid at 20 C at 30 C		 2.256 g/cm sec 1.72 g/cm sec
Boiling Point		97.4 C
Specific gravity at 20 C	0.8035	0.8035
[3]Weast, 1970		

APPENDIX B

ETHANOL PHASE GAS CHROMATOGRAPHY

An internal standard method using isopentyl alcohol (IPA) as the standard was used to determine the concentration of benzaldehyde in the aqueous phase. A Perkin-Elmer model 8500 equipped with a hot-wire thermal conductivity detector was used for the gas chromatography. The column was an Alltech Associates, Inc. Econo-Cap capillary column, catalog number 19653, 10 m long x 0.53 mm ϕ, with a 1.2 μm thick carbowax stationary phase.

Calibration mixtures of isopentyl alcohol and benzaldehyde were prepared according to Table B-1. The column was calibrated by injecting each of the sample mixtures multiple times and recording the number of area counts detected per unit of sample mixture injection volume. The data are presented in Table B-2. Calibration curves were prepared for both the internal standard, isopropyl alcohol, and benzaldehyde and are shown in Figure B-1 and Figure B-2.

The column operating conditions including the temperature versus time profile are shown in Figure B-3.

A sample chromatogram is shown in Figure B-4.

Table B-1. Ethanol Phase Calibration Standards

Sample Description	Ethanol g	IPA µl	Benz. µl	IPA Conc. ppm (wt)	Benz. Conc. ppm (wt)
1	14.7316	20	15	1100	1068
2	13.9332	30	25	1744	1882
3	13.6305	50	40	2971	3078
4	13.1170	75	55	4631	4398
5	12.1774	85	65	5654	5599
6	11.2367	100	85	7209	7935
7	8.3474	100	100	9704	12,567
Specific Gravity IPA = 0.81 at 20 °C Specific Gravity of Benzaldehyde = 1.049 at 20 °C					

Table B-2. Ethanol Phase G. C. Calibration Data

Sample Description	Injection Volume µl	IPA AC*/µl	Benz. AC*/µl
1	.3	16.67	17.28
1	.3	16.85	18.01
1	.3	16.89	17.86
1	.3	16.37	17.58
2	.3	26.44	30.66
2	.3	25.36	29.93
2	.3	27.33	31.89
2	.3	27.28	31.92
3	.3	41.22	45.76
3	.3	48.27	52.29
3	.3	48.16	53.23
3	.3	45.37	49.54
4	.3	74.13	74.42
4	.3	73.69	72.65
4	.3	70.85	70.81
4	.3	71.88	72.53

* AC = Area Counts

Table B-2. Continued

Sample Description	Injection Volume µl	IPA AC*/µl	Benz. AC*/µl
5	.3	89.90	93.91
5	.3	90.03	102.17
5	.3	88.15	91.83
5	.3	90.30	93.33
6	.3	106.74	122.35
6	.3	111.27	127.32
6	.3	102.71	118.56
6	.3	108.13	125.20
7	.3	152.05	206.48
7	.3	151.20	205.30
7	.3	136.65	185.03
7	.3	120.11	162.45

* AC = Area Counts

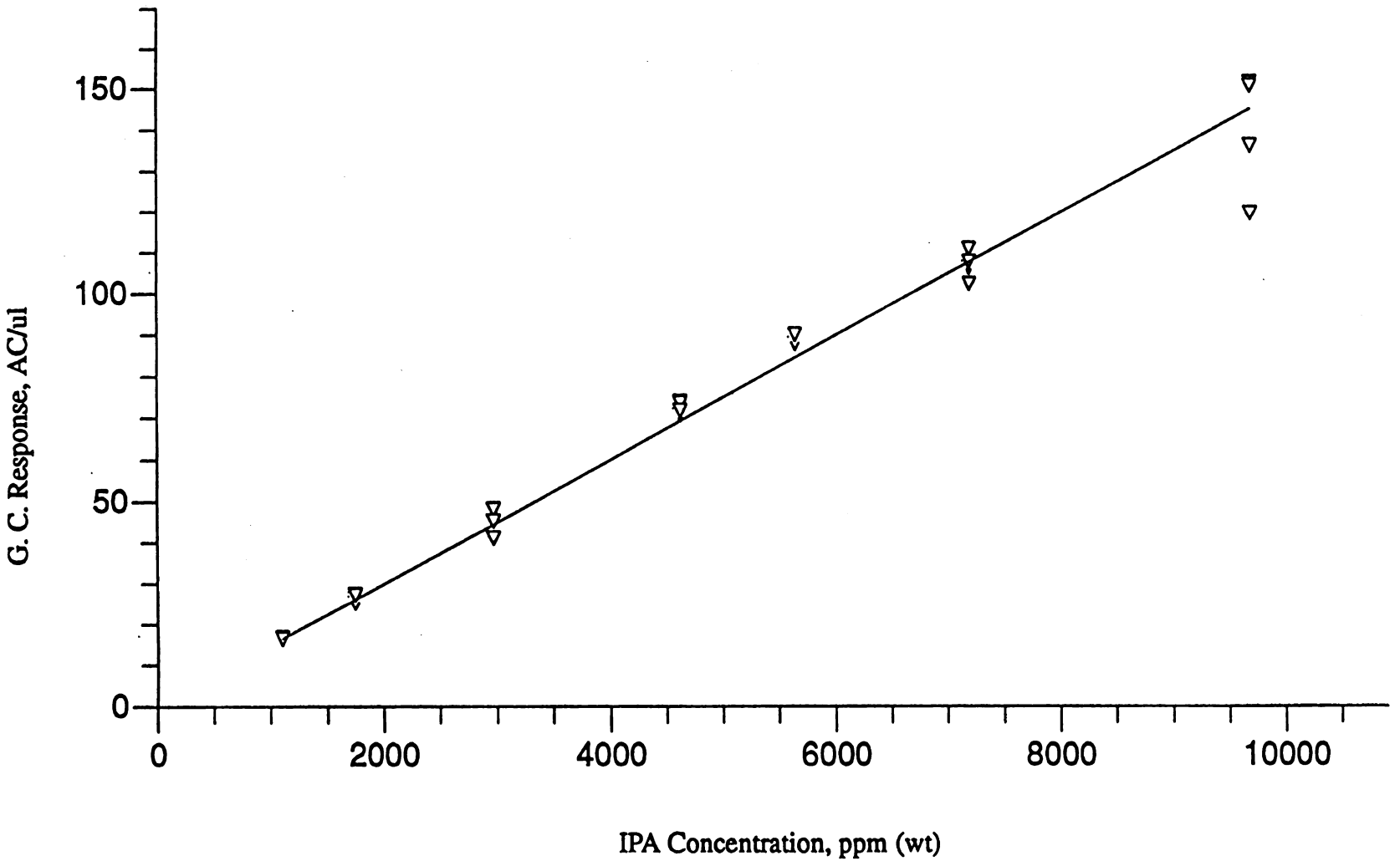

Figure B-1. IPA Concentration versus G.C. Response

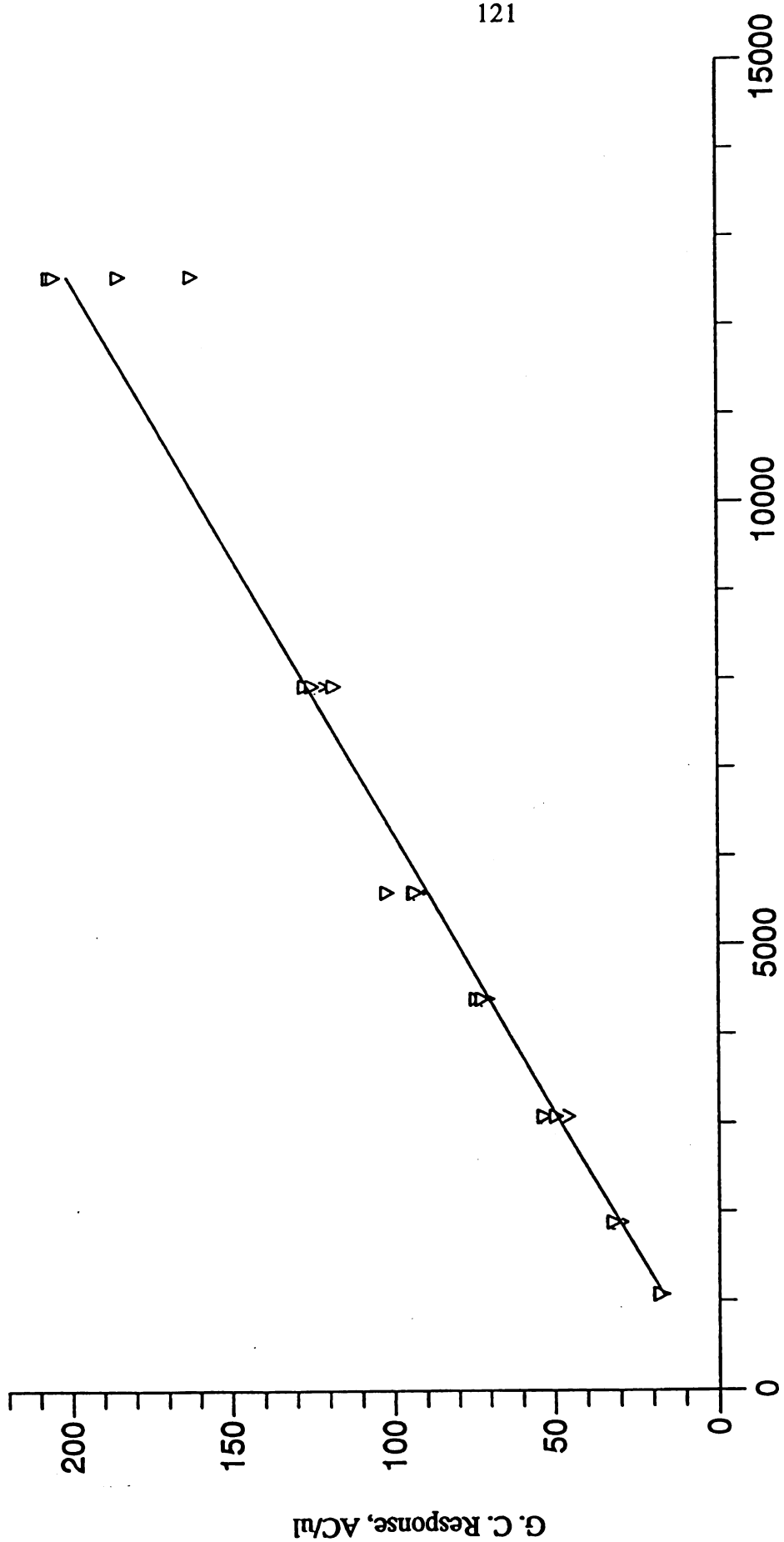

Figure B-2. Benzaldehyde Concentration versus G. C. Response

```
SECTION 1   GC CONTROL

                                  1        2
     OVEN TEMP (DEG C)           60      200
     ISO TIME  (MIN)            4.0      0.5
     RAMP RATE (DEG C/MIN)     30.0

     HWD 1 RANGE  OFF       HWD 1 POLARITY B-A
     FID 2 SENS   LOW

     DET ZERO      ON
     INITIAL DET    2

     INJ 1 TEMP   OFF
     INJ 2 TEMP   250
     DET 1 TEMP   250
     DET 2 TEMP   270

     FLOW  1    1 ML/MIN      FLOW  2    1 ML/MIN      PRESSURE 3    1.3 PSIG
     CARRIER GAS 1 HE         CARRIER GAS 2 HE

     EQUILIB TIME       0.0 MIN
     TOTAL RUN TIME     9.1 MIN

SECTION 3   DATA HANDLING

     DATA ACQUISITION                    REPORT

     START TIME     0.00 MIN             CALC TYPE       %
     END TIME       9.16 MIN             AREA/HT CALC    AREA
                                         PRINT TOL       0.0000
     WIDTH             3                 OUTPUT
     SKIM SENS        10                   SCREEN       YES
     BASELINE CORR    V-V                  PRINTER       NO
                                           EXT DEV       NO
     DET 1 AREA SENS  200
     DET 2 AREA SENS  200
     DET 1 BASE SENS    4
     DET 2 BASE SENS    4

     PEAK IDENTIFICATION                 QUANTITATION

     UNRETD PEAK TIME      0.00 MIN      SCALING FACTOR      25.3389
     AREA/HT REJECT      1.0000

     REF PK: TIME          3.36 MIN
             TIME TOL      0.10 MIN

     COMPONENT LIST

     RT        RF        STD AMT   NAME          GRP

       3.36    1.0000      199.1000  IBA            0
       6.22    1.0000        0.0000  BENZ           0
```

Figure B-3. G. C. Column Operating Conditions for Ethanol Phase

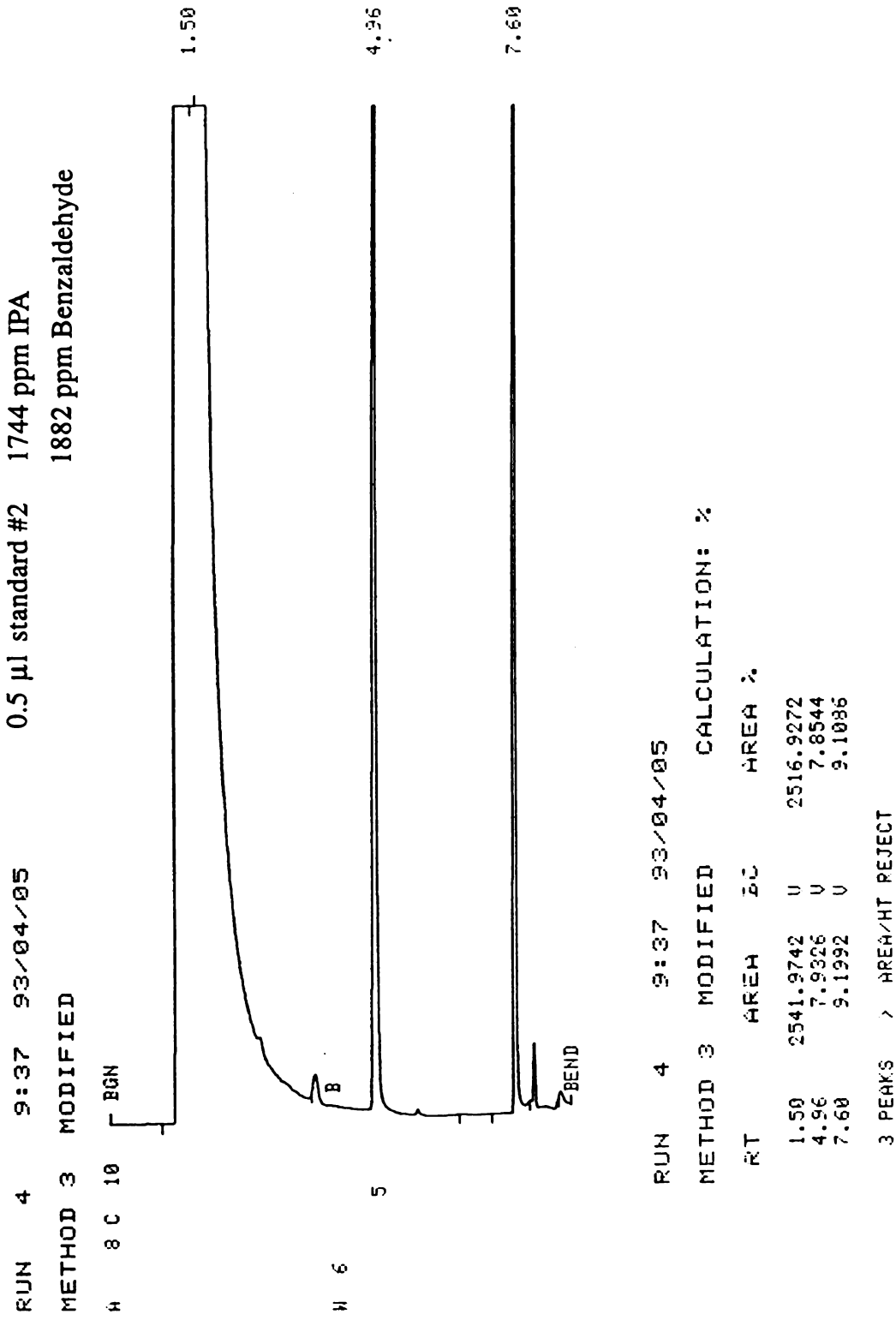

Figure B-4. Sample Chromatogram for Ethanol Phase

APPENDIX C

AQUEOUS PHASE GAS CHROMATOGRAPHY

An internal standard method using n-propanol as the standard was used to determine the concentration of benzaldehyde in the aqueous phase. A Perkin-Elmer model 8500 equipped with a hot-wire thermal conductivity detector was used for the gas chromatography. The column was an Alltech Associates, Inc. Econo-Cap capillary column, catalog number 19653, 10 m long x 0.53 mm ϕ , with a 1.2 μm carbowax stationary phase.

Calibration mixtures of n-propanol and benzaldehyde were prepared as shown in Table C-1, Table C-2, and Table C-3. The column was calibrated by injecting each of the mixtures multiple times and recording the number of area counts detected per unit of sample mixture injected into the gas chromatograph. The results are presented in Table C-4, Table C-5, and Table C-6. Calibration curves were prepared for both the aqueous phase internal standard, n-propanol, and benzaldehyde and are shown in Figure C-1, Figure C-2, and Figure C-3 respectively.

The column operating conditions including the temperature versus time profile are shown in Figure C-4.

A sample chromatogram is shown in Figure C-5.

Table C-1. G. C. Calibration Mixtures of n-Propanol/Water

Sample Description	Water g	n-Propanol g	n-Propanol ppm
4	13.9088	.0318	2286
5	15.8686	.0400	2521
6	14.8453	.0447	3011
7	16.4039	.0580	3536
8	15.9350	.0645	4048

Table C-2. G. C. Calibration Mixtures of Benzaldehyde/Water

Sample Description	Water g	Benzaldehyde g	Benzaldehyde ppm
1	99.47	.0136	137
2	99.47	.0220	221
3	99.38	.0325	327
R1	99.45	.0115	116
R2	99.49	.0275	276

Table C-3. G. C. Calibration Mixtures of Benzaldehyde/Water

Sample Description	Water g	Benzaldehyde g	Benzaldehyde ppm
F1	18.0231	.0272	1509
F2	13.5357	.0253	1869
F3	15.6002	.0332	2128
F4	11.7451	.0315	2682

Table C-4. n-Propanol/Water G.C. Calibration Data

Sample Description	Sample Volume µl	n-Propanol AC/µl
4	.5	31.0372
4	.5	31.9292
4	.5	30.1992
4	.4	32.3858
4	.3	32.1330
5	.4	35.1278
5	.4	35.7135
5	.3	36.156
6	.3	42.664
6	.3	43.2277
6	.3	42.7687
7	.3	49.654
7	.3	49.9863
7	.3	50.1897
8	.3	57.0787
8	.3	56.8027
8	.3	56.5543
AC = Area Counts		

Table C-5. Benzaldehyde/Water G.C. Calibration Data

Sample Description	Sample Volume µl	Benzaldehyde AC/µl
1	.5	2.4842
1	.5	2.4152
1	.5	2.4510
2	.5	4.0940
2	.5	4.1094
2	.5	4.0060
3	.5	6.1258
3	.5	6.0394
3	.5	6.2208
R1	.5	2.1376
R1	.5	2.0526
R1	.5	2.0264
R2	.5	4.8794
R2	.5	4.9504
R2	.5	4.8908

Table C-6. Benzaldehyde/Water G.C. Calibration Data

Sample Description	Sample Volume µl	Benzaldehyde AC/µl
F1	.5	26.9498
F1	.3	27.5753
F1	.3	27.4340
F2	.3	34.2380
F2	.3	34.0917
F2	.2	34.3615
F3	.3	39.3780
F3	.2	39.3450
F3	.2	39.5530
F4	.2	47.6050
F4	.2	48.7700
F4	.2	49.6200

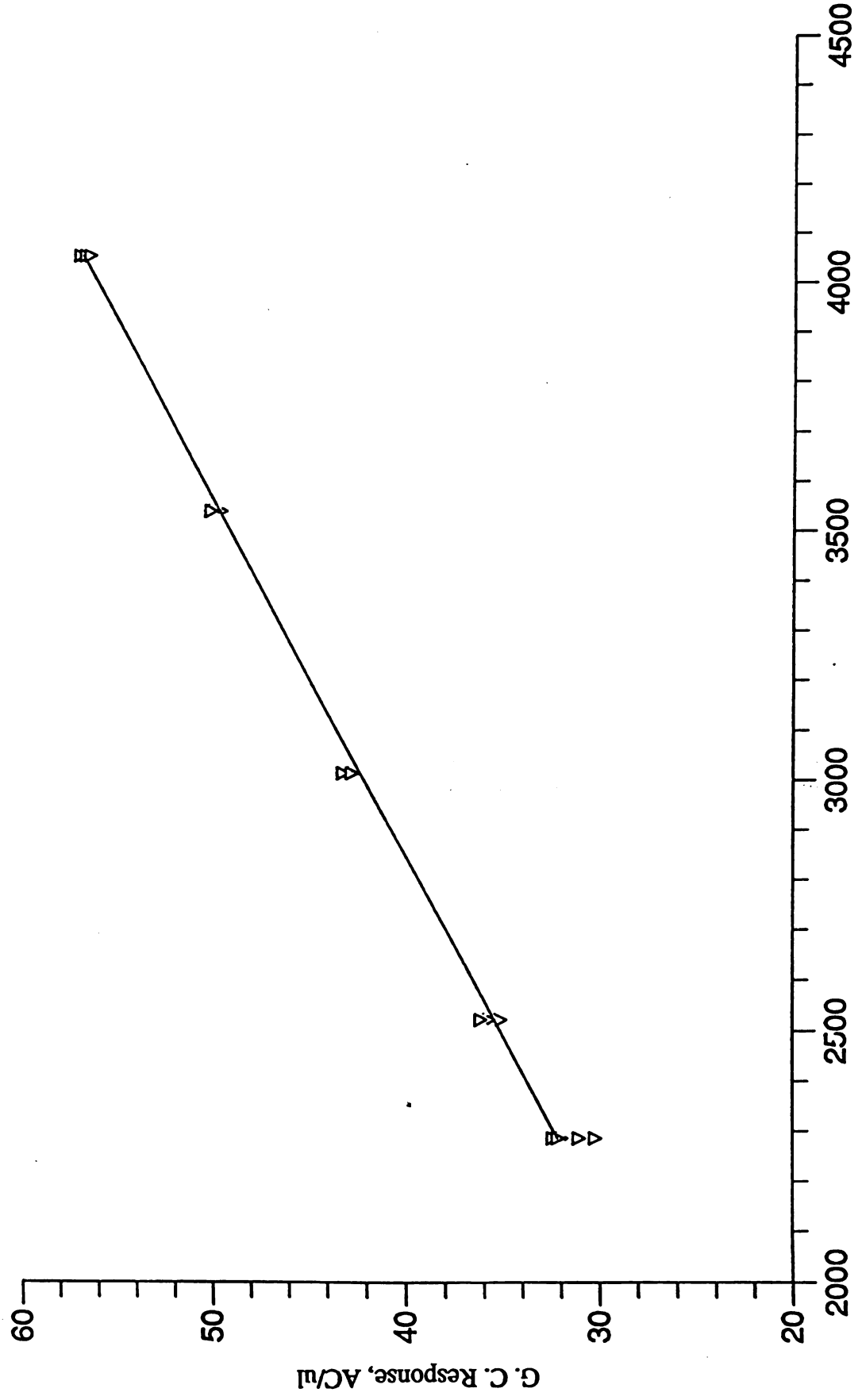

Figure C-1. n-Propanol Concentration versus G. C. Response

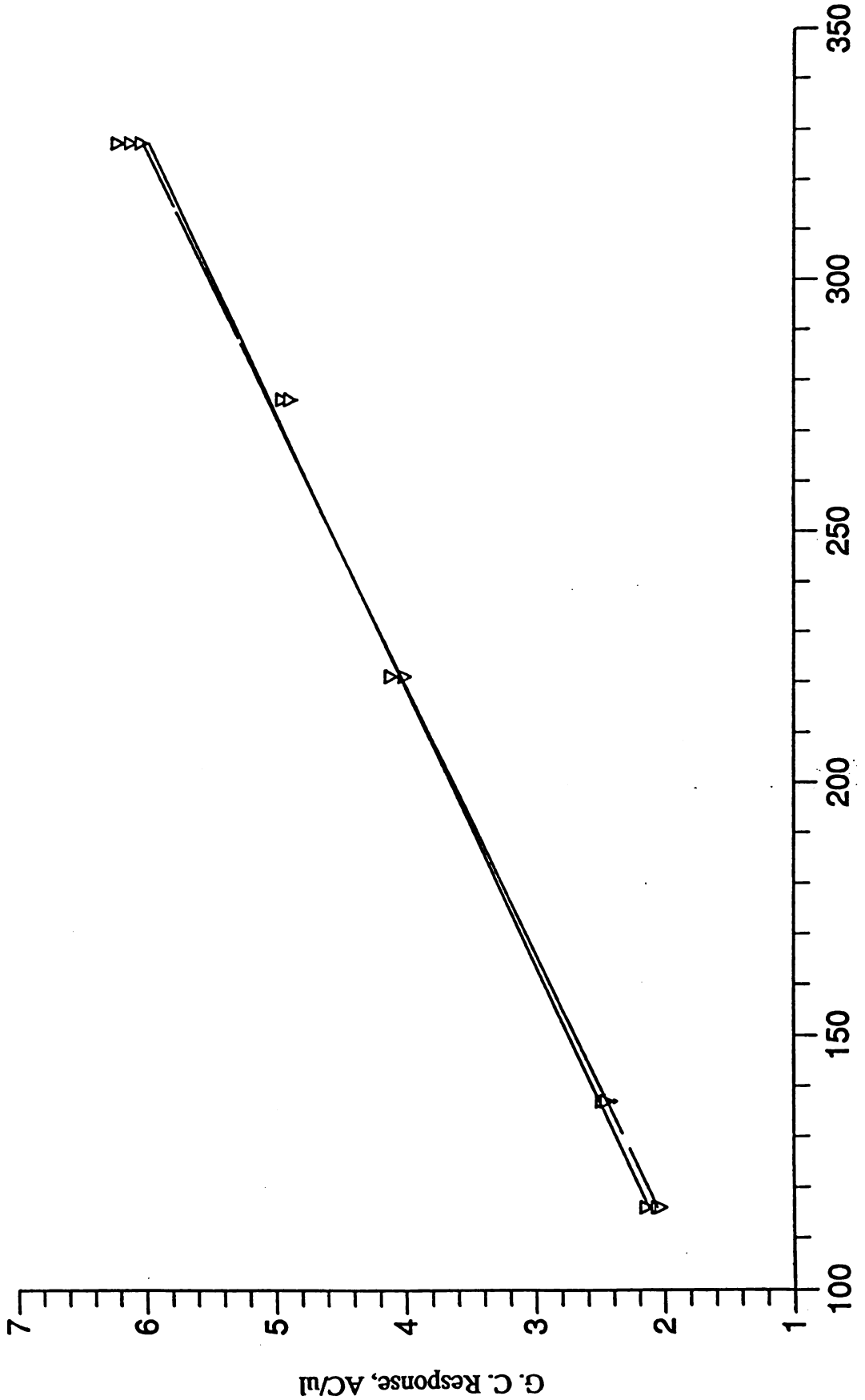

Figure C-2. Benzaldehyde Concentration versus G.C. Response

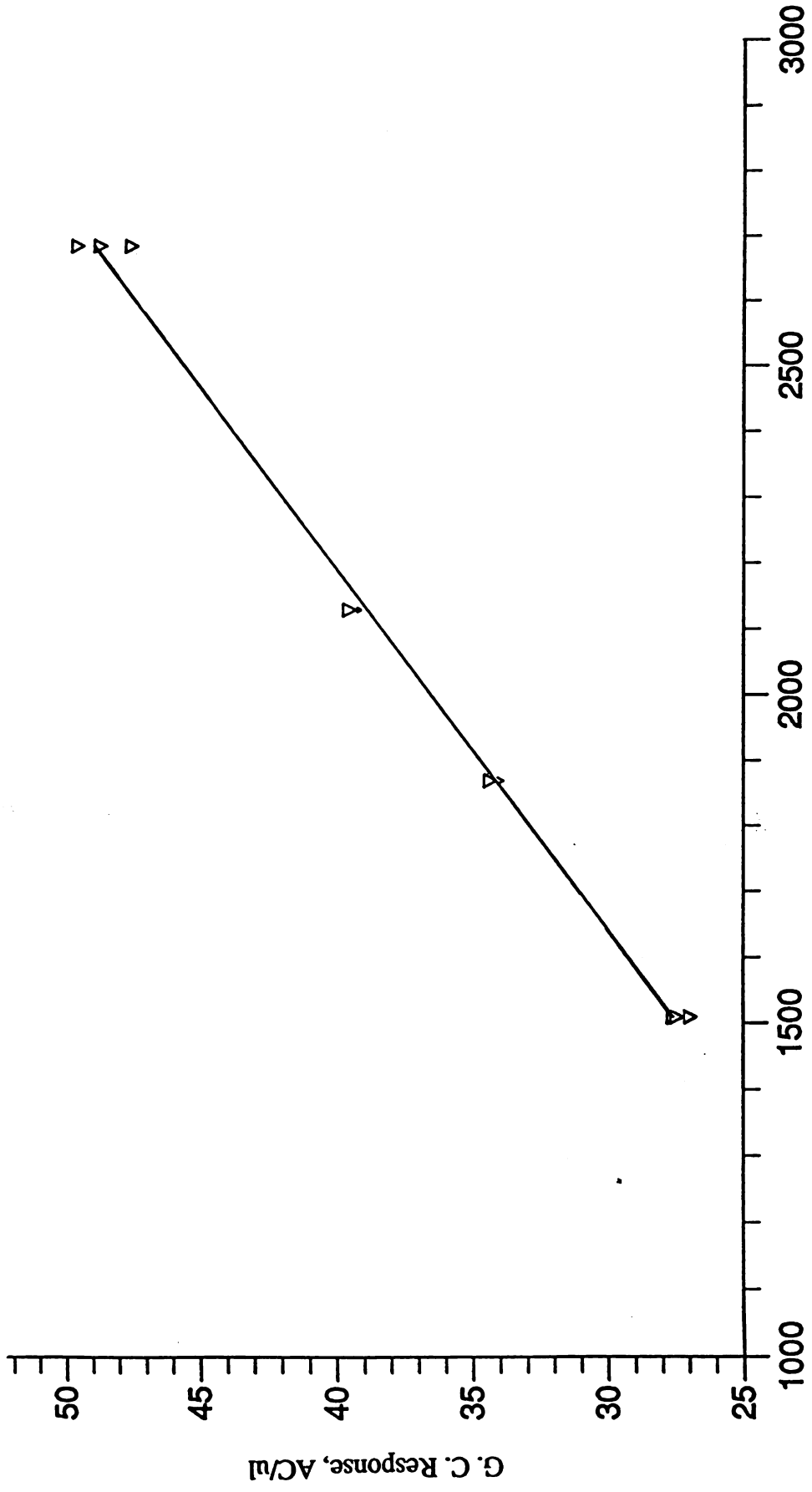

Figure C-3. Benzaldehyde Concentration versus G. C. Response

```
SECTION 1  GC CONTROL

                              1        2
   OVEN TEMP (DEG C)         70      200
   ISO TIME  (MIN)          0.0      1.0
   RAMP RATE (DEG C/MIN)   30.0

   HWD 1 RANGE  OFF      HWD 1 POLARITY B-A
   FID 2 SENS  LOW

   DET ZERO     ON
   INITIAL DET   2

   INJ 1 TEMP  OFF
   INJ 2 TEMP  250
   DET 1 TEMP  250
   DET 2 TEMP  270

   FLOW  1   1 ML/MIN      FLOW  2   1 ML/MIN      PRESSURE 3   1.3 PSIG
   CARRIER GAS 1 HE        CARRIER GAS 2 HE

   EQUILIB TIME      0.0 MIN
   TOTAL RUN TIME    5.3 MIN

SECTION 3  DATA HANDLING

   DATA ACQUISITION                    REPORT

   START TIME    0.00 MIN              CALC TYPE      %
   END TIME      5.33 MIN              AREA/HT CALC   AREA
                                       PRINT TOL      0.0000
   WIDTH            5                  OUTPUT
   SKIM SENS        1                    SCREEN      YES
   BASELINE CORR   V-V                   PRINTER      NO
                                         EXT DEV      NO
   DET 1 AREA SENS  200
   DET 2 AREA SENS  200
   DET 1 BASE SENS    4
   DET 2 BASE SENS    4

   PEAK IDENTIFICATION                 QUANTITATION

   UNRETD PEAK TIME     0.00 MIN       SCALING FACTOR       1.0000
   AREA/HT REJECT     0.2500

   REF PK: TIME         0.00 MIN
           TIME TOL     0.10 MIN
```

Figure C-4. G. C. Column Operating Conditions for Aqueous Phase

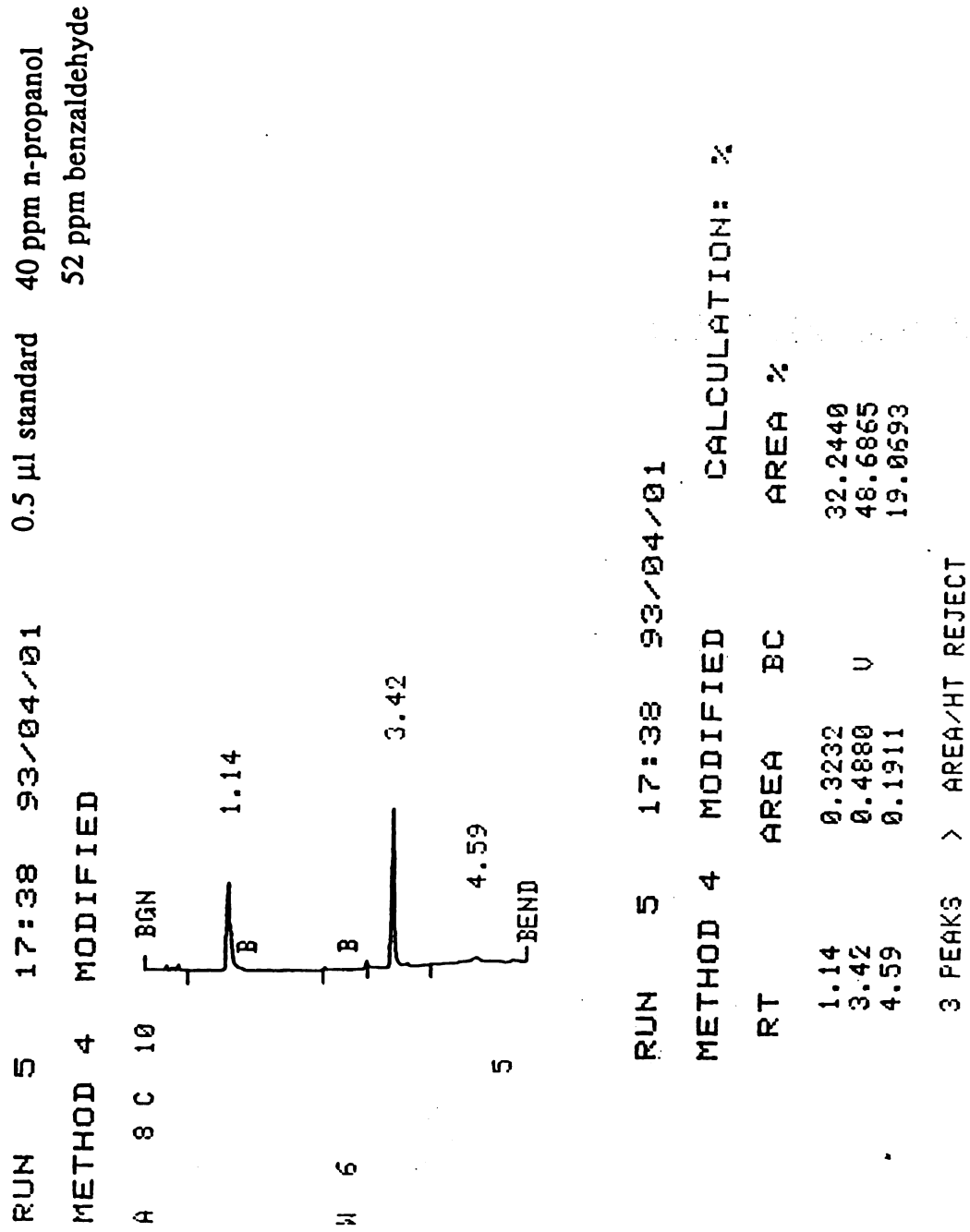

Figure C-5. Sample Chromatogram for Aqueous Phase G. C. Analysis

APPENDIX D

ULTRAVIOLET SPECTROPHOTOMETRY

Ultraviolet spectrophotometry was used to analyze for benzaldehyde in water. Benzaldehyde exhibits a strong absorption in the ultraviolet region of the electromagnetic spectrum at 241 nanometers as shown in Figure D-1 (Simons, W. W., Ed, spectra 2163).

Two calibration standards of 10 ppm (wt) and 210 ppm (wt) were prepared and used to calibrate the u.v. spectrophotometer. Aliquots of each of these standards were diluted and run on the u.v. to measure their absorbance. The results are presented in Table D-1. The results for both standards are plotted in the calibration curve shown in Figure D-2.

BENZALDEHYDE 2163

C_7H_6O

Mol. Wt. 100.12

B.P. 179°C (lit.)

Solvent: Cyclohexane

λ Max. mμ	^{a}m	Cell mm	Conc. g/L
352	22.2	10	5.13
338	27.3	10	5.13
327	26.3	10	5.13
317	24.2	10	5.13
305	19.4	10	5.13
288	974	10	0.103
278.5	1150	10	0.103
241	15200	10	0.010
* 214.5	2603	10	0.010

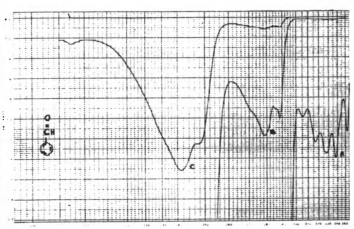

Figure D-1. U.V. Spectra for Benzaldehyde

Table D-1. Benzaldehyde/Water U. V. Calibration Data

Standard Concentration ppm (wt)	Dilution Ratio	Sample Concentration ppm (wt)	Absorbance Reading
10	1.5:1	6.67	.785
10	2:1	5.0	.606
10	3:1	3.3	.406
10	4:1	2.5	.306
10	10:1	1.0	.125
210	40:1	5.25	.596
210	40:1	5.25	.606
210	40:1	5.25	.616
210	50:1	4.2	.489
210	80:1	2.63	.306
210	80:1	2.63	.300

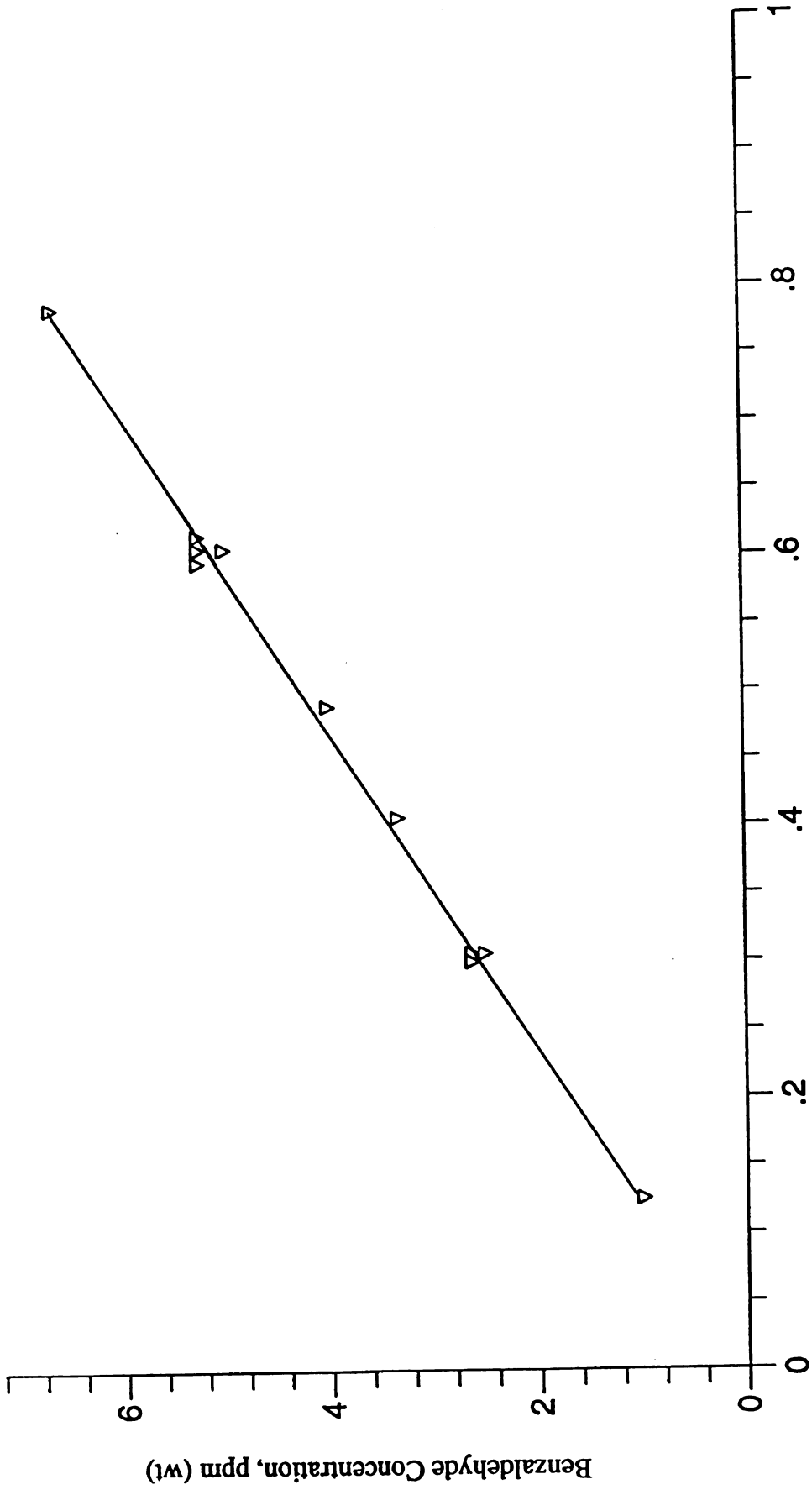

Figure D-2. Benzaldehyde/Water U.V. Spectophotometer Calibration Curve

APPENDIX E

SAMPLE CALCULATIONS

Number of Transfer Units

The defining equation for the number of transfer units developed from film-transfer theory is given by Equation 3-31:

E-1

$$NTU_{OR} = \int_{x_{R_2}}^{x_{R_1}} \frac{(1-x_R)_{OM}\, dx_R}{(1-x_R)\,(x-x_R^*)}$$

$$= \int_{x_{R_2}}^{x_{R_1}} \frac{dx_R}{(1-x_R)\ln\left[\dfrac{(1-x_R^*)}{(1-x_R)}\right]} = \frac{H}{HTU_{OR}}$$

Because the benzaldehyde concentrations were very dilute and the water and carbon dioxide solvents are relatively insoluble (0.014 g H_2O/g CO_2 and 6.4 g CO_2/g H_2O at 25 C, 1500 psig respectively) Equation 3-31 can be simplified using the assumption described in Chapter 3: Simplified Integration:

$$\int_{x_{R_2}}^{x_{R_1}} \frac{dx_R}{(x_R - x_R^*)} = \frac{1}{1-\dfrac{R}{mE}} \ln\left[\left(1-\frac{R}{mE}\right)\left(\frac{x_{R_1} - \dfrac{x_{E_2}}{m}}{x_{R_2} - \dfrac{x_{E_2}}{m}}\right) + \frac{R}{mE}\right] \qquad \text{E-2}$$

where x_{R_1} mole fraction benzaldehyde in feed

x_{R_2} mole fraction benzaldehyde in raffinate

x_{E_2} mole fraction benz. in carbon dioxide feed

m is the distribution coefficient = 52

R water flow rate, gmol/min

E carbon dioxide flow rate, gmol/min

For Run 3 the above parameters were:

mol fraction benz. in H_2O feed	2.84×10^{-5}
mol fraction benz. in CO_2 feed	0
mol fraction benz. in extract	1.87×10^{-3}
mol fraction benz. in raffinate	3.06×10^{-6}
water flow rate	0.95 gmol/min
carbon dioxide flow rate	0.21 gmol/min

Then

$$\frac{R}{mE} = \frac{0.95 \frac{gmol}{min}}{(52)\, 0.21 \frac{gmol}{min}} = 0.087 \qquad \text{E-3}$$

and

$$1 - \frac{R}{mE} = 1 - 0.087 = 0.913 \qquad \text{E-4}$$

$$\frac{1}{1 - \frac{R}{mE}} = 1.096 \qquad \text{E-5}$$

$$\frac{x_{E_2}}{m} = 0 \qquad \text{E-6}$$

Substitution into Equation E-3 yields:

$$\frac{1}{1-\frac{R}{mE}} \ln \left[\left(1-\frac{R}{mE}\right) \left(\frac{x_{R_1} - \frac{x_{E_2}}{m}}{x_{R_2} - \frac{x_{E_2}}{m}} \right) + \frac{R}{mE} \right] = (1.096) \ln \left[0.913 \left(\frac{2.84\times10^{-5}}{3.06\times10^{-6}} \right) + 0.087 \right]$$

$$= 2.52$$

The height of a transfer unit, HTU_{OR} is given by Equation 3-21

$$HTU_{OR} = \frac{H}{NTU_{OR}} = \frac{5ft}{2.52} = 1.98ft \qquad \text{E-8}$$

APPENDIX F

NOTATION

A	Mass flow of feed solvent alone in feed (mol/h)
A_T	Column (tower) cross-sectional area (m^2)
a	Interfacial area per unit volume of tower (m^2/m^3)
a_p	Surface area of packing (m^2/m^3)
C_E	Concentration of solute in extract phase ($kmol/m^3$)
C_{Ei}	Concentration of solute in extract liquid film interface ($kmol/m^3$)
C_R	Concentration of solute in raffinate phase ($kmol/m^3$)
C_R^*	Equilibrium concentration of solute in the raffinate, ($kmol/m^3$
C_{Ri}	Concentration of solute in raffinate liquid film interface ($kmol/m^3$)
$(\Delta C_R)_{lm}$	Logarithmic mean of $(C_R - C_R^*)_1$ and $(C_R - C_R^*)_2$
E	Extract
F	Packing factor
g	Gravitational acceleration, 32.2 ft/s^2
H	Extraction column height, (m)
H_E	Height of a transfer unit based on the extract phase mass transfer coefficient
H_{OR}	Height of an overall transfer unit based on raffinate phase mass transfer resistances (m)
H_{OE}	Height of an overall transfer unit based on extract phase mass transfer resistances(m)
H_R	Height of a transfer unit based on the raffinate phase mass transfer coefficient
HTU	Height of a film transfer unit, (m)
k_E	Extract liquid-film mass transfer coefficient (m/s)

k_R	Raffinate liquid-film mass transfer coefficient (m/s)
K_E	Overall mass transfer coefficient based on extract phase (m/s)
K_R	Overall mass transfer coefficient based on raffinate phase (m/s)
L_E	Extract volumetric flow rate per unit area (m^3/m^2 s)
L_R	Raffinate volumetric flow rate per unit area (m^3/m^2 s)
m	Distribution coefficient in weight or mole fractions
N	Solute transfer rate per unit area (kmol/m^2 s)
N_E	Number of transfer units based on extract mass transfer coefficient
N_R	Number of transfer units based on raffinate mass transfer coefficient
N_T	Number of film transfer units
P	Pressure, Pa
P_R	Reduced pressure
Q	Mass flow rate, g/min
R	Raffinate
S	Mass flow rate of extraction solvent alone in feed (mol/h)
T	Temperature, (°C)
T_R	Reduced temperature
U	Extraction factor
V_C	Continuous phase superficial velocity (m/s)
V_D	Distributed phase superficial velocity (m/s)
x_E	Weight fraction solute in extract
x_F	Weight fraction solute in feed
x_R	Weight fraction solute in raffinate
x_0	Mass fraction solute in aqueous phase into first equilibrium stage
x_1	Mass fraction solute in aqueous phase out of first equilibrium stage
x_2	Mass fraction solute in aqueous phase out of second equilibrium stage

X_E^*	Equilibrium mole fraction solute in extract
X_f	Mole fraction of solute in extraction column feed
X_i	Mole fraction of component i in extract
X_R^*	Equilibrium mole fraction solute in raffinate
y_0	Mass fraction solute in solvent phase into first equilibrium stage
y_1	Mass fraction solute in solvent phase out of first equilibrium stage
y_2	Mass fraction solute in solvent phase out of second equilibrium stage
Y_i	Mole fraction of component i in raffinate
Z	Height of packing (m)
β	Selectivity
γ	Activity coefficient
γ°	Activity coefficient at reference state
ε	Void fraction of packing
μ_C	Continuous phase viscosity (N s/m^2)
μ_D	Discontinuous phase viscosity (N s/m^2)
ρ	Density (kg/m^3)
ρ_C	Density of the continuous phase, (kg/m^3)
ρ_D	Density of the dispersed phase
$\Delta\rho$	Density difference between phases (kg/m^3)
σ	Interfacial tension (J/m^2)
σ_o	Interfacial tension of water in equilibrium with its pure vapor at 25°C (71.98 dyne/cm)

REFERENCES CITED

Akgerman, A., R. K. Roop, R. K. Hess, S. D. Yeo, "Supercritical Extractions in Environmental Control", pp 479-509, In: Supercritical Fluid Technology. Reviews in Modern Theory and Applications, T. J. Bruno, and J. F. Ely, Eds., CRC Press, Inc., Boco Raton, FL, (1991).

Breckenfeld, R. R., and C.R. Wilke, Chem. Eng. Prog., 66, p 305, (1942).

Briggs, D., "French Oil Mills machinery Company Pressing", Memo to the Cherry Marketing Institute, (October 25, 1991).

Compressed Gas Association, Handbook of Compressed Gases, 3rd ed., Van Nostrand Reinhold, New York, (1990).

Coulson, J. M., and J. F. Richardson, Chemical Engineering, Volume 2, Unit Operations, 2nd ed., Pergammon Press, New York, (1968).

Crawford, J. W., and C. R. Wilke, "Limiting Flows in Packed Extraction Columns", Chem. Eng. Prog., 47, (8), 423, (1951).

Cruess, W. V., Commercial Fruit and Vegetable Products, 4th ed., McGraw-Hill, New York, pp 738-743, (1958).

Donahue, D. J., and F. E. Bartel, "The Boundary Tension at Water-Organic Liquid Interfaces", Jour. Phys. Chem., 56, p 480, (1952).

Gaylor, R. N., and H. R. C. Pratt, "Transactions of Institution of Chemical Engineers", London, 35, p 267, (1957).

Gaylor, R. N., N. W. Roberts, and H. R. C. Pratt, "Transactions of Institution of Chemical Engineers", London, 57, (1953).

Gill, T., A. H. C. Chen, and H. Grethlein, "Feasibility Study Using Cherry Pits as a Natural Benzaldehyde Source", Report No. 2 to the Cherry Marketing Institute, (October 31, 1990).

Gribb, A., and C. T. Lira, "Benzaldehyde Recovery Process Design", Report to the Cherry Marketing Institute, (August 12, 1992).

Gore, G., "On the Properties of Liquid Carbonic Acid", Proc. Roy. Soc., London, 11, p 85.

Hannay, J. B., and J. Hogarth, "On the Solubility of Solids in Gases", Proc. R. Soc., London, 30, 324, (1879).

Holmes, M. J., and M. VanWinkle, "Prediction of Ternary Vapor-Liquid Equilibria from Binary Data", Ind. Eng. Chem., 62, (1), 21, (1970).

Kremser, Natl. Petrol. News., 22, (21), p 42, (1930).

Lira, C. T., "Physical Chemistry of Supercritical Fluids - A Tutorial", In: Supercritical Fluid Extraction and Chromatography: Techniques and Applications, B. A. Charpentier, and M. R. Sevenants, Eds., ACS Symposium Series 366, Washington D. C., 1-25, (1987).

Massoudi, R., and A. D. King, Jr., "Effect of Pressure on Surface Tension of Water. Adsorption of Low Molecular Weight Gases on Water at 25°.", Jour. Phys. Chem., 78, (22), p 2262, (1974).

McHugh, M. A., and V. J. Krukonis, Supercritical Fluid Extraction Principles and Practices, Butterworth, Stoneham, MA, (1986).

Nair, M. G., and A. Chandra, "HPLC Analyses of Kernel and its Cake from Montmorency Cherry Pits", Report to the Department of Horticulture, Bioactive Natural Products Laboratory, Michigan State University, (October 29, 1991).

Null, H. R., and D. A. Palmer, "Predicting Phase Equilibria", Chem. Eng. Prog., 65, (9), 47, (September, 1969).

Oberg, A., and S. C. Jones, "Liquid-Liquid Extraction", Chemical Engineering, 70, part 2, (15), p 119, (July 22, 1963).

Paulitis, M. E., et. al., "Phase Equilibria Related to Supercritical-Fluid Solvent Extraction", Ber. Bunsenges. Phys. Chem., 88, pp 869-875, (1984).

Perry, R. H., and C. H. Chilton, Eds., Chemical Engineers' Handbook, 5th ed., McGraw-Hill, New York, (1973).

Rao, M. R., and C. V. Rao, "Flooding Rates in Packed Extraction Towers", Chem. Eng. Sci., 9, pp 170-175, (1958)

Scheibel, E. G., "Fractional Liquid Extraction", Chem. Eng. Prog., 44, p 681, (1948).

Schultz, W. G., and J. M. Randall, "Liquid Carbon Dioxide for Selective Aroma Extraction", Food Technology, 24, pp 1282-1286, (November 1970).

Schultz, W. G., et. al., "Pilot Plant Extraction with Liquid CO_2", Food Technology, p 32, (June 1974).

Simons, W. W., Ed., The Sadtler Handbook of Ultraviolet Spectra, Sadtler Research Laboratories, Divison of Bio-Rad Laboratories, Inc., (1979).

Treybal, R. E., Liquid Extraction, 1st ed., McGraw-Hill, New York, (1951).

Treybal, R. E., Liquid Extraction, 2nd ed., McGraw-Hill, New York, Chap. 4, p 132, (1963).

Venkataraman, G., and G. S. Laddha, "Limiting Velocities, Holdup, and Pressure Drop at Flooding in Packed Extraction Columns", A. I. Ch. E. Jour., 6, 3, (1960).

Weast, R. C., Ed., CRC Handbook of Chemistry and Physics, 50th ed., The Chemical Rubber Company, Cleveland, Ohio, (1967-1970).

Weibe, R., "The Binary System Carbon Dioxide-Water Under Pressure", Fertilizer Research Division, Bureau of Plant Industry, U. S. Department of Agriculture, Washington, D. C., (1977)

Whitman, W. G., Chem. Met. Eng., 29, p 147, (1923).

Wiegand, J. H., Trans. Am. Inst. Chem. Engrs., 36, p 679, (1940).

Wohl, K., "Thermodynamic Evaluation of Binary and Ternary Liquid Systems", Trans. Am. Inst. Chem. Engrs., 42, 215, (1946)

Woods, W. S., et. al., "Carbon Dioxide Solubility in Water", Ind. Eng. Chem., 1, 1, (1956).